Bayesian Modeling and Simulation Methods for Fish Movements

by

Inesh Prabuddha, Munaweera Arachchilage

A Thesis submitted to the Faculty of Graduate Studies of

The University of Manitoba

in partial fulfilment of the requirements of the degree of

Doctor of Philosophy

Department of Statistics

University of Manitoba

Winnipeg

Abstract

Bayesian methods have been popular in modelling complex ecological data collected using modern animal tracking technologies such as acoustic telemetry for multiple reasons, including their extreme flexibility, ability to incorporate prior knowledge and better precision. Acoustic telemetry systems technology has been increasingly used to study fish movement patterns and habitat use and estimate demographic parameters, including survival probabilities and population size. However, the data generated using omnidirectional acoustic telemetry studies are complex, with multiple sources of variability. In this thesis, I develop methods to effectively analyze data generated with omnidirectional acoustic telemetry systems. The thesis consists of four manuscripts with three different Bayesian models in the first three manuscripts: (1) Bayesian state-space modelling approach to estimate the hidden fish movement paths of walleye in lake Winnipeg, (2) Bayesian multi-state mark-recapture models to estimate survival of Arctic char living in multiple habitats of the Cambridge bay region of Nunavut, and (3) Bayesian hierarchical modelling to understand the biological and environmental drivers behind the survival of Cambridge bay Arctic char. In the fourth manuscript, we develop a novel set of fishery metrics to further understand the vulnerability of walleye to fishing activities in lake Winnipeg. Furthermore, the thesis provides practical tools for many challenges that will arise from the planning stage of the study to the data analysis stage of acoustic telemetry studies. In addition, the finding of each study provides

valuable and influential information for fishery managers to make effective fish management and conservation decisions that will affect the future of the aquatic species in those regions.

Acknowledgement

First and foremost, I express my most profound appreciation to my supervisors, Dr. Saman Muthukumarana and Dr. Darren Gillis, for their invaluable guidance, support, patience, and motivation throughout my Ph.D. life. I could not have imagined more knowledgeable and supportive advisors for my Ph.D.

I want to thank my committee members, Dr. Aleeza Gerstein and Dr. Kevin Fraser, for their valuable comments, insights and encouragement in making this thesis successful. I would like to thank my external committee member Dr. Veronica Berrocal for the suggestions and constructive feedback given to further enhance the quality of my thesis. I would like to express my sincere gratitude to Dr. Derek Krepski, who chaired my dissertation defense.

Also, my sincere gratitude goes to my excellent collaborators Les Harris, Doug Watkinson, Eva Enders, Charles Collins, Jean-Sébastien Moore, Ross Tallman, Aaron Fisk, Brent Else, Mohamed Ahmed and Klein Geoff for their support in obtaining data and sharing the expertise in their fields with me.

Furthermore, I thank the staff members, my colleagues and friends in the Department of Statistics of the University of Manitoba for making my graduate life memorable.

I'm greatly indebted to my father and mother for everything. I have no words to express my love and gratitude for their immense support throughout my life. Also, I thank my sister and brother for their encouragement and love throughout my life.

Lastly, I thank my loving wife, Piyumi, and my little girl for their unconditional love and continuous encouragement. I love you two a lot.

Dedication

This thesis is dedicated to:

my loving parents...

Contents

List of Tables

List of Figures

Chapter 1

Introduction

The movement of an individual organism is one of the fundamental phenomena of life on Earth. Some interesting questions in studying animal movements are why they move, when and where they move, and the consequences of such movements (Hussey et al. 2015; Matley et al. 2022; Nathan et al. 2008). Modern technologies such as acoustic telemetry, GPS, camera traps, and radar allow for remotely collecting critical information on animals living in their natural worlds with minimum or no disturbance to their natural behaviour (Donaldson et al. 2014; Jonsen et al. 2003; Klimley et al. 1998). However, most of the data collected using such technologies are complex, and the paucity of suitable statistical tools limits the complete utilization of such data (Jonsen et al. 2005; Whoriskey et al. 2019). For instance, consider an acoustic telemetry system in an aquatic environment. An acoustic telemetry system consists of two components; an acoustic tag which is attached externally or surgically implanted in an animal, and a grid of receivers installed at fixed locations that detect and record the presence of the acoustically tagged animal. However, the commonly used omnidirectional acoustic

receivers cannot reveal the animal's exact location, and the animal can be anywhere inside the detection range of the receiver. Also, the receiver's ability to detect a tagged animal weakens as the animal moves away from the receiver. In addition, environmental conditions also affect the detection probability (Klinard et al. 2019; Reubens et al. 2019). For example, a receiver in an aquatic environment can better detect tagged fish in winter due to lower interference when the surface is covered in ice than in the open water season when wave actions and wind might interfere with the acoustic signals. Hence, accurate estimation of animal movement paths and population parameters (population size, survival probability, average swimming speed, etc.) has been challenging and requires complex statistical techniques that are still being developed (Alós et al. 2016; Jonsen et al. 2005). In this context, the Bayesian framework has been gaining popularity as the most natural approach in modelling such data due to its extreme flexibility in formulating complex process using a more straightforward set of sub-models. Also, the Bayesian framework facilitates the incorporation of prior knowledge about parameters and usually results in better precision compared to the more traditional likelihood approach (Gelman et al. 2004; Kéry and Schaub 2011; Muthukumarana et al. 2008).

Fish can be highly mobile in their quest for suitable foraging and spawning environments (Cooke et al. 2016). Studying freshwater fish presents a challenge for researchers due to the intricate nature of their habitats and the limited visibility underwater compared of most land-dwelling animals (Cooke et al. 2016). Some of the commonly used technologies to study the movements and behaviors of aquatic animals include; acoustic telemetry, radio telemetry, passive integrated transponders (PIT), and satellite telemetry (Cooke et al. 2013;

Donaldson et al. 2014; Ropert-Coudert and Wilson 2005). As technology has advanced, researchers have been able to significantly reduce the size of tags, enabling longer periods of monitoring for a wider range of species across various life stages (Block 2011; Cooke et al. 2013). Furthermore, some tags are specifically designed to infer predation, while certain modern tags are equipped with environmental and physiological sensors in addition to their tracking capabilities (Cooke et al. 2013; Villegas-Ríos et al. 2020).

Acoustic telemetry systems are increasingly used worldwide to study aquatic animal behaviour in freshwater and marine ecosystems (Matley et al. 2022; Reubens et al. 2019; Whoriskey et al. 2019). Acoustic receivers are usually arranged in two ways; (1) Traditional acoustic telemetry studies consist of receivers at geographical bottlenecks. (2) A systematically deployed two-dimensional array of receivers (Kraus et al. 2018). The first setting is frequently used to study broader animal movements, such as migration, or to estimate survival. The second setting is used to understand movements throughout a region. The objective of my thesis is to develop methods towards a modelling framework to analyze fish detection records generated from each of the above two scenarios to estimate unobserved fish positions or/and interesting population parameters. The thesis contains practical statistical tools that will help ecologists to understand animal movement patterns better and estimate population parameters by effectively analyzing data generated from acoustic telemetry systems. This thesis contains four manuscripts that are presented in the proceeding chapters.

In Chapter 2, we developed a Bayesian state-space modelling (SSM) framework to estimate individual Walleye (*Sander vitreus*) movement paths using data obtained from a systematically deployed two-dimensional grid of receivers in Lake Winnipeg, Manitoba. Also, we

compared the performance of the SSM approach against classical smoothing techniques, including simple weighted average method, kernel smoothing, and cross-validated local polynomial regression approach with Friedman's super smoother (Friedman 1984). In addition, we incorporated additional information within the SSM approach, such as prior knowledge of fish movements, detection probabilities, and seasonal variations, to further improve the model performance. Unlike the habitats of terrestrial animals, aquatic animal habitats are usually very complex. Hence, we must constrain the model, so the animal trajectory stays within suitable habitats. The Bayesian Markov Chain Monte Carlo sampler we used for the analysis ('JAGS') has limited functionalities in defining such constraints. Hence we used the constrained conditional likelihood methodology known as "One's Trick" to overcome this problem. Furthermore, we performed an intensive simulation study to compare the performance of the different modelling approaches in estimating the movement paths. The work is published in the Canadian Journal of Fisheries and Aquatic Sciences (Munaweera et al. 2021).

In Chapter 3, we propose a Bayesian multi-state capture–recapture model to estimate survival probabilities of Cambridge Bay Arctic char in different environments (marine, estuary and freshwater) using acoustic telemetry data from 2014 to 2018. The Arctic char in the region are anadromous. They migrate to the sea for forage and returns to freshwater to spawn. Previously, Caza-Allard et al. (2021) used Cormack-Jolly-Seber (CJS) framework to estimate survival probabilities for Arctic char in the region, but their study was limited to the marine environment. The recapture rates are lower in freshwater and estuary environments for this study. The survival and encounter probabilities estimates using conventional CJS models

are usually unstable and suffer from low precision when the recapture rates are low (Morris et al. 2006; O'Brien et al. 2005; Pollock et al. 1990). Therefore, in this study, we used more flexible Bayesian multi-state mark-recapture models to deal with sparseness by borrowing information across regions. Furthermore, the area is subjected to a long winter when fish are primarily inactive, resulting in lower detection probabilities during the winter (Mulder et al. 2018). Hence, the detection records were pooled over time intervals with unequal time bins under three different scenarios to avoid the sparseness caused by overwintering. This work is published in the Canadian Journal of Fisheries and Aquatic Sciences (Munaweera et al. 2022).

Chapter 4 introduces a sophisticated Bayesian hierarchical modeling approach that incorporates environmental and individual covariates, as well as varying detection probabilities within and among years, to further examine the survival probabilities of Cambridge Bay Arctic char. In most acoustic telemetry studies, the receiver array is not static over the study period due to changing study objectives, lost or repositioned receivers, and varying environmental conditions in different habitats. The model we developed in this study accounts for these variations, enabling the incorporation of all collected data instead of ignoring data from lost, removed, or repositioned receivers. As a result, the analysis of survival probabilities is more accurate and comprehensive.

In Chapter 5, we study the interaction between walleye movement paths and fishing activities in the south basin of lake Winnipeg combining fish movement paths estimated using the Bayesian SSM approach we proposed in Chapter 2, with fishery information on Lake Winnipeg, including fishing vessel information from 22 harbours observed through high-

resolution aerial images, quota allocation data for 13 licensing areas, and fish landing information (number of deliveries and their weight) obtained from 16 delivery points collected by Manitoba Natural Resources and Northern Development. We develop a set of novel metrics (probability of presence, probability of encounter, and potential fishing pressure) using the above data and compare the behaviour of those metrics seasonally against the spatial distribution of sampled Walleye in the Lake to study the potential interactions between walleye movements and fishing activity.

Finally, Chapter 6 presents concluding remarks with a discussion and future directions.

Chapter 2

Assessing movement patterns using Bayesian state-space models on Lake Winnipeg walleye

Assessing movement patterns using Bayesian state-space models on Lake Winnipeg walleye

Munaweera I[a], Muthukumarana S[a], Gillis D M[a], Watkinson D A[b], Charles C[b],

and Enders E C[b]

[a]University of Manitoba,

Winnipeg R3T 2N2.

[b]Fisheries and Oceans Canada,

501 University Cres.

Winnipeg MB R3T 2N6

This thesis contains the accepted version of the corresponding paper published in Canadian Journal of Fisheries and Aquatic Sciences (Munaweera et al. 2021).

Abstract

Acoustic telemetry systems technology is useful for studying fish movement patterns and habitat use. However, the data generated from omnidirectional acoustic receivers are prone to large observation errors since the tagged animal can be anywhere in the detection range of the receiver. In this study, we used the Bayesian state-space modeling (SSM) approach and different smoothing methods, including kernel smoothing and cross-validated local polynomial regression to reconstruct fish movement paths of Walleye (*Sander vitreus*) using data obtained from a telemetry receiver grid in Lake Winnipeg. Using the SSM approach, we obtained more realistic movement paths compared to the smoothing methods. In addition, we highlighted the advantages of the SSM approach to estimate undetected movement paths, over simple smoothing techniques, by comparing ecological metrics such as path length and tortuosity between different reconstruction approaches. Reconstructed paths could be useful in making effective fishery management decisions on Lake Winnipeg in the future by providing information on how Walleye move and distribute in Lake Winnipeg over space and time.

Keywords: Acoustic Telemetry, Walleye, Bayesian Inference, Markov Chain Monte Carlo, State Space Models, Fish Movements.

2.1 Introduction

Fish can be highly mobile in the search for suitable foraging and spawning habitats (Cooke et al. 2016). Fish movement paths reveal habitat use, migration patterns, survival, and behavioural changes across the years. Understanding how fish distribute and survive over space and time is important for sustainable resource management. For instance, by identifying critical habitats and movement patterns, a fishery manager can be informed of any potential risks that the fish in a population might experience from commercial fishing gear and other human activities. This will allow the manager to make effective fish management and conservation decisions (Brownscombe et al. 2019; Cooke et al. 2004, 2016).

Unlike most terrestrial animals, studying freshwater fish is not a simple task due to the complex nature of their habitats and the poor visibility in water (Cooke et al. 2016). However, modern tracking technologies such as acoustic telemetry allow for the collection of an enormous amount of data on animal movements over long distances without directly observing them in their natural habitats (Donaldson et al. 2014; Jonsen et al. 2003; Klimley et al. 1998).

Traditional acoustic telemetry studies frequently consist of an arrangement of receivers at geographical bottlenecks, which is suitable for a broader study of movements such as migration across the landscape or aquatic habitat Cooke et al. (2011). A linear arrangement of receivers does not help in understanding movements throughout a region. In this case, a systematically deployed two-dimensional array of receivers can be used (Kraus et al. 2018). However, the data collected by widely used omnidirectional acoustic receivers are subject to large observation errors, especially when the distance between two adjacent receivers in

the array is large (Alós et al. 2016). Hence, the detection of an acoustic tag only suggests proximity, but does not reveal the true location. Furthermore, the probability of a fish being detected by a receiver decreases as the fish moves away from the receiver, and the detection probability is also affected by environmental variables such as ice-cover, wind, and wave action (Klinard et al. 2019; Reubens et al. 2019). Two main approaches are available to estimate fish movement paths: (1) detection records can be smoothed to obtain the average fish locations for regular time bins, and (2) fish locations are estimated based on an underlying process model that describes fish behaviour.

Several different smoothing techniques have been applied to movement data. Simpfendorfer et al. (2002) used the weighted means algorithm to estimate the average fish locations. Hedger et al. (2008) suggested using the cross-validated local polynomial regression with Friedman's super smoother (Friedman 1984) to be the optimum interpolation method. Furthermore, Hedger et al. (2008) recommended kernel estimation with the Gaussian kernel to interpolate fish paths. Even though smoothing techniques provide an easily implemented and efficient way to reconstruct movement paths, simply smoothing the detection path masks the actual fish movement behaviour. This can lead to incorrect estimates of ecological metrics such as swimming speed and total distance travelled. These are important in quantifying individual fish movement for use in further analysis, such as comparing behavioural patterns among individual fish (Seidel et al. 2018).

Bayesian state-space modelling (SSM) is a promising approach for modelling individual-level animal movement. In ecology, SSMs are widely used for studying animal movements since they can account for both process variation, which is the natural variation of the

underlying movement process and observational error, which is the difference between the observed position and the true position of the animal (Albertsen et al. 2015; Alós et al. 2016; Bolker 2008; Patterson et al. 2017, 2008). Also, within the SSM approach, it is possible to incorporate additional information such as prior knowledge and detection probabilities in the estimation. Pedersen and Weng (2013) developed an SSM for observation network data to estimate animal movement using the Ornstein-Uhlenbeck (OU) process. They used the OU process based SSM to estimate movement paths and home range of Humphead Wrasse (*Cheilinus undulatus*; a coral reef fish). Through simulations, they showed that the SSM outperformed the smoothing techniques suggested by Hedger et al. (2008) and Simpfendorfer et al. (2002). Alós et al. (2016) used a more sophisticated SSM with a mechanistic movement model that accounted for the fish's home range behaviour to reconstruct individual movement patterns of Pearly Razorfish (*Xyrichtys novacula*) within a short time period of 20 days using acoustic telemetry data. They performed a simulation study to assess the accuracy and precision of their model and found that SSM models provide accurate and unbiased estimates for the movement parameters and locations.

The objective of this study was to develop a framework to effectively reconstruct individual fish movement paths to infer Walleye behaviour in Lake Winnipeg. As a part of the Lake Winnipeg Basin Fish Movement Project, 357 Walleye (*Sander vitreus*) were tagged and a grid of acoustic receivers was deployed in Lake Winnipeg and some of its major tributaries to detect the movements of tagged fish. From June 2017 to September 2018, the receivers recorded over 3.8 million detections. To achieve our objective, we used Bayesian SSMs and three popular smoothing approaches (simple weighted average method, kernel smoothing

with the Gaussian kernel, and cross-validated local polynomial regression approach) to reconstruct fish movement paths. Furthermore, we performed a simulation study to evaluate the performance of the different modelling approaches in estimating the movement paths.

2.2 Materials and methods

2.2.1 Study area

Lake Winnipeg, located in Manitoba, Canada, is the tenth largest lake in the world by surface area (24,514 km^2) and accounts for North America's second-largest freshwater fishery (Sheppard et al. 2015; Wassenaar and Rao 2012). It is a shallow lake that has two main basins (north basin and south basin), that are connected through the narrows (Fig. 5.1). The average depth of the north basin is 13.3 m and, the south basin is only 9 m deep on average (Brunskill et al. 1980; Stewardship et al. 2011). The lake typically has ice form around the middle of November in both basins, and ice melting usually at the end of April to mid-May in the south basin and mid-May to early June in the north basin. Despite its importance to commercial fisheries, little research has been conducted to understand how fish respond to the fishing pressure and changes in the physical environment (Johnston et al. 2012).

2.2.2 Study species

Walleye are large-bodied piscivorous fish that are commonly found in moderately productive lakes in North America (Hartman 2009). Adult Walleye typically reach maturity at lengths

ranging from 35–50 cm. Spawning occurs in early spring from mid-April to the end of May in Manitoba. Walleye is the most valuable species for commercial and recreational fisheries in Lake Winnipeg (Fisheries and Canada 2020; Stewart and Watkinson 2004; Thorstensen et al. 2020).

2.2.3 Experimental setup and procedure

For tagging, fish were captured by boat electrofishing. Only individuals with a body mass >1.2 kg were tagged ensuring that the transmitter was less than 2% of the mass of the fish. 'Vemco V16-4H' acoustic transmitters (16 mm diameter, 24 g, 6 $\frac{1}{2}$ years expected battery life, with an average transmission delay of 120 s with a pseudo-random uniform interval between 80–160 s) were surgically implanted in each fish.

Fish were sedated using a Portable Electroanesthesia System (PES™, Smith-Root, Vancouver, WA, USA). The PES™ was set to 100 Hz, 25% duty cycle, and 40 V. Pulsed direct current is appropriate sedation for adult fish because it provides a surgery window of 250–350 s and fish recover quickly with minimal impact to vertebral integrity. Fish were placed supine in a padded V-shaped trough (Vandergoot et al. 2011). Ambient water was continuously pumped over the gills (using a recirculating flow-through pump system) to maintain normal respiration during the surgical period (<5 min). A small incision was made posterior to the pectoral girdle just dorsal of the ventral midline. The acoustic transmitter was inserted posteriorly into the peritoneal cavity. The incision was closed with three interrupted sutures (standard surgical knots). Fish were put in the recovery tank and released 10–15 min post-surgery at the tagging location. Surgical procedures were carried out following approved

animal use protocols of Fisheries and Oceans Canada (FWI-ACC-2017-001) and the University of Nebraska-Lincoln (Project ID: 1208). The length, body mass, and sex (where discernible) of the fish were recorded while tagging. By June 2018, 357 Walleye were tagged (271 Females, 58 Males, and 28 unidentified).

Tagged fish were detected by a grid of Vemco VR2W acoustic receivers (47 in Section 1, 61 in Section 2, and 51 in Section 3) deployed near the bottom of Lake Winnipeg and its major tributaries (Red River and Winnipeg river). In the rivers, distances between receivers varied between 5 and 30 km. In the lake, the receivers were placed on a systematic grid varying between 5 km in the southern part of the south basin and 7 km for the rest of the south basin and narrows, and 14 km in the southern part of the north basin (Fig. 5.1). A feasibility study on the receiver array can be found in Kraus et al. (2018). Under good acoustic conditions, receivers detect the tag transmission up to 3 km and the probability of detecting a fish by a receiver decreases the further a fish is from the receiver (Fig. 2.2).

2.2.4 Classical approaches to movement path reconstruction

The simplest approach to reconstruct fish movement paths is to calculate the average locations of the fish at regular time intervals with the weighted average method (Simpfendorfer et al. 2002). For this approach, regular time bins are defined, and the number of detections is counted for each receiver and each time bin. If $\{\bar{x}_{E,n}, \bar{x}_{N,n}\}$ is the average location (easting and northing respectively) at the n^{th} time bin, then the average locations are obtained as

$$\bar{x}_{E,n} = \frac{\sum_{j=1}^{\mathrm{K}} \mathrm{R}_{n,j} x_{E,j}}{\sum_{j=1}^{\mathrm{K}} \mathrm{R}_{n,j}}, \qquad \bar{x}_{N,n} = \frac{\sum_{j=1}^{\mathrm{K}} \mathrm{R}_{n,j} x_{N,j}}{\sum_{j=1}^{\mathrm{K}} \mathrm{R}_{n,j}}, \tag{2.1}$$

where $R_{n,j}$ is the number of detections recorded at the j^{th} receiver within the n^{th} time bin, and $(x_{E,j}, x_{N,j})$ is the location of the j^{th} receiver. K denotes the number of receivers in the array (Simpfendorfer et al. 2002).

Interpolation approaches such as local polynomial regression and kernel estimations (smoothing) can also be used to construct individual movement paths (Hedger et al. 2008). The idea of local polynomial regression is to estimate the underlying smooth function by fitting a series of linear least squares regressions locally. The smoothness of the estimated curve depends on how many neighbouring observations are considered in each local regression, this is called the span (k). The selection of neighbouring points is usually done symmetrically so that half of the neighbouring points are at each side of the target point. Friedman's super smoother proposed by Friedman (1984) is an efficient algorithm that uses a variable span approach with a locally changing span. The optimum local span at each prediction point is selected with cross-validation.

Kernel estimations is similar to local polynomial regression. In kernel estimations, the smoothing is done by calculating local averages while assigning different weights to the neighbours with a kernel. The well-known Gaussian kernel applies more weight to the points closer to the target point, and the weights gradually decrease as the points are further away from the target. In their study, Hedger et al. (2008) identified the cross-validated local polynomial regression with Friedman's super smoother (Friedman 1984) to be the optimum interpolation method and also recommended kernel estimation with the Gaussian kernel over a box kernel to interpolate fish paths. In this paper, we used the '`sm`' package (Bowman and Azzalini 2018) in '`R`'(R Core Team 2020) to implement the cross-validated local polynomial

regression and kernel estimations.

2.2.5 Bayesian state-space models

An SSM contains two sub-models; process model and observation model. This can be expressed as

$$\boldsymbol{x}_t = f(\boldsymbol{x}_{t-1}, \epsilon_t), \tag{2.2}$$

$$\boldsymbol{y}_t = g(\boldsymbol{x}_t, \eta_t), \tag{2.3}$$

where $f(.)$ and $g(.)$ represent the process model and the observation model, respectively. Here, $\boldsymbol{x}_t$ is called the latent state and $\boldsymbol{y}_t$ is the observation of the state at time t. In the context of fish movement modeling, $\boldsymbol{x}_t$ represents the true position of the fish that can be in latitude-longitude or Universal Transverse Mercator (UTM) coordinates. $\boldsymbol{y}_t$ represents the observed position, which is usually subjected to errors. The errors associated with each model are denoted by ϵ_t and η_t (Patterson et al. 2008).

Due to the complex nature of SSMs, analytical solutions for the parameters are usually not feasible. One alternative is to use the Bayesian Markov Chain Monte Carlo (MCMC) approach. In the MCMC approach, the initial values of the true position and the model parameters are sequentially updated so that the values of the current step are updated conditioning on the values of the previous step. The simulation is continued until the parameter estimates converge (Patterson et al. 2008). One of the advantages of using the Bayesian MCMC approach is the ability to incorporate past knowledge about parameters to the models through prior distributions (Jonsen et al. 2003). However, the Bayesian MCMC approach

can be very computationally intensive as the SSM becomes more complex.

Constraining the paths

When using SSMs to reconstruct fish paths, it is important to avoid biologically impossible locations. Hence, we have to constrain the model so that the fish trajectory stays within feasible habitats. In our case, the predicted path should remain in the lake or rivers inflowing to the lake. Due to the limited functionality of Bayesian modeling programs such as `'BUGS'` and `'JAGS'`, constraining models is usually very problematic (Plummer et al. 2003; Spiegelhalter et al. 2003). One of the solutions to this problem is the methodology known as the "One's trick" among the `'BUGS'` and `'JAGS'` community. "One's trick" is usually used to specify distributions that have not yet been implemented as a standard distribution in those programs.

2.2.6 Model selection

The deviance information criterion (DIC) suggested by Spiegelhalter et al. (2002), is one of the most widely used measures of predictive accuracy in Bayesian model selection. DIC can be described as the Bayesian version of the Akaike information criterion (AIC) (Gelman et al. 2014) that measures the complexity and fit of a model. One of the reasons for the popularity of DIC is the computational convenience, since DIC is already incorporated into the `'BUGS'` and `'JAGS'` packages (Plummer et al. 2003; Spiegelhalter et al. 2003).

2.2.7 State space model implementation

Six Walleye with visibly different behavioural patterns were chosen for the modeling among the 100 inspected to test the methodology. Out of the selected fish, three stayed in the south basin for the entire year and the other three migrated between the south and north basins. The four female fish were larger in size than the two male fish (Table 2.1). The detection records during the period of June 1^{st}, 2017, to May 31^{st}, 2018, were considered for the movement path reconstruction to study the fish behaviour for the entire year. The detection paths were constructed by connecting the subsequent receiver locations, where the fish was detected (Fig. 2.3). Each point in Fig. 2.3 represents a detection, and the true location of the fish can be anywhere within the detection range of the receiver.

The detection records in our data set are in irregular time intervals. Hence, we made them regular by counting the number of detections recorded by each receiver within regular 3 h time bins. Data pooled into 3 h bins reduced the computing burden, and enabled us to estimate fish paths with enough resolution to study any behavioural changes within the day.

The process model

The simplest natural process model we can consider for fish movement is the random walk based on continuous turning angles and step lengths. The true position of the fish (which is unknown) at time t is given by $\boldsymbol{x}_t = \{x_{E,t}, x_{N,t}\}$, are in UTM coordinates. Since UTM coordinates are in meters, it is convenience to calculate distances and areas using the UTM coordinate system. The process model is given by

$$x_{E,t+1} = x_{E,t} + l_t \sin(\Phi_t), \qquad (2.4)$$

$$x_{N,t+1} = x_{N,t} + l_t cos(\Phi_t), \qquad (2.5)$$

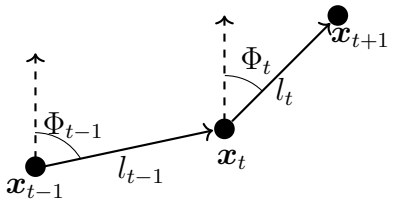

where l_t and Φ_t represent the step length and the turning angle at time t. We considered two scenarios for the distribution of l_t.

$$\text{Scenario 1:} \qquad l_t \sim N(\mu_l, 1/\tau_l), \qquad (2.6)$$

$$\text{Scenario 2:} \qquad l_t \sim P\phi(\mu_1, \sigma_1^2) + (1-P)\phi(\mu_2, \sigma_2^2). \qquad (2.7)$$

In Scenario 1, we considered the step lengths to arise from a single Gaussian distribution with parameters μ_l and τ_l, which represent the average step size and the precision (reciprocal of the variance) of the distribution of step size (l_t), respectively. The prior distribution for μ_l was set to be uniform and the prior for τ was set to be non-informative $Gamma(0.1, 0.1)$ based on swimming performance information for Walleye by Peake et al. (2000). In the second scenario, l_t was assumed to follow a Gaussian mixture distribution. Here, $\phi(.)$ denotes the Gaussian density and P defines the mixing probability, where μ_1 and μ_2 are the average step length sizes of the two mixing distributions and σ_1, σ_2 are the standard deviations of corresponding distributions. The ideology behind using the mixture distribution is that fish change their movement behaviour with two-step length distributions at any time step with the probability P. The prior distributions of μ_1 and μ_2 were set to be $Unif(0, 9000)$. The prior for σ_1 and σ_2 were set to be $Unif(0, 100000)$. The $Unif(0, 1)$ was used as the prior for P. The values for the hyper-parameters of μ_1 and μ_2 were defined with the information

in the literature (Peake et al. 2000). For both cases, the turning angle was assumed to be uniformly distributed as below.

$$\Phi_t \sim Unif(-\pi, \pi). \tag{2.8}$$

The scenario, which resulted in the lowest DIC scores in the final model, was selected as the best model.

The observation model

The second part of the SSM is the observational model, which describes the probability of detection at each receiver at a given time. To model detection probabilities, we used several non-linear functions which have been used in the literature for acoustic telemetry studies (Clark 2016; How and de Lestang 2012). The functions that resulted in the best fit for the observed data are given below. The distance from the true fish position to the j^{th} acoustic receiver at step n is denoted by $d_{n,j}$ and $\pi_{n,j}$ is the detection probability at j^{th} acoustic receiver at step n. Then, the detection probability was estimated with the following four functions:

1. Logistic function

$$log\left(\frac{\pi_{n,j}}{1-\pi_{n,j}}\right) = \alpha_n + \beta_n d_{n,j}, \tag{2.9}$$

2. Probit function

$$\Phi^{-1}(\pi_{n,j}) = \alpha_n + \beta_n d_{n,j}, \text{ where } \Phi^{-1} \text{ is the inverse cumulative distribution function of the standard normal distribution,} \tag{2.10}$$

3. Gaussian kernel function

$$\pi_{n,j} = p_0.e^{-d_{n,j}/2\sigma^2}, \qquad \text{where } p_0 \text{ is the probability of detection at } d_{n,j} = 0, \quad (2.11)$$

4. Hazard function

$$\pi_{n,j} = p_0 - exp\left(\frac{d_{n,j}}{\beta_1}\right)^{-\beta_2}. \quad (2.12)$$

The parameters of each model were estimated with the non-linear least squares approach using data from a reference tag experiment in Lake Winnipeg. A line of reference tags was placed in fixed locations with a spacing of 300 m between tags which extends to 3 km from the receiver. The data were obtained under (1) open water and (2) ice-covered conditions (November 9, 2017 to May 10, 2018). Each detection function was fitted for the two data sets separately. Root mean squared error (RMSE), Akaike information criterion (AIC), and Bayesian information criterion (BIC) were calculated for model comparison. The model with minimum error criteria was selected as the observation model for the SSM. Instead of estimating the observation model along with the process model of the SSM, we used the data from the reference tag experiment to estimate the observation model to reduce the computer burden and the variability in the parameter estimates.

Credible intervals for the reconstructed SSM path

The 95% credible intervals were obtained for estimated movement with the SSM approach. Each of the lower bounds was constructed with the 2.5% percentile values of the posterior distributions of x coordinates and y coordinates for the predicted location at each time bin.

The upper bounds were obtained similarly with the 97.5% percentile values of the corresponding posterior distributions. Some path segments of the credible intervals constructed in this manner fell outside the lake in the north basin and the narrows. This can be explained by how we defined the lower and upper credible intervals. Each of the lower bounds was constructed with the 2.5% percentile values of the univariate posterior distributions of x coordinates and y coordinates separately. Even though all the estimated locations in the MCMC simulation are constrained inside the lake, lower and upper paths constructed with univariate percentiles can still fall outside the lake. Hence, the credible intervals at each time step (n) were truncated at the lake boundary along a straight line from the average location at time step t and the upper or lower bound that fell outside the lake. In addition, to better understand the movements of each fish, a posterior density plot was created with a sample of points from the posterior densities of fish locations at each time step.

Model estimation

Model estimation was conducted using the Bayesian MCMC approach with `'JAGS'` in R using the package '`R2jags`' (Su and Yajima 2015). The "One's Trick" was used inside the model definition to truncate the conditional distributions at each time step to retain the movement paths in water. To determine if the current location is on land or water, we provided a habitat mask that has a 2 km resolution, which was defined in `'R'` and then provided to `'JAGS'` (Meredith 2013). We then fitted the SSM, by keeping α_n and β_n values fixed in (5.5). First 10,000 iterations were ignored as burn-in, and thinning was done by selecting each 10^{th} iteration to avoid possible autocorrelation in the converged series.

2.2.8 Movement path analysis

Once the fish movement paths were estimated, movement ecology metrics (step length, turning angle, path length, displacement, tortuosity, and residence time) were used to describe them (Seidel et al. 2018). Step length describes the distance that fish travelled during each consecutive location, and the turning angle measures the difference in the two consecutive headings (the direction). The path length is the total distance that fish travelled (or the sum of step sizes). The distribution of step length and turning angle can be used to compare the behavioural changes over time. Displacement measures the "straight-line distance" between the first point and the last point of a fish movement path. Tortuosity measures the wiggliness of the movement paths, which can be measured with either the straightness index or the sinuosity index. The straightness index is used when the movement path is oriented, and the sinuosity index is used otherwise (Benhamou 2004). Sinuosity index is defined as

$$\text{Sinuosity index} = \frac{\sigma_\Phi}{\sqrt{l}}, \tag{2.13}$$

where σ_Φ is the standard deviation of turning angles, and l is the constant step length. In our reconstructed movement paths, the step lengths were random. Hence, we discretized the trajectory with the '`adehabitatLT`' package in '`R`' (Calenge 2011) to obtain a trajectory with a constant step size. The parameter σ_Φ was estimated with the standard deviation of the turning angles of the estimated path. For each fish, the residence time was calculated for three sections of the lake (Fig. 5.1).

2.2.9 Simulation study

To evaluate the performance of the different modelling approaches in estimating the movement paths, we performed a simulation study. The study area was assumed to be a rectangle 32 km wide and 120 km long. First, we simulated ten fish paths inside the study area for 30 d with 2 min time increments, which corresponds to the average transmission delay of the 'Vemco V16-4H' acoustic transmitters. The receiver array for the simulation study was designed to mimic the real receiver array with increasing distances between receivers from south to north (Fig. 2.4). The array consists of 73 receivers in total with 42 receivers in the south that are 5 km apart, 25 receivers in the middle 7 km apart, and 6 receivers in the north 14 km apart. Also, we allowed an area with no receivers in the north. The detection probabilities were determined by the logistic function with parameters estimated with data from the reference tags representative of the ice-off period. Paths were estimated under nine settings with combinations of the three time bins (3 h, 6 h, 12 h) and three different lengths of tracking periods (10 d , 20 d, 30 d). The true simulated average paths were also obtained for each time bin and tracking period, using true simulated paths. To evaluate the accuracy of each reconstructed path, the root-mean-squared error between the true average path and the reconstructed path was calculated for the total distance travelled and the tortuosity.

2.3 Results

2.3.1 Simulation study

By visual inspection, we noticed that except for the paths reconstructed with the cross-validated local polynomial regression method, all other reconstruction paths gave satisfactory results in estimating true paths (Fig. 2.5). Cross-validated local polynomial regression paths were over smoothed and lost most of the true movement patterns. The weighted average paths and the kernel smoothing paths appeared similar. Furthermore, the SSM approach reconstructed some of the path segments even for the areas with no receivers. We observed that the SSM method resulted in lower RMSE values of total distance except for Simulation 3 where the bin size was the largest and the tracking period was the lowest (Table 2.2). Also, the SSM approach gave lower RMSE values for tortuosity for a longer tracking period with smaller bin sizes. In addition, we calculated the residence times for all movement paths under each simulation setting with respect to three sections in the study area (Table 2.3). However, except for the cross-validated local polynomial regression, all the reconstruction methods estimated the true residence time accurately in almost all cases. In most cases, the SSM method resulted in slightly lower RMSE values for residence time than the simple weighted average and kernel smoothing methods.

2.3.2 Movement path reconstruction

The estimated detection curves with logistic and probit functions were almost identical (Fig. 2.2) with the lowest errors (Table 2.4). Hence, we selected the logit model as the detection

function for the state space model.

For "Wall-001" and "Wall-007", the model with mixture step length distribution (Scenario 2) gave lower DIC scores while other fish paths favour the model having step lengths with a normal distribution (Scenario 1). Hence, in the proceeding sections, for each fish, the SSM path refers to the reconstructed paths with the SSM approach using the best scenario that resulted in the minimum DIC (Table 2.5).

For all fish, the weighted average paths constructed with 3 h time bins and the kernel smoothing paths with 3 h bandwidth, appeared almost identical (Fig. 2.6, Fig. 2.7). Cross-validated local polynomial regression paths were most smoothed, and do not provide any insight into the individual movement paths. Furthermore, all three smoothing methods predicted some path sections on land, which is unfavourable. However, the SSM approach resulted in movement paths that were constrained within the lake except for few path segments through islands and narrows. It is important to note that the SSM path is an average path that was constructed by connecting the means of the univariate posterior distributions of x coordinates and y coordinates at each time bin. Hence, when the simulated points at a certain time step are distributed around an island or an edge, the average of the posterior distribution can fall on the island.

In the lower part of the south basin of the lake, where the resolution of the grid of receivers is high, the 95% credible intervals for the SSM path did not deviate much from the average path (Fig.s 2.8 and Fig. 2.9). However, in the narrows and the north basin, the predicted paths were unstable and subject to high variation due to the low resolution of the receiver array. In some cases, we noticed that the posterior density around certain points was lower

than their neighbouring area. This can be seen as some light dots in the middle of dark areas (Fig.s 2.8 and Fig. 2.9). This occurred around some receivers, which did not detect the fish for a certain period of time. In this case, the Markov chain avoided simulating fish positions near those receivers.

2.3.3 Movement path analysis

The metrics for the weighted average paths and the kernel smoothing paths were very similar (Table 2.6 and Table 2.7). Due to the highly smoothed nature of the cross-validated local polynomial regression method, the metrics of those paths differed significantly from the SSM paths and other smoothed paths. It gives lower path lengths and tortuosity values than the other methods. For some fish, the path lengths for the SSM models were considerably larger than the path lengths for other smoothing approaches. Except for the cross-validated local polynomial regression approach, tortuosity values and residence times for all the approaches were similar (Table 2.6 and Table 2.7).

When there was no detection for a certain period or the fish was continuously detected by the same receiver for an extended period, the weighted mean method and other smoothing approaches failed to predict any fish movements. For the entire period that the fish was unobserved, the estimated step lengths were zero, and there was no any information on turning angles. However, the SSM approach predicted some fish movements even when there was no detection. This was clearly visible in the reconstructed paths for "Wall-001" (Fig. 2.6). The SSM approach showed three path segments between the Hecla and Gimli area, while other approaches predicted a single path. When fish moved north, it was detected

by receivers, and all the reconstructed approaches were able to estimate the path segment. Once the fish returned to the Gimli region, it was undetected for about two months in the winter. Hence, the smoothing approaches failed to estimate the path. However, the SSM approach still predicted a probable path segment based on the process model by borrowing information across regions.

In the case that the fish was detected by the same receiver for an extended period, the SSM approach did not assume that the fish stayed still as the smoothing methods do, and it predicted small movements around the receiver based on the underlying process model. This property allowed the SSM approach to produce more realistic paths that resulted in higher path lengths. This was clearly noticeable for the fish that migrated to the north basin, where the receiver density was lower.

2.4 Discussion

We reconstructed movement paths of tagged Walleye using detection records from the grid of acoustic receivers and analyzing the data by applying different classical smoothing techniques and Bayesian SSMs. In the SSM approach, we used a simple random walk model with normally distributed step lengths, and a Gaussian mixture to account for complex behavioural changes in fish movements (behavioural states) over time. Using DIC criteria, we selected the best SSM model for each fish. All the smoothing methods predicted some path sections on land while the estimated SSM paths were well constrained within the lake. The SSM approach also estimated the unobserved fish movement paths to some extent even with missing detections for a few weeks or portions of the north basin with no receivers, by

borrowing information from data-rich regions. This is not possible with classical smoothing techniques. Also, for SSMs, we incorporated available prior knowledge such as information on detection probabilities including temporal changes and swimming speed, to define suitable prior distributions and their parameters. Through simulation studies, we confirmed that the SSM approach can estimate ecological movement metrics with slightly better accuracy than the classical approaches, especially when using smaller time bins and longer tracking periods.

The presented SSM can easily be modified with different process models. If the fish movement paths show persistence in the movement direction, rather than using uniform turning angles, it is better to use wrapped normal, wrapped Cauchy, or Von Mises distribution with zero expectation (Codling et al. 2008) as the distribution of turning angles. Before settling with the process models that we presented in this paper, we explored the possibility of using more complex movement models such as the OU process, that accounts for any attraction towards spatially varying local home range centers following the work by Alós et al. (2016). However, the reconstructed paths showed a huge attraction towards the home range centers, that could not be justified by Walleye biology. Also, the large number of parameters in the OU process-based model caused a significantly higher computing burden in the estimation process compared to the random walk based model. When fish paths show different movement behaviour patterns (behavioural states) at different times, the multi-state random walk model suggested by Nicosia et al. (2017) may be a potential alternative to the Alós et al. (2016) approach.

Hostetter and Royle (2020) presented a similar framework to the SSM approach to estimate

animal locations using acoustic telemetry data with the assistance of a simple Gaussian Markov process model and an observation model that was estimated with observed data. However, estimating the observation model inside the SSM framework would add an additional computing burden and might result in convergence issues. Hence, we recommend estimating the detection functions using a reference tag experiment whenever possible. The frameworks presented by Alós et al. (2016),Breed et al. (2017),Pedersen and Weng (2013), and Hostetter and Royle (2020) seem to work well for small scale systematic acoustic telemetry studies that monitor a small region (i.e., a few km^2) with a few receivers with overlapping detection ranges. For large-scale movement tracking where the receiver grid has been spread over a large area (i.e., hundreds or thousands of km^2) non-uniformly with non-overlapping detection ranges, the use of complex models such as SSMs is challenging. In our study, using real data from a large-scale telemetry study and through a comprehensive simulation study, we compared the performance of classical approaches and the SSM approach in predicting unobserved fish movements. Furthermore, none of the aforementioned papers provided a framework to constrain the reconstructed paths inside the plausible area. In this paper, we illustrated how to constrain the reconstructed paths with widely used Bayesian MCMC sampler JAGS to maintain the model inside a complex shaped habitat.

The main limitation of the SSM approach is the high computing burden. For instance, to fit a model for a single Walleye with the Bayesian MCMC approach, it took around nine hours on Compute Canada Béluga computer facility (CPUs: Intel Gold 6148 Skylake @ 2.4 GHz). Hence, one has to maintain a trade-off among multiple factors including the model complexity, tracking period, time frequency, and computing burden. Due to these reasons,

we had to limit our simulation study to a few settings with fewer time steps. Another issue with modelling Walleye movement paths with our data was the high uncertainty of the paths for the regions where the resolution of the acoustic grid was lower. However, due to cost and other practical concerns, maintaining a higher resolution throughout a large water body such as Lake Winnipeg is difficult.

Reconstructed paths can be used to answer important questions related to Walleye in Lake Winnipeg. For instance, do the fish that migrate to the north basin move differently than fish that stay in the south basin? If they move differently, is this putting a portion of the population at risk relative to the other fish? For example, a Walleye that occupies the area along the shore is at higher risk due to commercial and recreational fishing activities compared to a fish that occupies off-shore area. Also, those fish that travel long distances have a higher chance to encounter a fishing net than the fish that travels less.

Finally, we conclude that SSM is a powerful, yet, sophisticated and computer-intensive tool that can be used to better understand acoustic telemetry data. In addition to the better accuracy in predicting unobserved animal paths, another advantage of using SSMs over smoothing methods is its ability to quantify the uncertainty associated with estimated animal movement paths. However, classical smoothing methods are still useful to have quick but comparatively accurate estimates for animal moment paths using acoustic telemetry data.

2.5 Acknowledgment

The study was funded by Fisheries and Oceans Canada (DFO) Partnership Fund, Fish and Wildlife Enhancement Fund, and the International Joint Commission. Also, we acknowledge our collaborators, Agriculture and Resource Development Manitoba, University of Nebraska, and Lakehead University. Furthermore, we thank the Department of Statistics, Department of Biological Sciences and Graduate Studies of the University of Manitoba for the financial support and assistance. Dr. Gillis and Dr. Muthukumarana have been partially supported by discovery grants from the Natural Sciences and Engineering Research Council of Canada.

Table 2.1: Biological information of the six Walleye selected for testing the modelling approach for the movement path reconstruction.

Fish ID	Gender	Body mass (kg)	Fork length (mm)	No. of detections
Wall-001	Male	2.25	572	60 940
Wall-004	Female	3.80	678	63 828
Wall-006	Female	3.55	630	35 940
Wall-007	Male	1.45	519	58 030
Wall-010	Female	3.30	640	68 015
Wall-032	Female	5.15	711	30 776

Table 2.2: RMSE values of path lengths and tortuosity for simple weighted average method (WA), kernel smoothing with the Gaussian kernel (KS), cross-validated local polynomial regression approach (LPR), and the state-space modelling approach (SSM) under different simulation settings.

Simulation	Number of days	Bin size (hrs)	RMSE - Path length (km)				RMSE - Tortuosity			
			WA	LPR	KS	SSM	WA	LPR	KS	SSM
1	10	3	0.0390	0.1175	0.1094	0.0481	55.82	204.53	97.11	51.70
2	10	6	0.0417	0.1015	0.0426	0.0353	28.08	98.22	59.99	24.60
3	10	12	0.0382	0.0783	0.0782	0.0563	10.79	33.97	42.54	17.83
4	20	3	0.0571	0.1857	0.0674	0.0519	177.45	541.90	218.95	168.54
5	20	6	0.0483	0.1418	0.0623	0.0396	96.70	299.41	137.36	88.42
6	20	12	0.0388	0.0938	0.0435	0.0365	62.78	144.55	109.62	59.31
7	30	3	0.0631	0.2229	0.0720	0.0450	312.18	888.72	376.12	271.20
8	30	6	0.0433	0.1633	0.0688	0.0421	187.38	526.76	242.32	158.06
9	30	12	0.0310	0.1223	0.0265	0.0330	117.22	291.84	170.55	100.97

Table 2.3: RMSE values of residence time (as a proportion of the total time) at three sections of the study area for simple weighted average method (WA), kernel smoothing with the Gaussian kernel (KS), cross-validated local polynomial regression approach (LPR), and the state-space modelling approach (SSM) under different simulation settings.

Simulation	No of days	Bin size (h)	Section 1 (Y<40 km)				Section 2 (40 km<Y<80 km)				Section 3 (Y>80 km)			
			WA	LPR	KS	SSM	WA	LPR	KS	SSM	WA	LPR	KS	SSM
1	10	3	0.0438	0.0333	0.0387	0.0181	0.0444	0.0505	0.0397	0.0240	0.0040	0.0373	0.0125	0.0158
2	10	6	0.0306	0.0296	0.0512	0.0250	0.0345	0.0518	0.0530	0.0306	0.0158	0.0426	0.0177	0.0177
3	10	12	0.0224	0.0158	0.0316	0.0224	0.0224	0.0387	0.0316	0.0224	0.0000	0.0354	0.0000	0.0000
4	20	3	0.0276	0.0262	0.0243	0.0128	0.0307	0.0926	0.0270	0.0140	0.0114	0.1719	0.1484	0.0084
5	20	6	0.0153	0.0250	0.0377	0.0158	0.0271	0.0980	0.0458	0.0227	0.0224	0.1738	0.1476	0.0163
6	20	12	0.0079	0.0158	0.0418	0.0112	0.0137	0.0829	0.0447	0.0158	0.0112	0.1622	0.1510	0.0112
7	30	3	0.0310	0.0385	0.0301	0.0062	0.0412	0.0605	0.0336	0.0113	0.0215	0.1560	0.1416	0.0116
8	30	6	0.0179	0.0401	0.0387	0.0149	0.0376	0.0681	0.0465	0.0269	0.0300	0.1578	0.1425	0.0220
9	30	12	0.0118	0.0253	0.0435	0.0118	0.0269	0.0503	0.0447	0.0204	0.0242	0.1528	0.1442	0.0167

Table 2.4: The error measurements for different detection functions.

Model	Open water			Ice Covered		
	RMSE	AIC	BIC	RMSE	AIC	BIC
Logit	0.0338	-33.38	-32.47	0.0932	-13.07	-12.16
Probit	0.0340	-33.23	-32.32	0.0918	-13.39	-12.49
Gaussian kernel	0.0351	-32.63	-31.73	0.0977	-12.14	-11.23
Hazard	0.0362	-29.97	-28.76	0.0975	-10.18	-8.97

Table 2.5: DIC scores for fitted models. For each fish, model with the lower DIC was selected as the best SSM (marked with *) to reconstruct the movement paths. ΔDIC is the difference in the DIC scores for the models under two scenarios.

Fish ID	Wall-001	Wall-004	Wall-006	Wall-007	Wall-010	Wall-032
Scenario 1	92954.2	*110287.0	*35757.0	134017.6	*90910.9	*42822.5
Scenario 2	*92948.5	110355.2	35878.2	*134011.6	91125.2	42902.5
ΔDIC	5.7	68.2	121.2	6.0	214.3	80.0

Table 2.6: Path lengths and tortuosity for simple weighted average method (WA), kernel smoothing with the Gaussian kernel (KS), cross-validated local polynomial regression approach (LR), and the state-space modelling approach (SSM) for six selected Walleye.

Fish ID	Path length (km)				Tortuosity			
	WA	LR	KS	SSM	WA	LR	KS	SSM
Wall-001	1,336	343	1,305	1,643	0.0175	0.0082	0.0163	0.0167
Wall-004	1,724	194	1,691	1,592	0.0213	0.0140	0.0211	0.0209
Wall-006	1,417	405	1,437	1,620	0.0175	0.0105	0.0184	0.0168
Wall-007	1,688	231	1,688	1,668	0.0203	0.0111	0.0206	0.0217
Wall-010	1,550	191	1,583	1,549	0.0225	0.0181	0.0227	0.0221
Wall-032	1,370	419	1,376	1,752	0.0192	0.0113	0.0189	0.0186

Table 2.7: Residence time (as a proportion of the total time) at three sections of the lake for simple weighted average method (WA), kernel smoothing with the Gaussian kernel (KS), cross-validated local polynomial regression approach (LR), and the state-space modelling approach (SSM) for six selected Walleye.

Fish ID	Section 1				Section 2				Section 3			
	WA	LR	KS	SSM	WA	LR	KS	SSM	WA	LR	KS	SSM
Wall-001	0.1083	0.0902	0.1083	0.1086	0.5489	0.5645	0.5482	0.5475	0.3428	0.3452	0.3435	0.3439
Wall-004	0.3326	0.3646	0.3428	0.3435	0.6674	0.6354	0.6572	0.6565	0	0	0	0
Wall-006	0.4921	0.4959	0.4928	0.4948	0.2717	0.2631	0.271	0.2672	0.2362	0.241	0.2362	0.2379
Wall-007	0.099	0.0983	0.1069	0.1089	0.901	0.9017	0.8931	0.8911	0	0	0	0
Wall-010	0.0354	0.0079	0.0354	0.0347	0.8863	0.9763	0.886	0.886	0.0783	0.0158	0.0786	0.0793
Wall-032	0.5943	0.5836	0.5957	0.5967	0.2425	0.2734	0.2418	0.2401	0.1632	0.1429	0.1625	0.1632

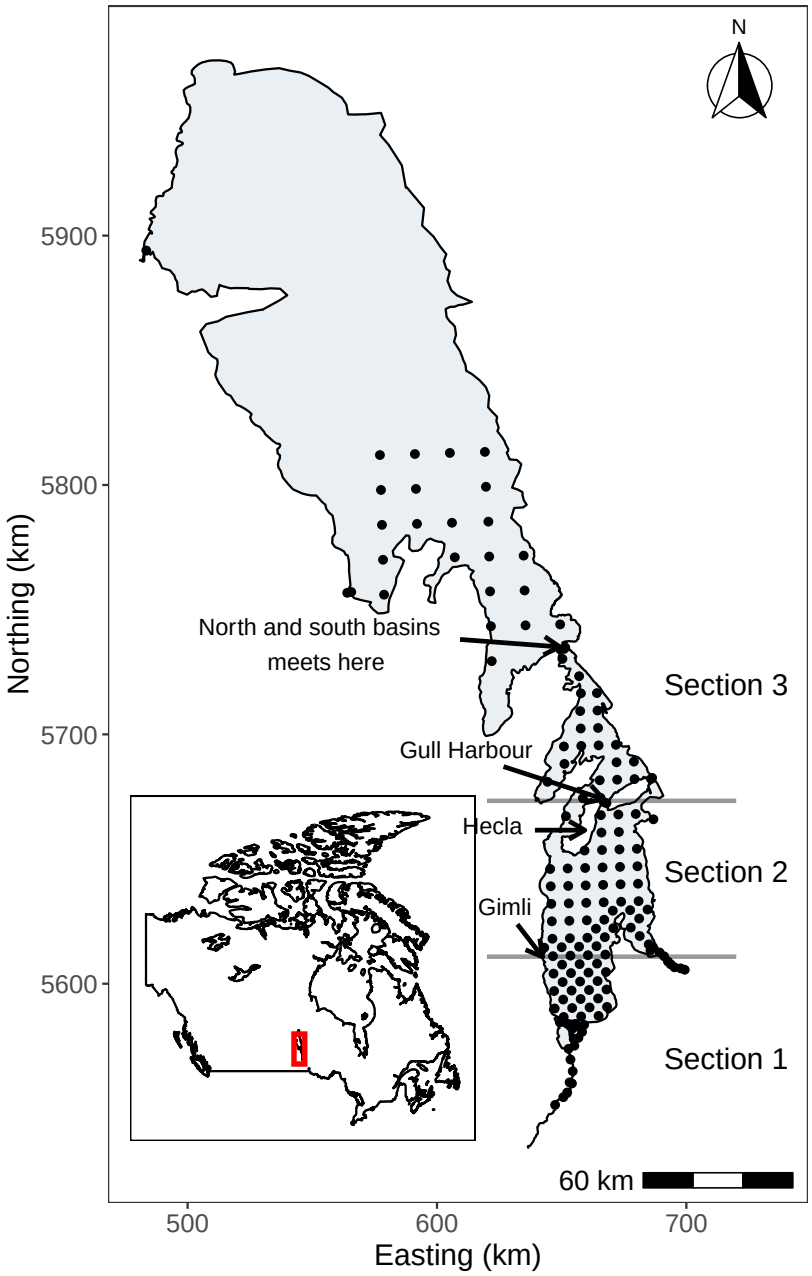

Figure 2.1: Lake Winnipeg and the locations of the acoustic receivers indicated by '•'. The study area was divided into three sections. Section 1 is the area south of Gimli, Section 2 is the area between Gimli and Gull Harbour, and Section 3 is the area north of Gull Harbour. Map was made using R (R Core Team 2020) with ggplot2 (Wickham 2016).

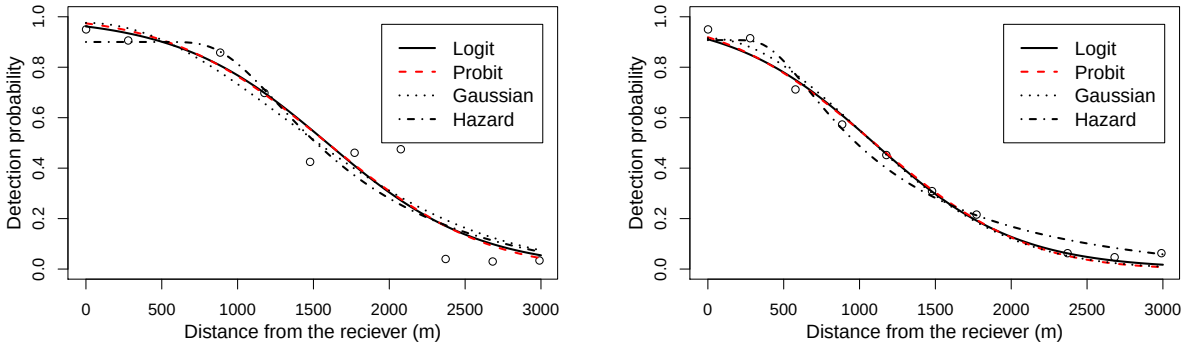

(a) Ice covered.

(b) Open water.

Figure 2.2: Detection data and estimated detection functions. The curves were estimated separately for open-water data and ice-covered data.

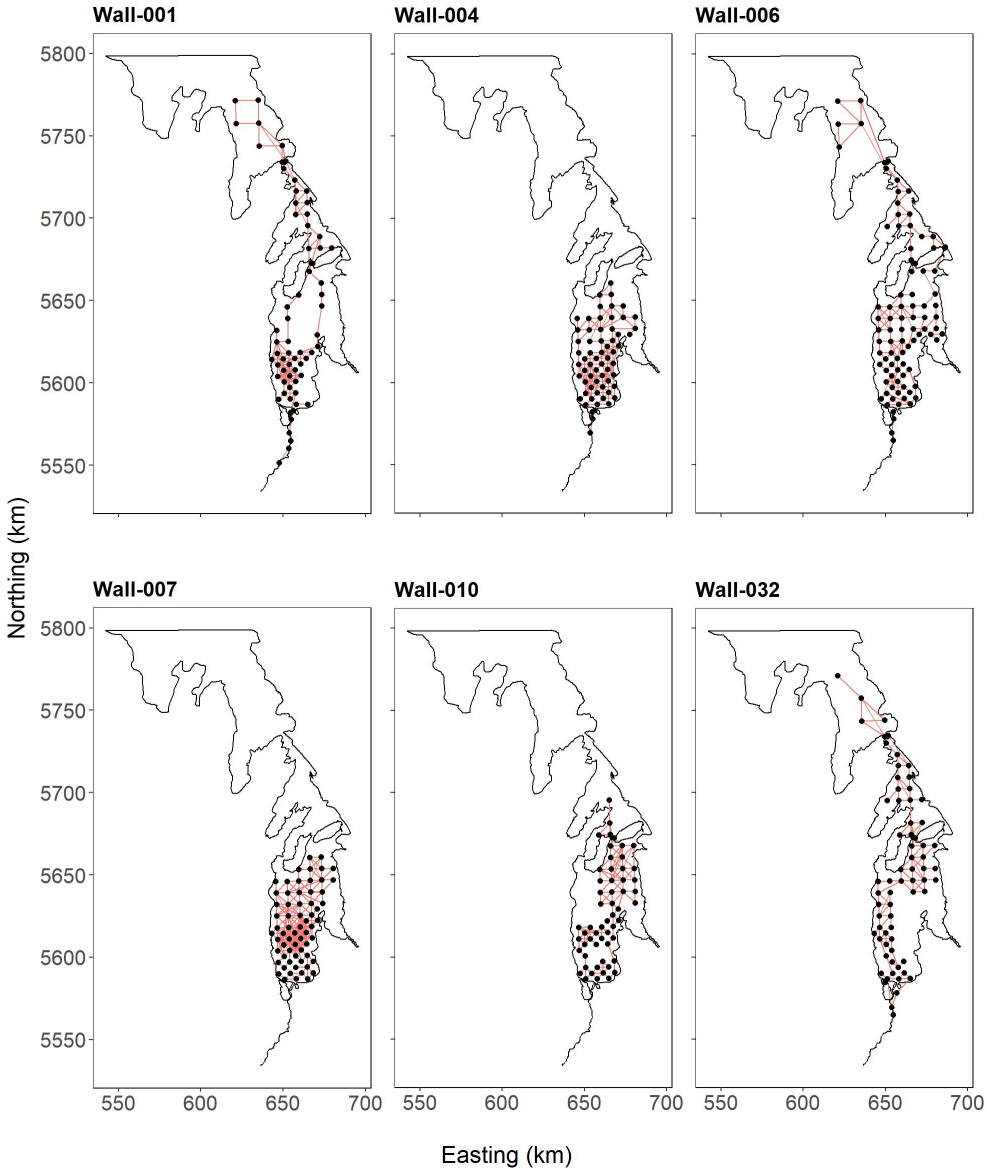

Figure 2.3: Detection paths for six selected Walleye that were constructed by connecting the consecutive receiver locations where fish were detected. Maps were made using R with ggplot2.

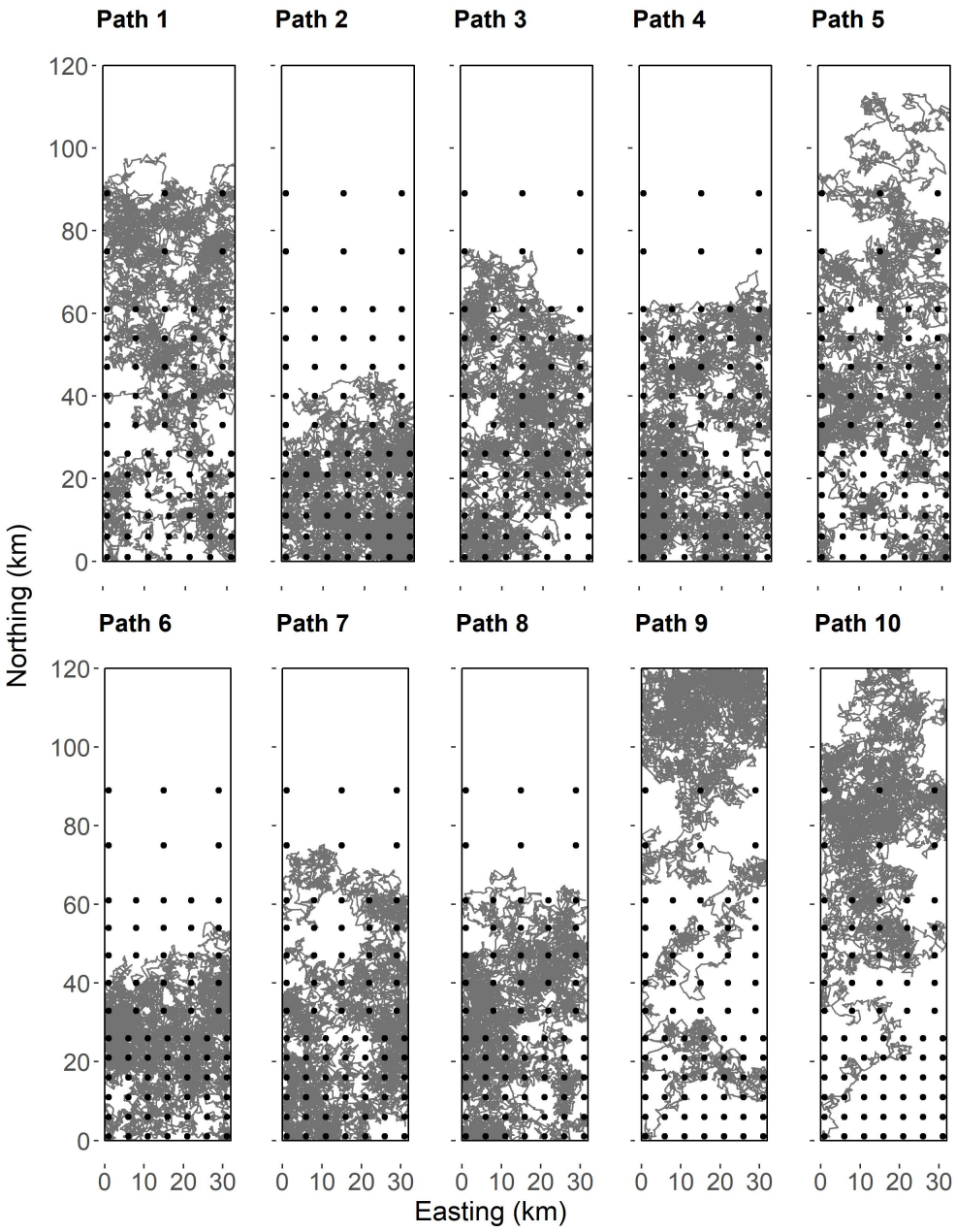

Figure 2.4: Simulated trajectories for 30 d with 2 min time increments. The receiver locations are denoted by '•'. The spacing between the receivers changes from the bottom to top (4 km, 7 km, and 14 km).

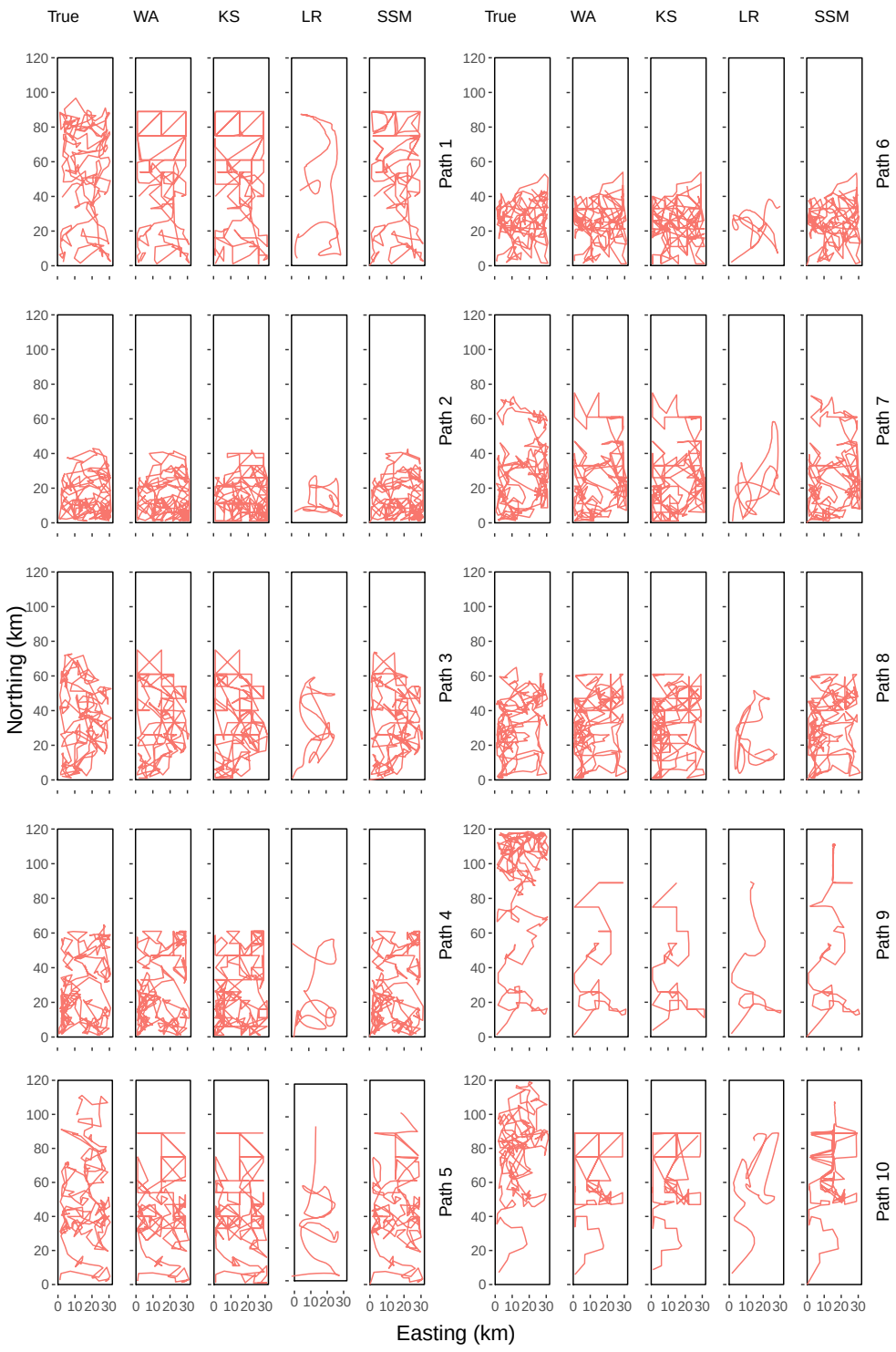

Figure 2.5: The true average path using 3 h time bins (True), reconstructed movement paths with the simple weighted average method (WA), kernel smoothing with the Gaussian kernel (KS), cross-validated local polynomial regression approach (LR), and the state-space modeling approach (SSM) for Simulation 7 (time bin = 3 h and tracking period = 30 d).

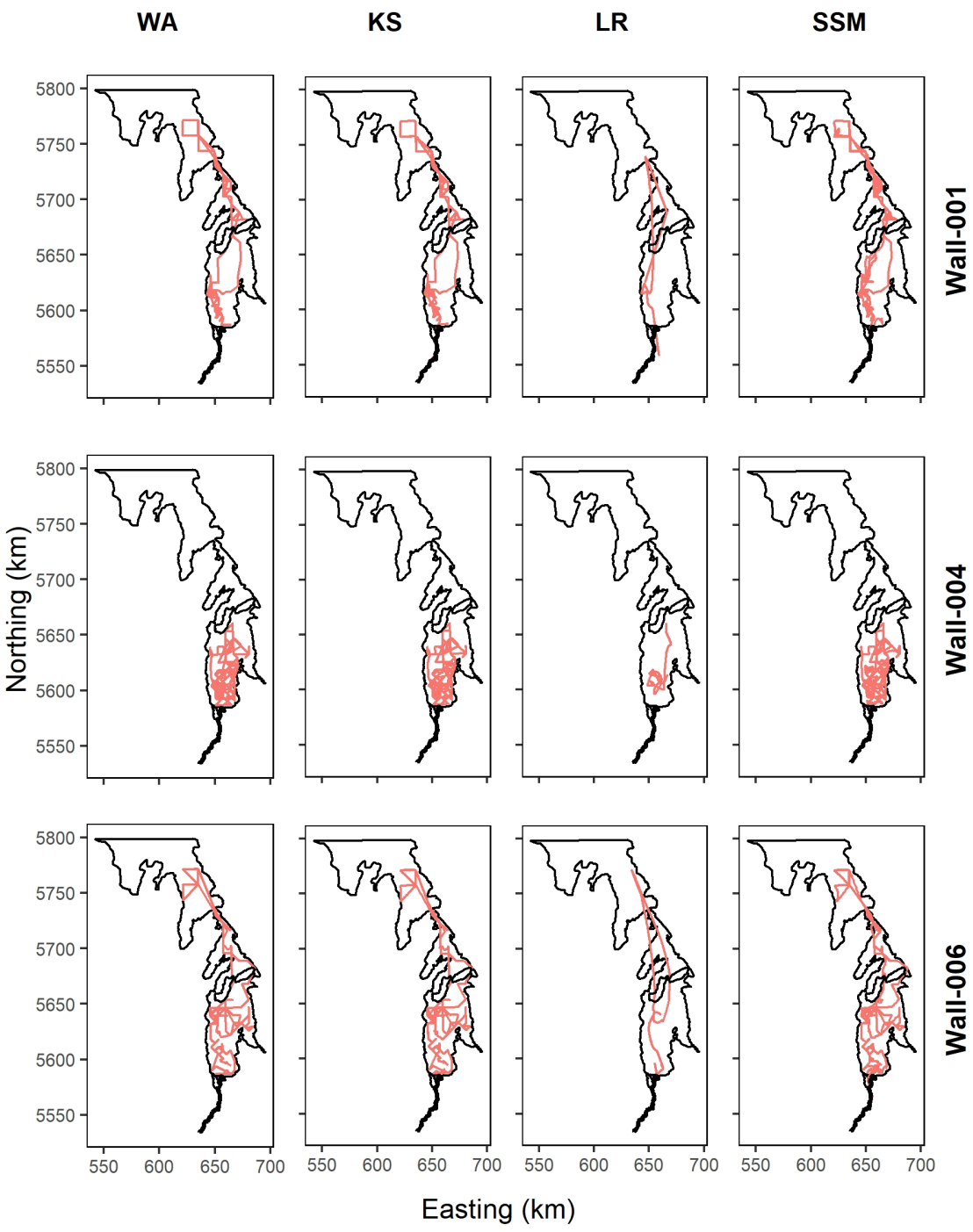

Figure 2.6: Reconstructed movement paths with the simple weighted average method (WA), kernel smoothing with the Gaussian kernel (KS), cross-validated local polynomial regression approach (LR), and the state-space modeling approach (SSM) for the fish "Wall-001", "Wall-004", and "Wall-006". Maps were made using R with ggplot2.

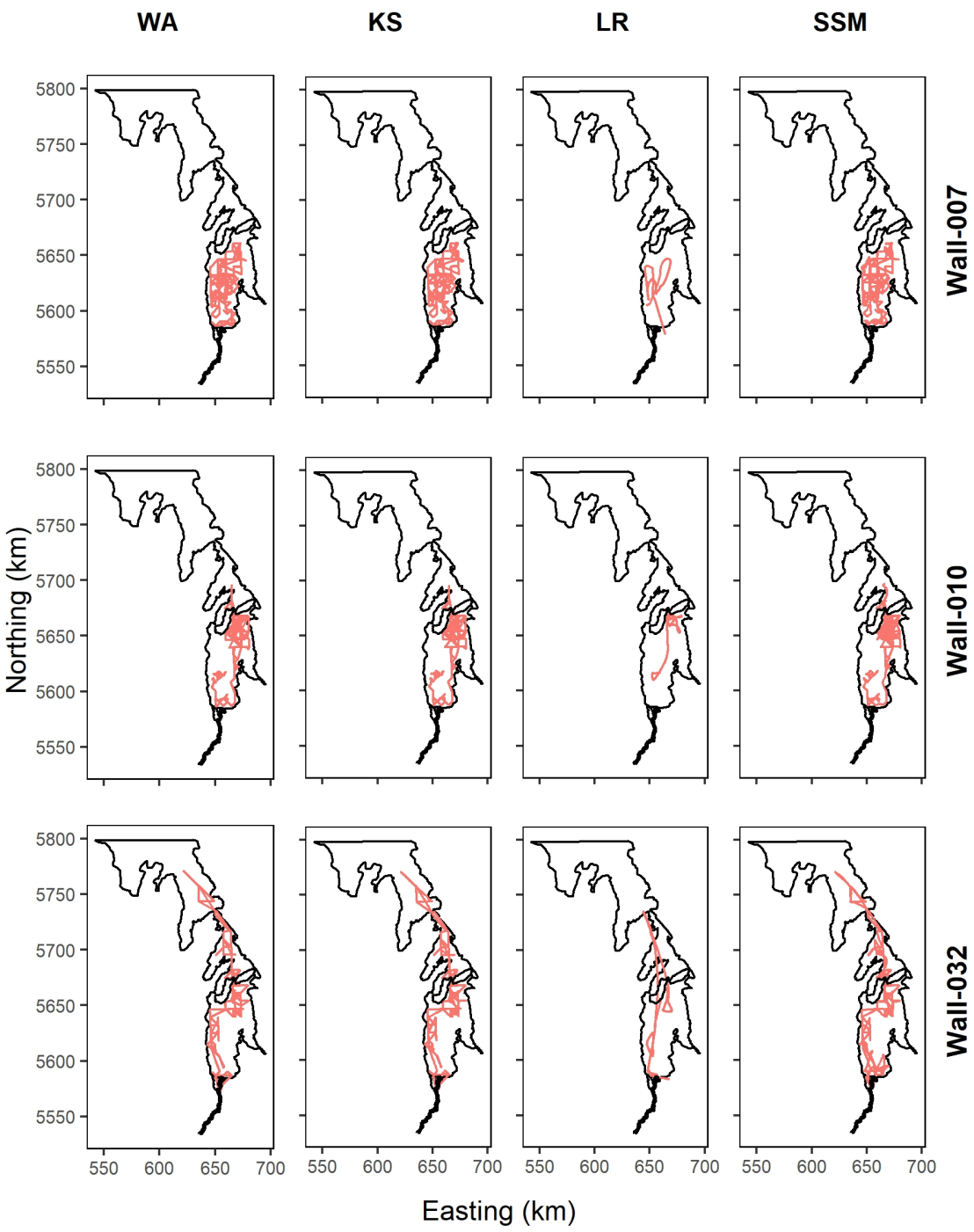

Figure 2.7: Reconstructed movement paths with the simple weighted average method (WA), kernel smoothing with the Gaussian kernel (KS), cross-validated local polynomial regression approach (LR), and the state-space modeling approach (SSM) for the fish "Wall-007", "Wall-010", and "Wall-032". Maps were made using R with ggplot2.

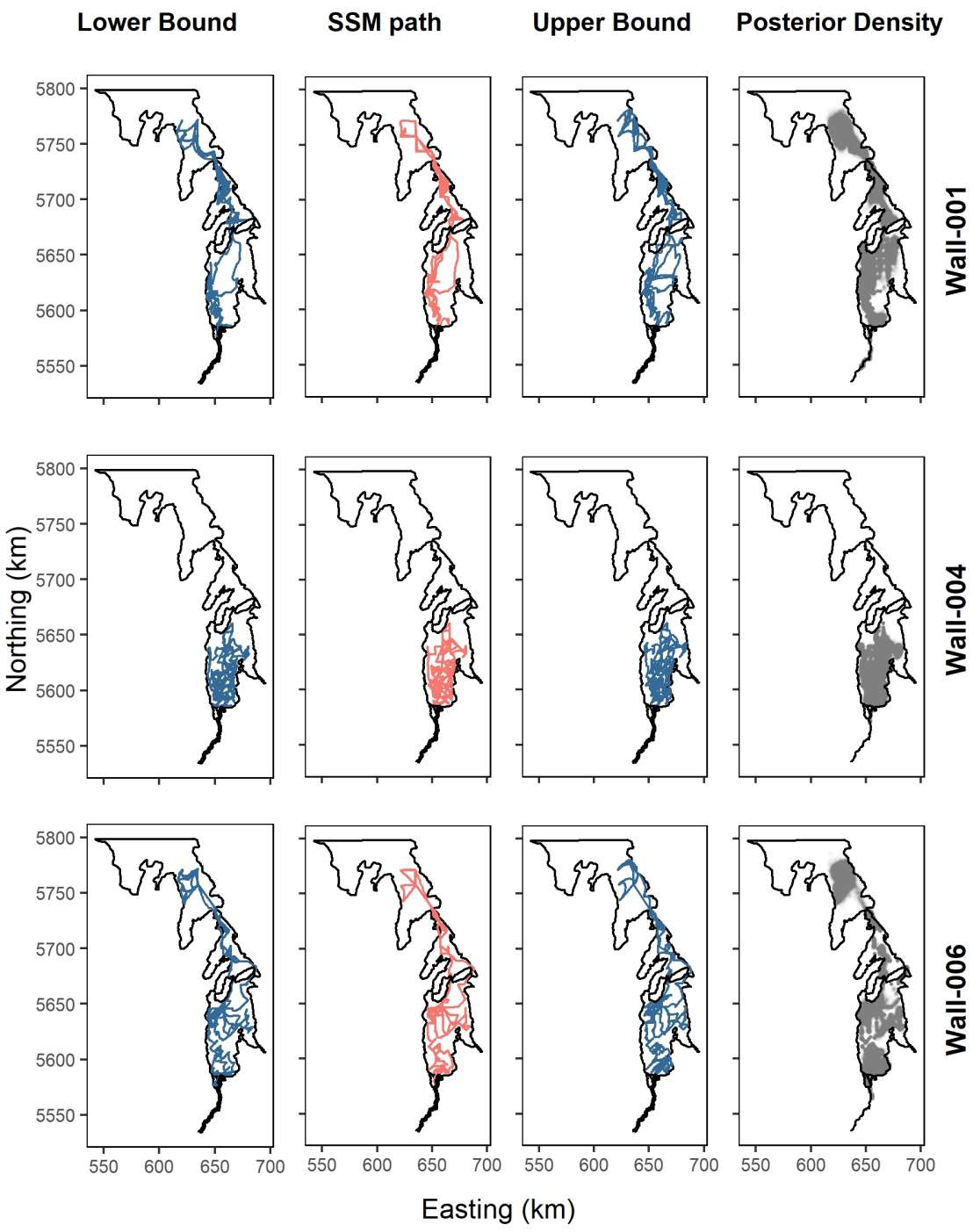

Figure 2.8: 95% credible paths and posterior density plots for the paths reconstructed with the SSM approach for the fish indexed "Wall-001", "Wall-004", and "Wall-006". Map made using R with ggplot2. Maps were made using R with ggplot2.

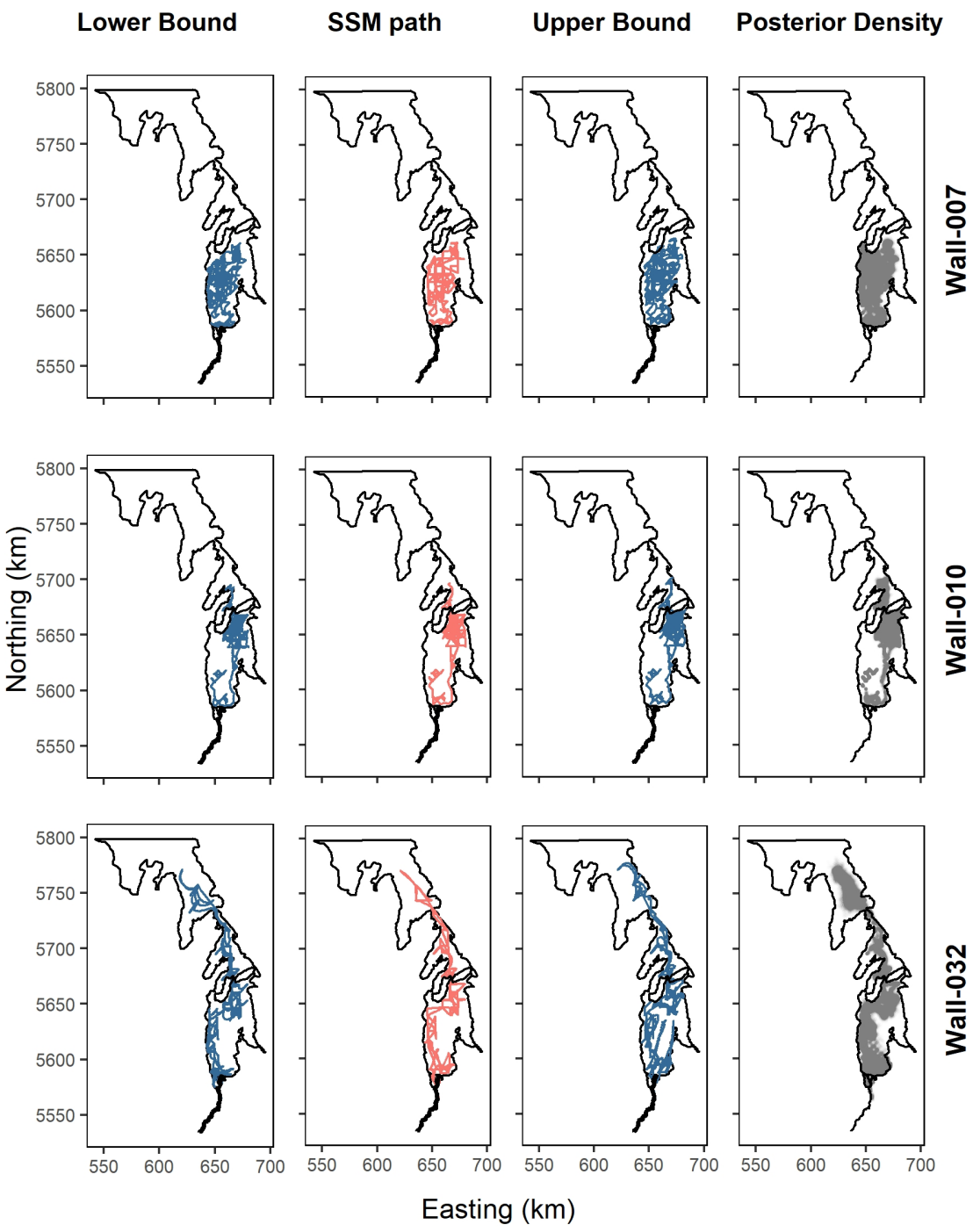

Figure 2.9: 95% credible paths and posterior density plots for the paths reconstructed with the SSM approach for the fish indexed "Wall-007", "Wall-010", and "Wall-032". Maps were made using R with ggplot2.

Chapter 3

Estimating survival probabilities of Cambridge Bay Arctic char using acoustic telemetry data and Bayesian multi-state capture–recapture models

Estimating Survival Probabilities of Cambridge Bay Arctic Char Using Acoustic Telemetry Data and Bayesian Multi-state Capture–recapture Models

Inesh Munaweera[a], Les N. Harris[b], Jean-Sébastien Moore[c], Ross F. Tallman[b],

Aaron T. Fisk[d], Darren M. Gillis[a], Saman Muthukumarana[a]

[a]University of Manitoba,Winnipeg R3T 2N2.

[b]Fisheries and Oceans Canada, Arctic and Aquatic Research Division, Winnipeg, MB, R3T 2N6, Canada.

[c]Institut de Biologie Intégrative et des Systèmes and Département de Biologie, Université Laval, Québec, QC, G1V 0A6, Canada.

[d]Great Lakes Institute of Environmental Research, University of Windsor, Windsor, ON, N9B 3P4, Canada.

This thesis contains the accepted version of the corresponding paper published in Canadian Journal of Fisheries and Aquatic Sciences (Munaweera et al. 2022).

Abstract

Arctic fishes are threatened by climatic change and other anthropogenic stressors, yet information on how such changes impact survival remains scarce. Acoustic telemetry has become valuable for studying aspects of fish ecology, including survival which is invaluable in understanding potential responses to changing conditions. In Cambridge Bay, NU, we have been using acoustic telemetry to study movements and habitat use of the culturally and commercially important Arctic Char (*Salvelinus alpinus*). Here, we combine acoustic telemetry data and Bayesian multi-state mark-recapture models to study the survival of Arctic Char from 2014-2018 in the region in freshwater and marine/estuarine habitats. We found that survival probabilities were high (>0.87), and models considering two environments (freshwater and marine) performed better than those considering three (including estuarine habitats). Furthermore, the survival in freshwater was higher than survival in marine/estuary environments. Overall, the results of this study further our understanding of important demographic parameters (i.e., survival) for Arctic Char in the region which will be useful in refining fishery management plans for the largest commercial fishery for this species in Canada.

Keywords: Acoustic Telemetry, Arctic char, Bayesian Statistics, Mark–recapture models, Survival Ecology.

3.1 Introduction

Climate change in the Canadian Arctic is occurring at some of the fastest rates on Earth (Barber et al. 2008; Pithan and Mauritsen 2014; Prowse et al. 2006). This rapid climate change, coupled with other human-related factors such as increased harvesting and negative impacts from increased shipping activities, poses clear and significant threats to the survival and population persistence of many freshwater and anadromous Arctic fish species (Caza-Allard et al. 2021). Due to a paucity of data and a subsequent poor understanding of the biology and ecology of many Arctic fish species, predicting how those species will respond and adapt to changing climatic conditions and anthropogenic pressures has been challenging (Crossin et al. 2017; Reist et al. 2006). Some climate change effects noted for Arctic anadromous fishes include, among other things, changes in trophic positioning and diet (Ulrich and Tallman 2021), declines in fish condition (Lehnherr et al. 2018), impacts to early-year growth, and life history variation (Grenier and Tallman 2021), shifting geographic ranges and potentially local extinctions (Reist et al. 2006). Few studies to date, however, have assessed changes in survivorship and mortality in anadromous fishes relating to climate change in the Canadian North. All told, the impacts of Arctic climate change on anadromous fishes remain enigmatic and future studies at high latitudes will be important for understanding the potential and realized impacts on this important group of fishes.

Recent advances in animal tracking technologies such as acoustic telemetry, have enabled researchers to collect enormous amounts of data on animal movement and habitat use over large geographic scales (Donaldson et al. 2014; Hussey et al. 2015; Klimley et al. 1998) significantly increasing the overall understanding of the ecology and biology of high-latitude

fish species (Hussey et al. 2017, 2015; Peklova et al. 2012). For example, data from acoustic telemetry have primarily been used for studying spatiotemporal aspects of animal movements in both marine and freshwater environments (Heupel and Simpfendorfer 2002; Lees et al. 2021; McMichael et al. 2010). More recently, acoustic telemetry data have been used to estimate demographic parameters such as survival probability and population size, with comparable or better precision than conventional capture-mark-recapture studies (Dudgeon et al. 2015; Lees et al. 2021; Pollock et al. 2004). Estimating survival using acoustic data has become particularly important for understanding how fishing and natural mortality impact population persistence (Crossin et al. 2017; Lees et al. 2021).

Incorporating acoustic telemetry data, the most popular approach for estimating survival probabilities has been the use of the Cormack-Jolly-Seber (CJS) model (Cormack 1964; Jolly 1965; Seber 1965). However, when there are few detection records from certain sites, the estimated survival probabilities with CJS models suffer from low precision due to low recapture rates (Morris et al. 2006; O'Brien et al. 2005; Pollock et al. 1990). As such, using CJS models, it is often not possible to obtain stable estimates for individual survival probabilities for all sites and/or environments. In this context, multi-state mark-recapture models can be used to deal with sparseness in data by borrowing information across regions (Calvert et al. 2009). Early applications of multi-state mark-recapture models can be found in Arnason (1972), Hestbeck et al. (1991), and Brownie et al. (1993). Parameter estimation of the multi-state mark-recapture models can be done using either the frequentist or Bayesian framework. The Bayesian framework has been gaining popularity for a variety of reasons including its extreme flexibility, greater precision, and ability to incorporate prior knowledge

about parameters (Calvert et al. 2009; Harwood and Stokes 2003; Kéry and Schaub 2011). Through simulation studies and real world applications, Calvert et al. (2009) showed that using a hierarchical Bayesian approach to multi-state mark-recapture, one can obtain more precise and accurate parameter estimates than non-hierarchical approach. Thus, hierarchical Bayesian approaches using acoustic telemetry data and mark-recapture methods hold promise for estimating demographic parameters using non-conventional methods.

The objective of this study was to use the multi-year acoustic telemetry data set that has been generated for Arctic Char (*Salvelinus alpinus*) in the Cambridge Bay region of Nunavut to estimate survival probabilities of this culturally and commercially important species. Here, we have been using acoustic telemetry since 2013 to further our understanding of movements and freshwater and marine habitat use of Arctic char in the region (Harris et al. 2020a; Moore et al. 2016). The region is home to the largest commercial fishery for this species in Canada yet there is still a paucity of information on many demographic parameters highlighting the need to employ non-conventional methods for parameter estimation. Previously, Caza-Allard et al. (2021) employed conventional CJS methodology to estimate survival and encounter probabilities for Arctic char in the region. However, due to low recapture rates in freshwater and estuary environments, CJS models are not ideal to estimate survival probabilities of Arctic char in those environments. Furthermore, Caza-Allard et al. (2021) estimated survival solely in the marine environment despite the fact the Arctic char in the region spend more than 10 months of the year in freshwater. Hence, in this study, we used more flexible hierarchical Bayesian multi-state mark-recapture models to estimate survival probabilities over multiple years (2014–2018) in marine/estuarine and freshwater environments for Arctic

Char tagged specifically in the Ekalluk River/Ferguson Lake system where much of our acoustic telemetry efforts have been focused.

3.2 Materials and methods

3.2.1 Study area and fishery information

The study takes place on southern Victoria Island in the Cambridge Bay region of Nunavut (Figure 3.1). Our acoustic telemetry array in the area consists of stations that cover marine (Wellington Bay and adjacent coastal areas), estuary (Lauchlan, Halokvik, Surrey and Ekalluk river estuaries), and freshwater (Ferguson Lake) environments. Detailed descriptions of the acoustic array and station information can be found in Moore et al. (2016) and Harris et al. (2020a). Commercial fishing for Arctic Char in the Cambridge Bay region started in 1960, and as mentioned above, the region now accounts for the largest commercial fishery for Arctic Char in Canada (Harris et al. 2020a). Presently, five waterbodies are actively fished with a combined available annual quota of 56,100 kgs (Harris et al. 2020b). The Ekalluk River commercial fishery, which now takes place in Ferguson Lake targeting Arctic Char after they have returned to freshwater from summer foraging, is the largest in the region with a 20,000 kg quota (DFO 2014).

3.2.2 Experimental setup and data

This study is based on a sample of 188 Arctic Char acoustically tagged (VEMCO V16 transmitters) between 2014–2018 focusing on those from, or presumed to be from, the Ekalluk

River/Ferguson Lake system (Table 3.1). Over the years, acoustic data have been collected using 99 receivers (VEMCO VR2W) including estuary and marine stations in the region and freshwater stations in Ferguson Lake (Figure 3.1). Some receivers were re-positioned during the study. Hence, we incorporated acoustic detections from 30 receivers which were fixed or moved slightly (less than the detection range of the acoustic tags (Moore et al. 2016)) and continuously in operation between 2014–2018. Additional information on the tagging process and the experimental setup can be found in Moore et al. (2016) and Harris et al. (2020a). For each year of study, our acoustic tagging procedure was approved by the Fisheries and Oceans Canada (DFO) Animal Care Committee and the procedure conforms to all animal care laws in Canada (permit no. FWI-ACC-2013-2019). Licenses to Fish for Scientific Purposes (LFSP) were also approved annually by DFO.

3.2.3 Multi-state Capture–recapture models

The models we present in this paper are based on the multi-state capture-recapture with Bayesian framework using state-space formulation presented in Kéry and Schaub (2011). State-space models are a type of hierarchical models that are increasingly used to model complex ecological data observed with error (Auger-Méthé et al. 2021; King 2012). Using a state-space formulation for capture-recapture data, we can specify the model as two separate sub-models (levels) for the demographic process and the observation process (Gimenez et al. 2007; King 2012). This can be generally expressed as

$$x_t = f(x_{t-1}), \tag{3.1}$$

$$y_t = g(x_t, \epsilon_t), \tag{3.2}$$

where x_t denotes the true state (e.g., alive or dead), and y_t denotes the observed state (e.g., observed or not observed). Here, $f(.)$ and $g(.)$ represent the process model and the observation model, respectively. The process model describes the true state, and the observation model maps the true state to the observed state. The parameter ϵ_t is the observation error.

The process model

Consider a mark-recapture setting where n number of fish were captured and observed in T number of recapture occurrences. Let $x_{i,t}$ denotes the true state of the i^{th} fish at time t, and $y_{i,t}$ denotes the observed state. Let x_{i,e_i} to be the true state of the i^{th} fish at the first capture occurs at time e_i that is observed without error. Then, conditioning on the known first capture, the process model (state equation) can be written as

$$x_{i,t+1} \mid x_{i,t} \sim multinomial(1, \Omega_{x_{i,t},1\ldots K}) \qquad , i = 1 \ldots n, \text{and} \quad t \geq e_i \tag{3.3}$$

where K is the total number of true states and $\Omega_{x_{i,t},1\ldots K}$ is a vector of length K, where the elements are the transition probabilities of a fish given it's true state at time t (i.e., $x_{i,t}$). Given the capture occasion and state, we assume that the survival/transition probabilities ($\Omega_{x_{i,t},1\ldots K}$) to be independent of the fish.

First, consider a state-space process with two environments (M-Marine/Estuary, F-Freshwater). Let ϕ_M and ϕ_F be environment-specific survival probabilities for the marine-estuary envi-

ronment and freshwater environment respectively. Let ψ_{MF} and ψ_{FM} denote movement probabilities between each environment. Then, the process can be represented by a 3×3 matrix, which is usually referred to as the transition matrix (Table 3.2). Note that the rows of the transition matrix are $\Omega_{x_{i,t},1\ldots K}$ in Equation 4.7. In this formulation, as used in Kéry and Schaub (2011) we assume that a fish is alive in the environment at time t and then moves to the next environment between t and $t+1$. That is, transitions among states are instantaneous and hence, there is no mortality while moving between environments.

Consider a state-space process with three environments (M-Marine, E-Estuary, F-Freshwater). Now, the list of states at a given time point is "alive in the Marine environment", "alive in the Estuary environment", "alive in the Freshwater environment", and "dead". Similarly to the previous case, the process can be represented by a 4×4 transition matrix (Table 3.3).

Observation model

The second component of the model is the observation model given by

$$y_{i,t} \mid x_{i,t} \sim multinomial(1, \Theta_{x_{i,t},1\ldots K}) \qquad , i = 1 \ldots n, \text{and} \quad t \geq e_i \tag{3.4}$$

where $\Theta_{x_{i,t},1\ldots K}$ is also a vector of length K, where the elements are the observation probabilities of a fish at each state given it's state at time t (i.e., $x_{i,t}$). Here as well, we assume, given the capture occasion and state, observation probabilities ($\Theta_{x_{i,t},1\ldots K}$) to be independent of the fish.

Again, consider a process model with two environments; M and F. Let $p_{s,t}$ be the probability of observing a tagged fish that is alive in environment s at time t. Here, we assume that

a fish in environment s can only be observed in environment s, but cannot be observed in another environment. Thus the observation process is conditional on the state process and the first capture and this can be represented by a 3×3 matrix (Table 3.4). The rows of this matrix are $\Theta_{x_{i,t},1...K}$ in Equation 3.4. Similarly, the observation matrix for a state-space process with three environments can be written as in Table 3.5.

We further assume that the fish are independent of each other, the fish and states are recorded without error, and no tags are lost. The posterior distribution can be written as

$$P(\boldsymbol{\phi}, \boldsymbol{\psi}, \boldsymbol{p} \mid \boldsymbol{y}) = f(\boldsymbol{y} \mid \boldsymbol{x}, \boldsymbol{p}) \times f(\boldsymbol{x} \mid \boldsymbol{\phi}, \boldsymbol{\psi}) \times f(\boldsymbol{\phi}, \boldsymbol{\psi}, \boldsymbol{p}). \tag{3.5}$$

Here, $\boldsymbol{\phi}, \boldsymbol{\psi}, \boldsymbol{p}$ are the vector of environment-specific survival probabilities, the vector of transition probabilities, and the vector of observation probabilities respectively. For all the models, since all the parameters are probabilities with the support [0,1], $Beta(\alpha, \beta)$ distribution was used as the prior for all parameters. In the model estimation, we used $\alpha = 1$ and $\beta = 1$ so that the priors were non-informative uniform for all parameters.

Data preparation

Since the transmission of an acoustic ping from an individual fish to receiver takes just a few milliseconds, each detection can be considered as an instantaneous sampling point. There were millions of such detection records in our data set. If we consider the time point of each detection to be a sampling point, only one fish will be detected at each point. This will result in the detection matrix (the matrix with detection records in which each row represents a fish and columns are sampling points) having a large number of entries with the unobserved

state which is usually represented by zeroth state. To avoid that, we pooled the detection record over time bins and the initial date of the bin is considered as the sampling point. If the fish was detected at least once during a certain time interval, we recorded the state of the fish corresponding to the environment in which the fish was observed. When the fish was detected in multiple environments, the state in which the fish stayed the longest was assigned.

The area is subjected to a long winter where detection probabilities are lower due to inactivity on freshwater (Mulder et al. 2018). This sparseness caused non-convergence issues in our initial models and therefore we pooled the detection records over time intervals under three different scenarios. We used binning intervals with unequal lengths to avoid the effect of overwintering (Table 3.6). For Scenario 1, the detection records were binned into two time intervals for each year: June-September and October-May. June to September would be representative of times when Arctic Char would be migrating between freshwater and marine environments and when they would be foraging in marine environments (Moore et al. 2016). October to May, Arctic Char in the region would be overwintering. In Scenario 2, detection records were binned into three periods annually: June-September, October-December, and January-May. The interval October-December would capture the spawning and post-spawning period of Arctic Char in the region. In Scenario 3, annual detections were binned into six Periods as June, July, Aug, September, October-December, and Jan-May.

3.2.4 Model estimation and evaluation

The models were fitted using the Bayesian MCMC approach with 'JAGS' (Plummer et al. 2003) in R using the package 'R2jags' (Su and Yajima 2015). The models were run on Compute Canada, Graham cluster that mostly used 2×Intel E5-2683 v4 Broadwell @ 2.1GHz processors with 32 cores in each node. Three parallel chains were run for each model. Thinning is a common practice done to reduce autocorrelation in the MCMC sequence by selecting each k^{th} iteration and discarding the rest. However, thinning is considered to be very inefficient and unnecessary by many researchers (Geyer 1992; Link and Eaton 2012; Maceachern and Berliner 1994). Hence we performed thinning minimally with $k = 5$ for each model. For each model, the number of MCMC iterations and burn-in (the number of iteration to ignore in the beginning of the chain) were decided based on the number of steps needed for all parameters of the model to converge. The exact number of MCMC iterations and burn-in have been mentioned in the model summary table of each model (Table 8 and Table S1 to S5). To assess the convergence, in addition to inspecting trace plots and posterior densities, Gelman-Rubin statistics (Gelman and Rubin 1992) and Effective Sample Size (ESS) suggested by Kass et al. (1998) were used.

The Gelman-Rubin statistics that is usually denoted by $\hat{R}$ is widely used to determine whether the MCMC chain has achieved convergence. Calculation of $\hat{R}$ requires multiple MCMC chains (usually 3 to 5). Then, $\hat{R}$ for a parameter of interest is the variance of the parameter calculated using all the MCMC chains combined, divided by the average of the variances within each chain (Kass et al. 1998). A converged series should result in a $\hat{R} \approx 1$.

ESS is calculated as

$$\text{ESS} = \frac{B}{1 + 2\sum_{k=1}^{\infty} \rho_k}, \tag{3.6}$$

where B is the length of the MCMC chain after burn-in and ρ_k is the autocorrelation of the sequence at lag k. In practice, the infinite sum in the formula is cutoff at a finite k when the ρ_k is sufficiently small ($\rho_k < 0.05$) (Kruschke 2014). ESS can be used to measure the amount of independent information in MCMC chain.

To evaluate how well each model fits the data, posterior predictive checks were performed (Gelman et al. 2013; King 2012). First, we drew a sample of 1500 parameter vectors from the joint posterior distribution (obtained from the converged MCMC chains) along with the unobserved states corresponding to each parameter vector (Equation 4.7). Then, we predicted a dataset using each sampled set of values and compared the predicted data with the observed data. In our case, since the predicted values are categorical, instead of calculating the Bayesian p-value, we explored the probability of accurately predicting the observed state of a fish in different environments of the study area.

Model identifiability was accessed by inspecting Bayesian MCMC outputs (posterior density and trace plots) and pairwise correlations between the model parameters obtained using MCMC chains. A posterior density that is not unimodal and extends over a large fraction of the parameter space, and the trace plot with multiple chains that do not converge/mix indicate non-identifiable models (Siekmann et al. 2012; Simpson et al. 2020). Furthermore, nonidentifiable models also result in strong correlations between model parameters (Gimenez et al. 2009; Hines et al. 2014).

3.2.5 Model selection

In this study, the fitted models were compared using the deviance information criterion (DIC) proposed by Spiegelhalter et al. (2002) that measures both the fit and the complexity of a model and DIC is described as the predictive measure of choice in Bayesian model selection (Gelman et al. 2013). DIC can be written as

$$DIC = D(\bar{\theta}) + 2p_D, \tag{3.7}$$

where $\bar{\theta}$ is the posterior mean and p_D is the effective number of parameters given by

$$p_D = \overline{D(\theta)} - D(\bar{\theta}), \tag{3.8}$$

where

$$D(\theta) = -2\log p(y|\hat{\theta}) + 2logf(y). \tag{3.9}$$

Here, $f(y)$ is the standardizing term that is a function of data (Spiegelhalter et al. 2002). DIC is "a somewhat Bayesian version" of the well-known Akaike information criterion (AIC) which measures both the model fit and the complexity (Gelman et al. 2013, 2014). In this work, we used a version of DIC that uses an alternative formulation to p_D suggested by Gelman et al. (2004) which is given below.

$$p_V = Var(D(\theta))/2. \tag{3.10}$$

A model with lower DIC is preferred over a model with larger DIC. One of the reasons for the popularity of DIC is the computational convenience since it has been incorporated into the Bayesian programming languages such as `'BUGS'` and `'JAGS'` (Plummer et al. 2003; Spiegelhalter et al. 2003).

3.3 Results

There were 2.34 million records of detection of the selected 188 fish from 2014-07-01 to 2018-07-01 by 30 receivers. The majority of the detections were recorded by the receivers in freshwater (1.76 million). The receivers in the estuary environment recorded 1.52 million detections and the receivers in the marine environment only recorded 0.42 million detections. Among the 188 selected fish, 158 fish were detected at least once after the initial release.

For all models, the trace plots showed a good mixing and the Gelman-Rubin statistics was very close to 1 for all the parameter estimates ($\hat{R} < 1.01$). Also, the posterior distributions were unimodal and the bivariate correlation among most parameters was weak with a few pairs having moderately strong correlations indicating no convergence or identifiability issues. Effective sample size estimates were large for all parameters showing that the MCMC chains contain a sufficient amount of independent information. The posterior predictive check shows all models satisfactory fit to observed data where the model fitted with three environments under binning scenario 3 showed the best fit (Table 3.7). Parameter estimates of all models had small standard errors. All the models and convergence evaluation results can be found in the supplementary material (Figures 2, 3, S1 to S10, and Tables 9, 10 and S1 to S10). The model with two environments under scenario 1 showed the minimum DIC value while the model with three environments under Scenario 3 resulted in the highest DIC (Table 3.8). Hence for making conclusions, we used the model that resulted in the lowest DIC.

The survival probability in the freshwater (0.95 ± 0.02) was higher than the survival probability in the marine and estuary environments (0.87 ± 0.02). The recapture probability was also higher in the freshwater environment than in the marine and estuary environments

(Table 3.9). The standard errors of all parameter estimates were small. Furthermore, we observed a difference between the freshwater to marine and marine to freshwater transition probabilities.

3.4 Discussion

Acoustic telemetry is a powerful tool in fisheries research for studying movement and habitat use (Donaldson et al. 2014; Kraus et al. 2018). More recently acoustic data have been used in novel ways for estimating and inferring demographic parameters such as survival and population size (Crossin et al. 2017; Donaldson et al. 2014; Lees et al. 2021). In this study, we estimated the survival and recapture probabilities of Arctic Char in marine-estuary and freshwater environments using Bayesian multi-state mark-recapture models and acoustic telemetry data. We found that the survival probability was generally high (> 0.87) and survival estimates were typically higher in the freshwater compared to that estimated for marine and estuary environments. We also found that the recapture probability was higher in the freshwater compared to marine and estuary environments. To our knowledge, this is the first time a Bayesian multi-state capture-recapture framework has been used to estimate the survival of an Arctic anadromous salmonid. The results of the study further our understanding of survival in Arctic Char from Canada's largest commercial fishery for this species, the results of which may inform fisheries management in the region. The Cambridge Bay commercial fishery is the largest in Canada, employing dozens of Nunavummiut annually (DFO 2014) and having information on annual survival will be valuable in understanding the viability of these populations and potential responses to warming Arctic conditions.

Demographic parameter estimation using hierarchical Bayesian models is becoming more common and has now been used across a variety of taxa (Clark 2005). For example, Calvert et al. (2009) applied a hierarchical Bayesian multi-state mark-recapture model with three states to estimate daily transience and departure of migratory birds. They found that the parameter estimation can be improved by using the hierarchical Bayesian approach compared to frequentist non-hierarchical models. Wu and Holan (2017) also used a Bayesian hierarchical multi-population multi-state Jolly–Seber model to estimate the abundance of Pallid Sturgeon (*Scaphirhynchus albus*) in the Lower Missouri River. These authors also incorporated covariates (sampling efforts for different gear types) to further improve the model in terms of reducing computational burden and precision. These studies highlight that the Bayesian framework when combined with acoustic telemetry data can be an effective method for estimating demographic parameters when traditional methods/data are not available.

Similar to our study, Jensen et al. (2019) also presented evidence for higher annual mortality rates for the Arctic Char in the marine environment (Arctic region of Norway) than in freshwater for fish that were captured using permanent fish traps during the ice-free period between 1987-2012. These authors suspected that mortality was higher in the marine environment due to osmoregulation difficulties in the salt water and higher number of predators in the marine habitats. Recently, Caza-Allard et al. (2021), also using a CJS framework, estimated high annual survival probabilities (varying between 0.79 and 0.88) for Cambridge Bay Arctic Char in the marine environment, with recapture probabilities varying between 0.64 and 0.90. However, the standard errors of survival estimates in our study were much lower than those reported in Caza-Allard et al. (2021) which were estimated using ordinary

CJS models. The lower error resolved in this study is likely because the Bayesian multi-state mark-recapture models borrow information through all environments to estimate the parameters, highlighting the utility of the Bayesian framework used here. Finally, recent stock assessments completed on stocks of commercially harvested Arctic char in the region also suggest that overall natural mortality is low with values between 0.15 and 0.18 (Zhu et al. 2021). However, these authors estimated mortality for every age class while in this study, we only considered adult Arctic char in parameter estimation. Including all age classes would likely inflate mortality estimates as younger age classes (e.g., juvenile) would be expected to have much higher mortality. Therefore mortality for adults alone should be even lower than what Zhu et al. (2021) reported in their assessment. Thus our results corroborate previous findings for Arctic char in that survival is generally high in this species once they are adults.

Adult Arctic Char in the study area inhabit freshwater during the long winter (September to June/July) and migrate to forage in the marine environment in late June or early July before returning to freshwater in August or September for spawning and/or overwintering purposes (Harris et al. 2020a; Moore et al. 2016). High survival in both environments is not surprising, given that Arctic Char are a top predator with few competitors. During the winter months while in freshwater, the survival probability is likely higher since there are fewer risks of mortality compared to the marine environment. For example, there are likely no predators for adult Arctic Char in the freshwater environment, and most fisheries (subsistence and commercial) are executed in marine and estuarine habitats (Day and Harris 2013). The activity level of Arctic char is also greatly reduced when overwintering in freshwater (Mulder et al. 2018) possibly reducing their chances of encountering potential threats to survival. In

the marine environment, the mortality can be expected to be higher due to these fishing activities and possibly due to predators such as seals which are known to predate on Char in other regions (Jensen et al. 2019; Moore 1975). The difference in the detection probability between the two environments can be accounted for by the difference in the receiver cover. In freshwater, there is a higher probability that the receiver would detect a fish than in the marine and estuary environments. One reason for the higher detection probability in freshwater is that the river funnels the fish that migrate to estuary and marine environments. Also, once there is ice on the lake surface, the detection range of the tags improves resulting in a higher probability of detection (Moore et al. 2016; Munaweera et al. 2021).

The model we developed in this study is directly applicable for analyzing acoustic telemetry data from other studies incorporating a fixed array of receivers and where the study species is monitored in multiple habitats (i.e., anadromous and catadromous fishes) for which survival estimates are wanted. However, for long-term studies (>5 years) it is possible that the acoustic array may not be static throughout the study period due to a variety of reasons (e.g., lost receivers, changed objectives, etc.). In these cases, we recommend the reader maintain an approximately fixed receiver array throughout the duration of the study in order to improve parameter estimates. In our study, we filtered the data set by removing some receivers and some fish tagged before 2014 so that the receiver array was fixed throughout the study period. Even though we had to remove a significant amount of data, this allowed us to assume that the detection probabilities for each environment were fixed over time allowing us to use a simpler model with lower number of parameters. Using a simpler model allowed us to avoid issues such as non-convergence and large computational burden. All the models we

attempted in this study were completed in less than 2 hours except for the model with three environments under Scenario 3 which required about 4 hours to complete. Further, users of this model must take into consideration varying detection probability among environments. A reference tag experiment conducted in different environments under different conditions (e.g., ice on/off) would be ideal in this situation to support the constant detection probabilities assumption over time (Munaweera et al. 2021). However, such data do not exist for the study region at this point. As a consequence of model violation due to temporal varying detection probabilities, we can expect the estimated parameter to be biased and hence, less accurate. Another alternative is to account for the annual changes in the receiver array by adding temporally varying detection probabilities to the model. Even though this would allow us to use all the detection records from all receivers, this will significantly increase the number of parameters in the model and the computational burden that can result in non-convergence. However, as more data become available, this will be a natural extension of the model presented here. The framework we used in this study can be easily generalized for a larger number of states. Even though we did not use the three-environment model (Model 2) to draw conclusions, the model still converged and the standard errors of the parameter estimates under all three binning scenarios were also satisfactory for obtaining separate estimates of survival for marine, estuary and freshwater environments.

Acoustic telemetry data are more commonly being incorporated into fishery and habitat management decision-making processes (Crossin et al. 2017; Lees et al. 2021), for example in determining protected areas to preserve critical fish habitats (Goodchild 2004; Halpern 2003; Lea et al. 2016) and fisheries stock assessments aimed at resolving sustainable removal levels

(Cooke et al. 2016; Kneebone et al. 2014; Tim et al. 2015). Acoustic telemetry results in higher recapture rates than conventional capture-mark-recapture studies and therefore the analysis of acoustic telemetry data often results in more precise estimates of demographic parameters including survival, mortality, and abundance compared to conventional capture-mark-recapture studies (Dudgeon et al. 2015; Kraus et al. 2018; Pollock et al. 2004). Hence, the management decisions based on acoustic telemetry information can be developed with less uncertainty (Lees et al. 2021). Our data have provided a multi-year perspective on the annual survival of adult Arctic Char highlighting differences among environments (freshwater vs. estuary/marine). It is not clear what mortality rates would be detrimental to Arctic char population persistence in the region but Johnson (1980) suggested that an 11% harvest rate would be excessive. This would suggest that our estimates of survival leave the possibility that the mortality rate is above the level considered safe which might be concerning from a fisheries management perspective. However, our estimates are for annual survival which would include other mortality-related factors such as predation and senescence. Furthermore, others have estimated mortality rates (Harris et al. 2021) and exploitation rates (Day and Harris 2013) in excess of 11% for fisheries in the region that have still been deemed sustainable. As mentioned above, it is unclear as to what harvest rates would be considered detrimental to stock health, and further work is required in order to shed light on this important knowledge gap in the region and for Arctic char in general. Overall, the relatively high survival rate for adult Arctic Char for all the environments in the region, combined with recent assessments that have suggested at least some stocks are considered healthy (Day and Harris 2013; Harris et al. 2021; Zhu et al. 2021), suggests that the contemporary fishery management strategies in the region are likely effective.

In this study, we used acoustic telemetry data to estimate the survival and recapture probabilities of adult Arctic Char in different environments. The parameter estimates in this study generated using Bayesian multi-state mark-recapture models were more precise than those reported in previous studies in the region using the traditional CJS models. The models we used did not suffer from convergence issues and convergence was achieved quickly. Hence, Bayesian multi-state mark-recapture models incorporating acoustic telemetry data can be recommended as a suitable alternative for estimating demographic parameters such as survival compared to the conventional CJS models. Anadromous fishes that migrate between marine and freshwater environments throughout their lives are common across the Canadian Arctic. These fishes, including the Arctic char studied here but also Dolly Varden Char *(S. malma malma)*, anadromous lake trout *(S. namaycush)*, and multiple whitefishes and ciscoes *(Coregonus spp.)*, all share a relatively similar life history in that they forage in marine habitats in the summer before migrating back to freshwater to spawn and/or overwinter. This group of fishes is also highly sought after in subsistence and commercial fisheries throughout the Canadian Arctic where they are important for local economies, food security, health, and maintaining traditional cultures (e.g., Government of Nunavut (2016)). The results of our study are relevant for future telemetry projects on Arctic anadromous fishes and the Bayesian multi-state capture-recapture models we employed here could inform survival and mortality in other regions on other important species with similar life histories. Furthermore, there are currently multiple projects across the Canadian Arctic that are using, or have recently used, acoustic telemetry for inferring spatiotemporal aspects of migrations and habitat use in anadromous Arctic char (Hammer et al. 2022; Hollins et al. 2022; Smith 2020). Therefore our results are widely applicable to these other studies that have already generated

acoustic telemetry data for anadromous Arctic char and the model proposed here may prove valuable for shedding additional light on the mortality and survival of this species which will be useful in developing future fishery conservation and management plans effectively. This will be valuable in ensuring the long-term sustainability of this culturally and commercially important resource to Inuit across the Canadian Arctic.

3.5 Acknowledgment

We would first like to thank the Ekaluktutiak Hunters and Trappers Organization for their ongoing support for our acoustic telemetry program in the region. Koana! We thank all Elakututiakmiut who provided support while in the field over the years including M. Omilgoetok, R. and M. Ekpakohak, J. Haniliak, D. Kanayok, K. Kanayok, C. Amegainik, R. Emingak, B. Mala, R. Klengenberg, E. Maniyogina, B. Klengenberg, T. Ekpakohak, D. Oniak, C. Evalik, J. Panioyak, G. Angohiatok, R. Angohiatok, A. Maksagak, B. Vandenbrink and S. Marriott. Field support was also provided by B. Malley, M. Gilbert and M. Falardeau. Logistical support was provided by Dal Aviation (Fred Hamilton), the Polar Continental Shelf Project and the Arctic Research Foundation crew of the RV 'Martin Bergmann'. Accommodations were provided by Polar Knowledge Canada. We thank the associate editor and X anonymous reviewers for comments that greatly improved the manuscript.

Competing Interests Statement

The authors declare there are no competing interests.

Data Availability Statement

Data generated or analyzed during this study are available from the corresponding author

upon reasonable request.

Funding Information Statement

This work was funded by the Ocean Tracking Network, Fisheries and Oceans Canada (Nunavut Implementation Funds), the Nunavut Wildlife Management Board, Polar Knowledge Canada and the Marine Environmental Observation Prediction, Response Network and Arctic Net. Dr. Gillis and Dr. Muthukumarana have been partially supported by discovery grants from the Natural Sciences and Engineering Research Council of Canada.

Table 3.1: Tagging information for acoustically tagged Arctic Char used in this study. Shown are the tagging location (and location code), coordinates for the tagging location, dates of tagging, sample sizes and length and weight information.

Location/Fishery	Lat	Lon	Year	Number Tagged	Dates	Length (mm) (mean ± sd)	Weight (g) (mean ± sd)
Ekalluk River (EKA)	69.406836°	-106.316685°	2013	30	July 10-12	717 ± 57	4013 ± 1065
			2014	30	July 11-12	670 ± 85	3192 ± 1183
			2015	75	July 9-11	729 ± 83	4103 ± 1212
Spawning Lake (SPW)	69.363741°	-105.045023°	2016	23	August 14-15	761 ± 62	4601 ± 1056
Wishbone Lake (WIS)	69.555709°	-104.178389°	2016	19	August 20-21	734 ± 66	4247 ± 8330
Roberts Bay (ROB)	69.366612°	-104.976021°	2016	21	August 25-26	783 ± 68	5319 ± 1467
Ferguson Lake (FER)	69.461544°	-106.107964°	2017	6	August 13-14	784 ± 81	5450 ± 2056
Heart Lake (HRT)	-104.386835°	-104.386835°	2017	19	August 22-23	671 ± 52	3345 ± 6980

Table 3.2: State transition matrix for a state-space process with two environments. Here, ϕ_M and ϕ_F are environment-specific survival probabilities for the marine-estuary environment (M) and the freshwater environment (F) while ψ_{MF} and ψ_{FM} are movement probabilities.

		True state at time $t+1$		
		Environment M	Environment F	Dead
True state at time t	Environment M	$\phi_M(1-\psi_{MF})$	$\phi_M\psi_{MF}$	$1-\phi_M$
	Environment F	$\phi_F\psi_{FM}$	$\phi_F(1-\psi_{FM})$	$1-\phi_F$
	Dead	0	0	1

Table 3.3: State transition matrix for a state-space process with three environments. Here, ϕ_M, ϕ_E, and ϕ_F are environment-specific survival probabilities for the marine (M), estuary (E) and freshwater (F) environments respectively while ψ_{ME}, ψ_{MF}, ψ_{EM}, ψ_{EF}, ψ_{FM}, and ψ_{FE} are movement probabilities.

	Marine	Estuary	Freshwater	Dead
Marine	$\phi_M(1-\psi_{ME}-\psi_{MF})$	$\phi_M\psi_{ME}$	$\phi_M\psi_{MF}$	$1-\phi_M$
Estuary	$\phi_E\psi_{EM}$	$\phi_E(1-\psi_{EF}-\psi_{EM})$	$\phi_E\psi_{EF}$	$1-\phi_E$
Freshwater	$\phi_F\psi_{FM}$	$\phi_F\psi_{FE}$	$\phi_F(1-\psi_{FM}-\psi_{FE})$	$1-\phi_F$
Dead	0	0	0	1

Table 3.4: Observation matrix for a state-space process with two environments. Respectively, p_M and p_F are the observation probabilities at marine-estuary environment (M) and freshwater (F) at time t.

		Observation at time t		
		Environment M	Environment F	Not seen
True state at time t	Environment M	p_M	0	$1 - p_M$
	Environment F	0	p_F	$1 - p_F$
	Dead	0	0	1

Table 3.5: Observation matrix for a state-space process with three environments. Respectively, p_M, p_E, and p_F are the observation probabilities at marine (M), estuary (E), and freshwater (E) environments at time t.

	Observed at Marine	Observed at Estuary	Observed at Freshwater	Not Observed
Marine	p_M	0	0	$1 - p_M$
Estuary	0	p_E	0	$1 - p_E$
Freshwater	0	0	p_F	$1 - p_F$
Dead	0	0	0	1

Table 3.6: Binning scenarios that were used to avoid the effect of overwintering.

Scenario	Bins per year	Months
1	2	June-September and October-May
2	3	June-September, October-December, and January-May
3	6	June, July, Aug, September, October-December, and Jan-May

Table 3.7: Prediction probabilities for the models under different binning scenarios. Model 1 and Model 2 refer to the model with two environments and the model with three environments respectively. Scenarios 1, 2 and 3 refer to the binning scenarios in Table 3.6.

	Scenario 1	Scenario 2	Scenario 3
Model 1	65.9%	69.0%	77.2%
Model 2	75.5%	65.6%	84.7%

Table 3.8: DIC (ΔDIC) values for the models under different binning scenarios. The best model is the model with the lowest DIC (marked by '*'). ΔDIC is the difference in the DIC scores from the best model. Model 1 and Model 2 refer to the model with two environments and the model with three environments respectively. Scenarios 1, 2 and 3 refer to the binning scenarios in Table 3.6.

	Scenario 1	Scenario 2	Scenario 3
Model 1	1942.6*	2811.2 (868.6)	6789.7 (4847.1)
Model 2	2626.9 (684.3)	2603.3 (660.7)	9691.9 (7749.3)

Table 3.9: Parameter estimates for the model with two environments under Binning scenario 1. Here, ϕ_M and ϕ_F are environment-specific survival probabilities for the marine-estuary environment and freshwater environment while ψ_{MF} and ψ_{FM} are movement probabilities; p_M and p_F are the corresponding detection probabilities. $\hat{R}$ denotes Gelman-Rubin statistics and ESS is the effective sample size. The model was estimated using three MCMC chains each with 20,000 iterations, 5,000 burn-in with thinning by selecting each 5^{th} iteration.

Parameter	Mean	Standard Error	95% Credible Interval		$\hat{R}$	ESS
			Lower	Upper		
p_M	0.43	0.04	0.36	0.51	1.001	9000
p_F	0.73	0.07	0.62	0.88	1.001	9000
ϕ_M	0.87	0.02	0.82	0.91	1.001	9000
ϕ_F	0.95	0.02	0.91	0.99	1.002	2700
ψ_{MF}	0.25	0.03	0.19	0.32	1.001	9000
ψ_{FM}	0.47	0.05	0.38	0.57	1.001	5900
Deviance	1489.13	30.12	1426.87	1543.83	1.002	2700

Table 3.10: Bivariate correlations between parameters for the model with two environments under Binning Scenario 1. Here, ϕ_M and ϕ_F are environment-specific survival probabilities for the marine-estuary environment (M) and freshwater environment (F) while ψ_{MF} and ψ_{FM} are movement probabilities; p_M and p_F are the corresponding detection probabilities.

	p_M	p_F	ϕ_M	ϕ_F	ψ_{MF}	ψ_{FM}
p_M	1.00					
p_F	-0.53	1.00				
ϕ_M	-0.11	0.13	1.00			
ϕ_F	-0.31	0.01	-0.27	1.00		
ψ_{MF}	0.33	-0.31	-0.12	-0.11	1.00	
ψ_{FM}	-0.52	0.61	0.02	0.23	-0.04	1.00

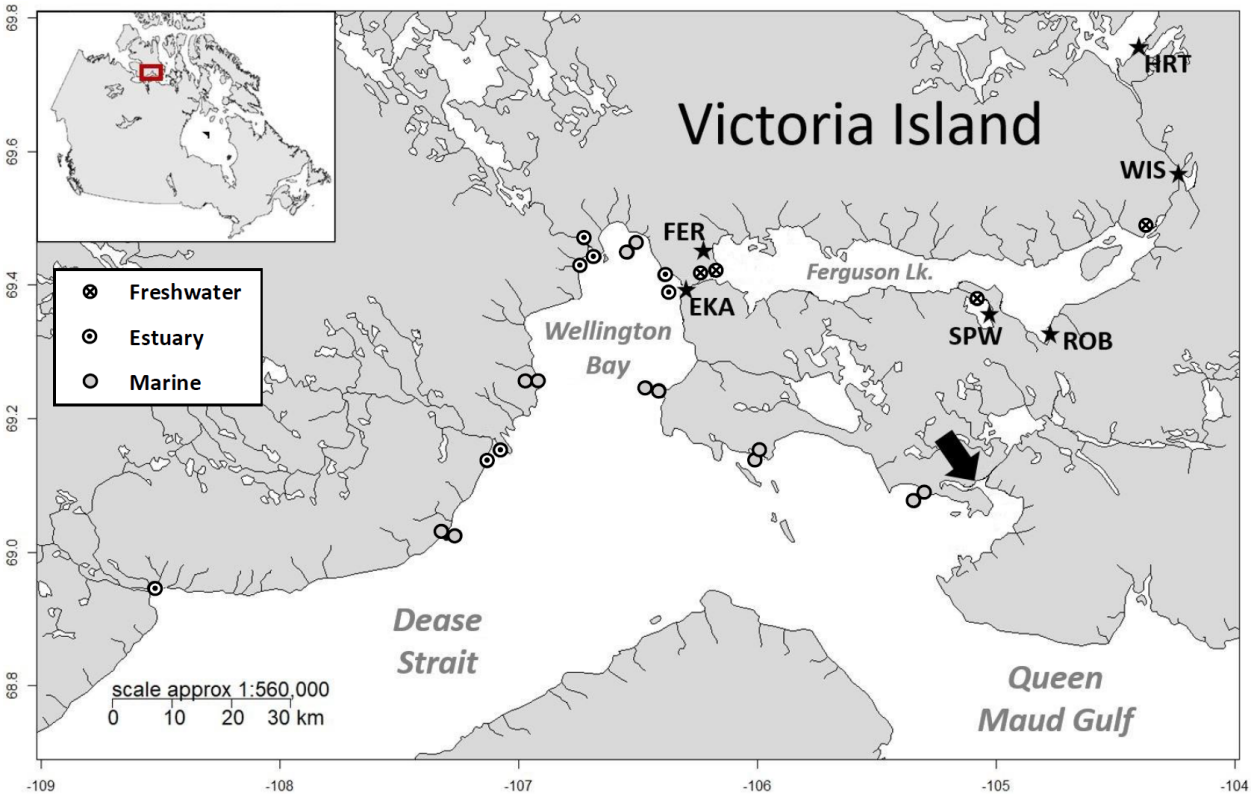

Figure 3.1: Study area on southern Victoria Island within the Kitikmeot Sea region of Nunavut showing receivers that we considered in this study (circles), and acoustic tagging locations (stars). The location of the community of Cambridge Bay is shown with a black arrow. Tagging information is described in Table 3.1. Map was modified form Harris et al. (2022). The original map was created with R package 'maps' (Becker et al. 2018) using NAD83 projection, and layers for rivers and lakes were downloaded from the National Topographic Database of Canada.

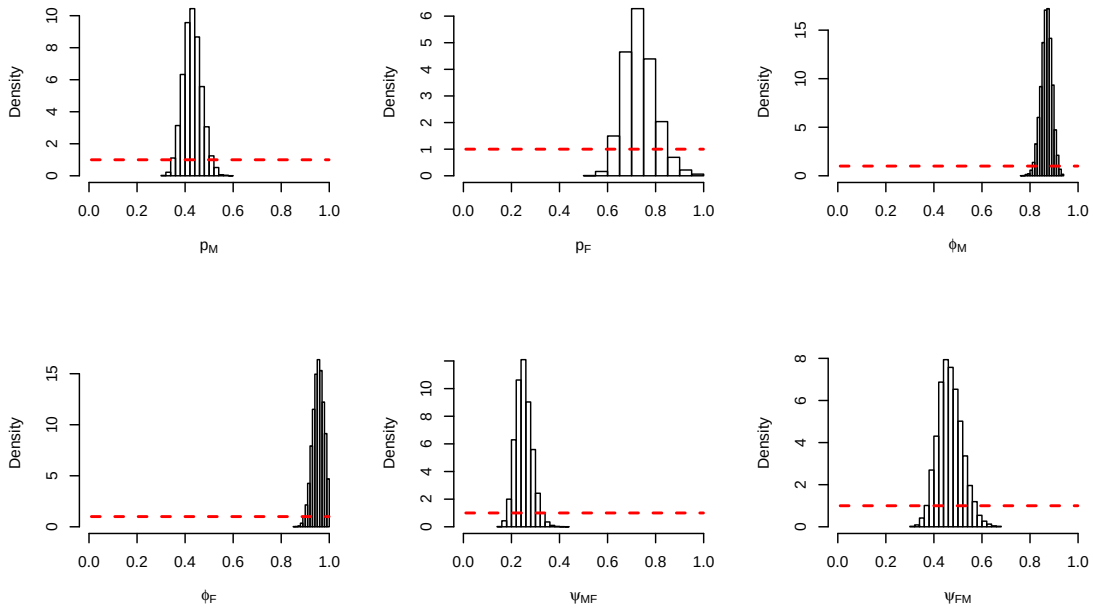

Figure 3.2: Posterior plots of parameter estimates for the model with two environments under Binning Scenario 1. Here, ϕ_M and ϕ_F are environment-specific survival probabilities for the marine-estuary environment (M) and freshwater environment (F) while ψ_{MF} and ψ_{FM} are movement probabilities; p_M and p_F are the corresponding detection probabilities. Dashed horizontal lines represent the prior distributions.

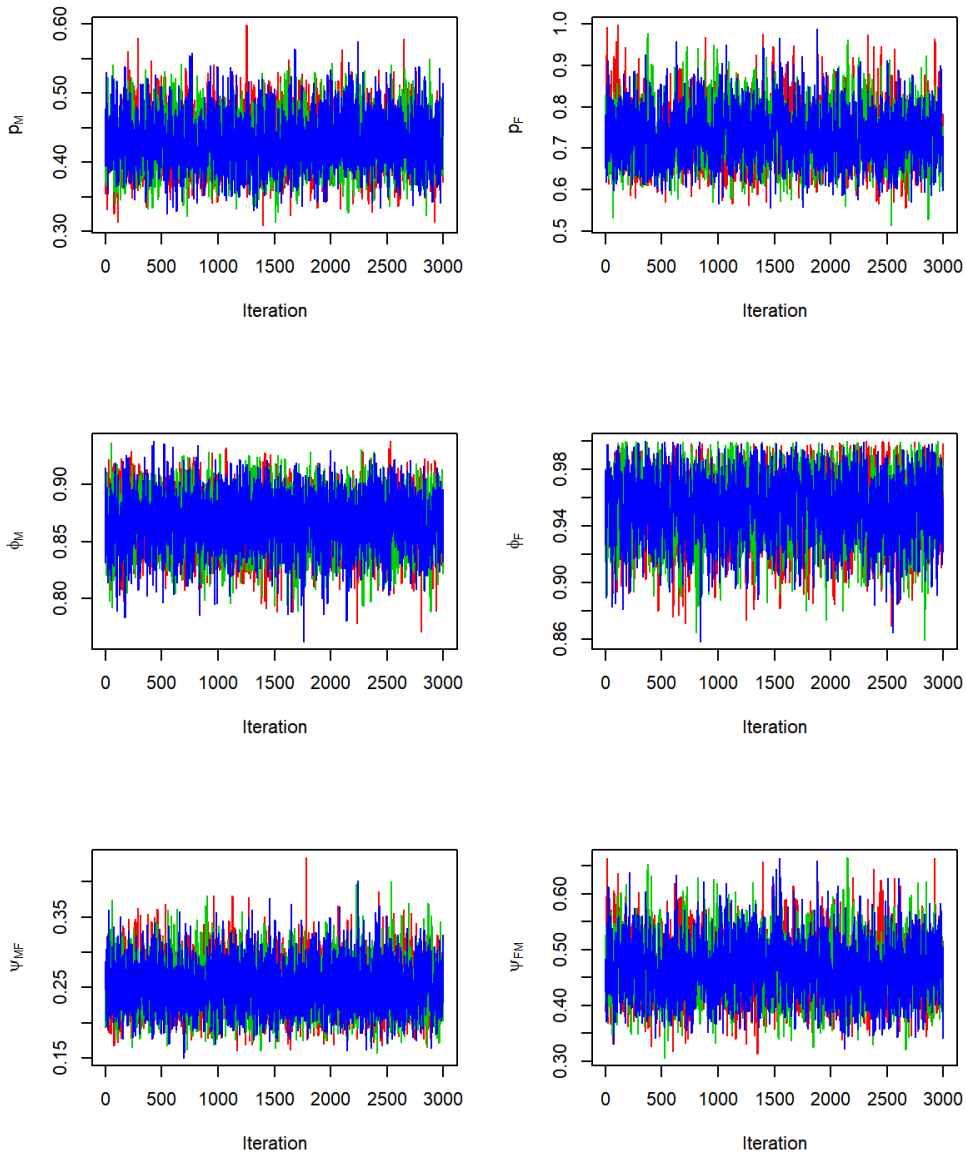

Figure 3.3: Trace plots of parameter estimates for the model with two environments under Binning Scenario 1. Here, ϕ_M and ϕ_F are environment-specific survival probabilities for the marine-estuary environment (M) and freshwater environment (F) while ψ_{MF} and ψ_{FM} are movement probabilities; p_M and p_F are the corresponding detection probabilities.

Chapter 4

Bayesian hierarchical models to estimate survival probabilities of Cambridge Bay Arctic char with environmental and individual covariates

Bayesian hierarchical models to estimate survival probabilities of Cambridge Bay Arctic char with environmental and individual covariates

Inesh Munaweera[a], Les N. Harris[b], Darren M. Gillis[a], Saman Muthukumarana[a]

[a]University of Manitoba,Winnipeg R3T 2N2.

[b]Fisheries and Oceans Canada, Arctic and Aquatic Research Division, Winnipeg, MB, R3T 2N6, Canada.

Abstract

Hierarchical modelling is frequently used to model complex ecological processes because of its ability to model complex ecological phenomena by decomposing them into naturally explainable sub-models. In this study, we combine Bayesian hierarchical models with acoustic telemetry data to estimate survival probabilities for Arctic char in the Cambridge Bay region of Nunavut while incorporating environmental and individual covariates to assess the impact of these factors on survival in this species. Also, the model we present here can account for temporally varying detection probabilities due to changes to the acoustic receiver array over the study period and seasonal variations in the detection probabilities within the year (e.g., ice vs. no ice). We found that the covariates pertaining to sea ice coverage and Fulton's condition factor explained the variability in the survival probabilities of Arctic char. Also, the Arctic char survival was considerably lower during the summer (open water) compared to winter. The results of this work further our understanding of anadromous Arctic char at high latitudes, including the environmental and biological drivers influencing survival. More importantly, we present a hierarchical Bayesian model that accounts for varying detection probabilities, a major concern of acoustic telemetry studies. The model can be easily adapted for other taxa with similar life histories.

4.1 Introduction

Most ecological processes are complicated and hierarchical in nature with multiple levels of spatiotemporal hierarchies (Lele and Dennis 2009; Royle and Dorazio 2009; Wikle 2003). Hierarchical modelling is frequently used to model such processes given its ability to model complex ecological phenomena by decomposing them into naturally explainable sub-models to account for different sources of variance and various sources of data (Bolker 2008; Richardson and Best 2003; Royle and Dorazio 2008). Hierarchical models can essentially be defined as the family of models that connect multiple parameters according to the structure of the problem (Gelman et al. 2004). With the development of computing power, the Bayesian approach to hierarchical models has been gaining popularity due to its extreme flexibility, better precision, and ability to incorporate prior knowledge about parameters compared to more traditional non-hierarchical models (Calvert et al. 2009; Gelman et al. 2004; Kéry and Schaub 2011).

Bayesian hierarchical models have been widely applied to various types of data, including in the financial (Chib and Greenberg 1995; Kantorová et al. 2020; Ying et al. 2005), health science (Grieve et al. 2010; Kantorová et al. 2020; Prevost et al. 2000) and environmental fields (Apputhurai and Stephenson 2013; Fuentes and Raftery 2005; Sahu et al. 2009). Bayesian hierarchical models have also been increasingly used in fisheries ecology and management for many applications such as estimation of fish movement paths (Patterson et al. 2017, 2008), parameter estimation for mark-recapture studies (Calvert et al. 2009; Harley and Myers 2001; Rivot and Prevost 2002), and in fisheries stock assessment (Aanes et al. 2007; Aeberhard et al. 2018). More recently, combining hierarchical Bayesian models with acoustic

telemetry data has facilitated the estimation of fish movement paths and other parameters of interest, such as survival probabilities and recapture rates, with better precision than traditional capture-mark-recapture models (Alós et al. 2016; Dudgeon et al. 2015; Munaweera et al. 2022, 2021).

Having a clear understanding of survival and mortality in fisheries ecology is essential for effective fishery conservation and management decision-making. For example, survival estimates for a particular species over time may provide insights into fishing and natural mortality, how these change over time and with changing environmental conditions allowing managers to make decisions on how best to facilitate the long-term sustainability of the species (Brooks et al. 2000; Murray and Patterson 2006). Recently, we used Bayesian multistate capture-recapture models combined with acoustic telemetry data to estimate survival probabilities over multiple years (2014–2018) in marine/estuarine and freshwater environments for Arctic char *(Salvelinus alpinus)* in the Cambridge Bay region of Nunavut where the largest commercial fishery in Canada takes place (Munaweera et al. 2022). We found that the survival probability of Cambridge Bay Arctic char was generally high (> 0.87), and survival probability was higher in the freshwater compared to marine and estuary environments. Long-term acoustic telemetry studies are often hindered by the fact that acoustic telemetry arrays are often not static over the entire study period. This is due to changing study objectives where the receiver array design changes to answer new questions or because the equipment is lost and not recovered. Also, for multi-year and multi-seasonal telemetry studies, detection probabilities vary over time, often due to varying environmental conditions that affect the acoustic signal emitted from the transmitter (e.g., when there is ice vs.

no ice). This creates problems for data analyses and interpretation of results when using the traditional Cormack–Jolly–Seber (CJS) model unless varying detection probabilities are properly incorporated into the model. In our previous study, we had to filter out a large number of detection records recorded by some receivers and some fish tagged before 2014 so that the receiver array was fixed throughout the study period. Our previous model did not account for temporally varying detection probabilities due to seasonal factors such as the surface ice cover, and we did not consider environmental and biological drivers of survival that might impact the accuracy/precision of estimates.

Arctic char is widely considered one of the most important natural resources in Nunavut, where it is harvested in every community in the territory (Priest and Usher 2004). Despite this, there is still a paucity of information on many demographic parameters in harvested stocks of this species, and this is especially true for survival. Additionally, little is known regarding the environmental and biological variables that influence survival and even less is known on how interannual variation in these variables influences annual survival in this species. This has implications for fully understanding population viability in this species and, thus, population persistence and long-term sustainability.

In this study, we extended our previous work by developing a more complex Bayesian hierarchical model to examine survival probabilities of Cambridge Bay Arctic char that now incorporates environmental and individual covariates to assess how variation in these impact survival in this species. Specifically, we included sea surface temperature (SST), surface ice conditions, Fulton's condition factor (k) and the sex of each fish and assumed variable detection probabilities within and among years. Also, we now incorporate a monthly detection

variability index that was calculated using reference tag data. This factor (i.e., varying detection probability) is rarely considered in the majority of acoustic telemetry studies. Overall, this model is flexible, and it can account for any changes in receiver array design across years and variations in monthly detection probability due to changing environmental conditions.

4.2 Materials and methods

4.2.1 Study area and fishery information

Our study took place in the Cambridge Bay area of Nunavut on southern Victoria Island (Figure 4.2). The area is subject to long winters, and the marine environments are covered in ice from November to July. The largest commercial fishery for Arctic char in Canada takes place in the Cambridge Bay region (Harris et al. 2020a) where five waterbodies are mainly used with a combined annual quota of 56,100 kgs (Harris et al. 2020b). An acoustic telemetry array of 99 receivers was used from 2013-2021 to study the habitat use and migrations of acoustically tagged Arctic char between marine, estuary, and freshwater environments. More information on the acoustic telemetry study and fishery in the region can be found in Moore et al. (2016) and Harris et al. (2020a).

4.2.2 Experimental setup and data

This study includes data from 218 Arctic char (122 female and 96 male) that were acoustically tagged between July 2013 to August 2018 (Table 4.1). For each tagged Arctic char, we recorded fork length (±1 mm) and round weight (± 25 g). For each fish, Fulton's relative

condition factor (K) was calculated as $K = [W \times 10^5]/L^3$, where W and L are weight (g) and fork length (mm), respectively. We used the genetic-sex determination protocol of Yano et al. (2013) to determine the sex of all tagged Arctic char. We estimated the daily sea surface temperature (SST) values for the marine environment in our study area from the NOAA 0.25° Daily Optimum Interpolation Sea Surface Temperature (OISST) dataset. The OISST dataset incorporates observations from different platforms (satellites, ships, buoys, and Argo floats), and the product also uses sea ice datasets and includes a large-scale adjustment of satellite biases with respect to the in-situ data (Banzon et al. 2016; Huang et al. 2021; Reynolds et al. 2007). The dataset is interpolated using an optimum interpolation (OI) technique to fill gaps in the data and create a spatially complete map of SST over the globe. After clipping the downloaded dataset to our study area, we calculated the average monthly temperature for June, July, August, and September (when Arctic char would potentially be using the marine environment) from 2013 to 2019. After September until June, Arctic char will be in freshwater, but the surface temperature during this time period can safely be assumed to be less than 5^oC. Weekly sea ice charts from the Canadian Ice Service (`https://iceweb1.cis.ec.gc.ca/IceGraph/page1.xhtml?lang=_en`) were used to determine sea surface ice conditions (SIC) for the marine environment. When the marine environment is covered in ice, we also assume that all freshwater habitats would be covered in ice. The ice cover in the marine environment is minimum in August and September, with less than 25% ice cover (Figure 4.3).

4.2.3 Bayesian hierarchical models

Bayesian hierarchical modelling is a key framework in Bayesian statistics that allows for the modelling of complex population dependencies using a much simpler set of layers to represent different levels of hierarchy (Gelman et al. 2013; Shaddick and Zidek 2015). The state-space model is one of the most popular hierarchical models that has three layers: 1) the observation model that describes observed data generated from a latent process (complete data likelihood), 2) the process model that represents the underlying latent process (latent data density), 3) the prior densities (model for the parameters) based on prior knowledge (Congdon 2010; Shaddick and Zidek 2015). The popular Cormack–Jolly–Seber (CJS) model (Cormack 1964; Jolly 1965; Seber 1965) can be easily formulated using state-space formulation (Kéry and Schaub 2011; King 2012). Figure 4.1 shows a graphical representation of the state-space formulation of the CJS model.

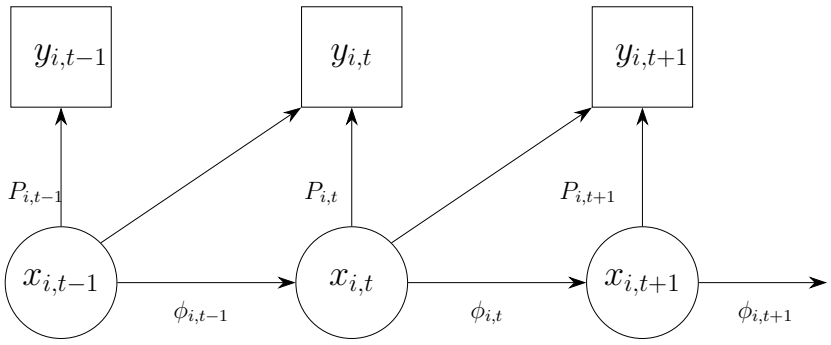

Figure 4.1: A graphical representation for the state-space formulation of the Cormack–Jolly–Seber model. Here, x is the latent process, y is the observation process, while ϕ and P are parameters that are to be estimated.

Consider a regular mark-recapture setting with n number of tagged fish observed through

T number of recapture instances. Then, the joint density can be generally expressed below (Congdon 2010; Fouley 2013; Kéry and Schaub 2011).

$$f(\boldsymbol{y}, \boldsymbol{x}, \boldsymbol{\phi}, \boldsymbol{p}) = f(\boldsymbol{y} \mid \boldsymbol{x}, \boldsymbol{p}) f(\boldsymbol{x} \mid \boldsymbol{\phi}) \pi(\boldsymbol{\phi}, \boldsymbol{p}), \tag{4.1}$$

where $f(\boldsymbol{y} \mid \boldsymbol{x}, \boldsymbol{p})$ is the observation model for the observed data ($\boldsymbol{y}$). The observation model is conditioned on the latent (hidden) states of captured fish ($\boldsymbol{x}$) and the detection probability ($\boldsymbol{p}$). Note that $\boldsymbol{x}$ and $\boldsymbol{y}$ are $n \times T$ matrices where the elements of each matrix are defined as:

$$x_{i,t} = \begin{cases} 0, & \text{if } t < e_i \text{ or the } i^{th} \text{ fish is dead at time } t, \\ 1, & \text{otherwise,} \end{cases}$$

where e_i is the tagged time step of the i^{th} fish, and

$$y_{i,t} = \begin{cases} 0, & \text{if } t < e_i \text{ or the } i^{th} \text{ fish is not captured at time } t, \\ 1, & \text{otherwise.} \end{cases}$$

Then, the observation model can be written as

$$f(\boldsymbol{y} \mid \boldsymbol{x}, \boldsymbol{p}) = \prod_{t=1}^{T} f(\boldsymbol{y}_t \mid \boldsymbol{x}_t, \boldsymbol{p}), \tag{4.2}$$

where $\boldsymbol{y}_t = \{y_{1,t}, y_{2,t}, \ldots, y_{n,t}\}$ and $\boldsymbol{x}_t = \{x_{1,t}, x_{2,t}, \ldots, x_{n,t}\}$ are the vector of observed status and the vector of latent states respectively at time step $t \in \{1, 2, \ldots, T\}$.

The second part of the joint density in (4.1), $f(\boldsymbol{x} \mid \boldsymbol{\phi})$ is the process model that describes the latent states ($\boldsymbol{x}$) of the fish that depend on the survival probability ($\boldsymbol{\phi}$) given by

$$f(\boldsymbol{x} \mid \boldsymbol{\phi}) = \prod_{t=1}^{T} f(\boldsymbol{x}_t \mid \boldsymbol{x}_{t-1}, \boldsymbol{\phi}), \tag{4.3}$$

The third component of the joint density, $\pi(\boldsymbol{\phi}, \boldsymbol{p})$ is the joint prior density of the parameters $\boldsymbol{p}$ and $\boldsymbol{\phi}$ (Congdon 2010; Shaddick and Zidek 2015).

The posterior density can be written as

$$f(\boldsymbol{\phi}, \boldsymbol{p}, \boldsymbol{x} \mid \boldsymbol{y}) = \frac{f(\boldsymbol{y} \mid \boldsymbol{x}, \boldsymbol{p}) f(\boldsymbol{x} \mid \boldsymbol{\phi}) \pi(\boldsymbol{\phi}, \boldsymbol{p})}{f(\boldsymbol{y})}, \tag{4.4}$$

where, $f(\boldsymbol{y})$ is called the normalizing constant. The marginal posterior distribution for the parameters $\boldsymbol{\phi}, \boldsymbol{p}$ can be obtained by

$$f(\boldsymbol{\phi}, \boldsymbol{p} \mid \boldsymbol{y}) = \frac{\pi(\boldsymbol{\phi}, \boldsymbol{p}) \int f(\boldsymbol{y} \mid \boldsymbol{x}, \boldsymbol{p}) f(\boldsymbol{x} \mid \boldsymbol{\phi}) dx}{f(\boldsymbol{y})}. \tag{4.5}$$

The posterior distribution in Eq. 4.5 is obtained indirectly by simulating samples using the Bayesian Markov chain Monte Carlo (MCMC) approach since the analytical solution for the posterior distribution is intractable (Congdon 2010; King 2012). In the MCMC approach, we use the much simpler conditional distributions $f(\boldsymbol{\phi}, \boldsymbol{p} \mid \boldsymbol{x}, \boldsymbol{y})$ and $f(\boldsymbol{x} \mid \boldsymbol{\phi}, \boldsymbol{p}, \boldsymbol{y})$ to fully characterize the posterior in Eq. 4.5. In the k^{th} iteration, MCMC will alternatively sample from the conditional distributions $f(\boldsymbol{x}^{(k)} \mid \boldsymbol{\phi}^{(k-1)}, \boldsymbol{p}^{(k-1)}, \boldsymbol{y})$ and $f(\boldsymbol{\phi}^{(k)}, \boldsymbol{p}^{(k)} \mid \boldsymbol{x}^{(k)}, \boldsymbol{y})$ (Congdon 2010; King 2012).

The process model in Eq. 4.2 is defined by a Bernoulli distribution given by

$$x_{i,t+1} \mid x_{i,t} \sim Bernoulli(\boldsymbol{x_{i,t}} \phi_{i,t}) \qquad , i = 1 \ldots n, \text{and} \quad t \geq e_i, \tag{4.6}$$

where e_i is the tagged time step of the i^{th} fish. Similarly, the observation model in Eq. 4.3 is defined as

$$y_{i,t} \mid x_{i,t} \sim Bernoulli(\boldsymbol{x_{i,t}} p_{i,t}) \qquad , i = 1 \ldots n, \text{and} \quad t \geq e_i. \tag{4.7}$$

We will assume that the survival probability $\phi_{i,t}$ is associated with the temporal covariates: sea surface temperature (SST) and surface ice condition (SIC), and individual covariates; Fulton's condition factor (FC) and sex. Also, we will assume an individual random effect (ϵ_i) to account for any remaining individual variability (Kéry and Schaub 2011). Then, we will model the survival as below

$$\log\left(\frac{\phi_{i,t}}{1-\phi_{i,t}}\right) = \beta_0 + \beta_1 \text{SST}_t + \beta_2 \text{ SIC}_t + \beta_3 \text{FC}_i + \beta_4 \text{Sex}_i + \beta_5(\text{SST}_t \times \text{ SIC}_t) + \epsilon_i, \tag{4.8}$$

$$\epsilon_i \sim Normal(0, \sigma^2),$$

where the SST is obtained by taking the average sea surface temperature for the month as below 5°C (SST=0) or above 5°C (SST=1) to assess if SST impacts survival at lower and higher values, we were restricted to lower values of temperature given that the highest monthly average temp was 8°C; however, this model can be extended to any range of temperatures the study organism would experience in nature. Fulton's condition factor was recorded as below 0.9 (FC=0) or above 0.9 (FC=1) to assess if there were survival differences between fish with lower and higher FC when they were acoustically tagged. Finally, we also recorded the marine surface ice condition as a binary variable that reflects whether the surface is covered in ice (SIC=0, if the marine ice cover is >25%) or mostly open water (SIC=1, otherwise) during the given month to assess the potential impact of surface ice conditions on survival (Figure 4.3).

Since the detection probabilities exhibited monthly variation within and among years, we used a monthly detection variability index (DVI) calculated with reference tag data for each habitat separately (marine, estuary, and freshwater) to account for the within-year variability in the detection probabilities. Each reference tag was approximately 500 m away from the closest receiver, and any missing values during the study period were imputed with the monthly averages across years. For each fish, the DVI at time t was assigned according to the location of the most recent detection record before time t. Note that DVI is just an indicator of the variability in the detection probabilities within a year for each environment. The exact probability that a fish would be detected by at least one of the receivers during the given period depends on how far the fish is from the nearest receiver, how many receivers were active during the period and other environmental conditions (e.g., ice and wind). DVI can account for the monthly variability in detection probabilities due to these environmental variables that change seasonally and spatially (since we calculate DVI for each environment). A DVI above 1 indicates above-average detection probability, and below one indicates lower than average detection probability. Our acoustic array changed annually by adding new receivers, removing receivers and/or repositioning current receivers. Hence, we assume annually varying detection probabilities to account for those changes to the receiver array. Furthermore, tags were programmed to automatically turn off at 72 months. Hence, the detection probability was assigned zero for all the fish once the time from tagging was greater than 72 months. Then we modelled the detection probability as below:

$$p_{i,t} = p_{year_t} \times \text{DVI}_t \times I(i,t),$$

where p_{year} is the average detection probability for the year of month t which is unknown. Here, $I(i,t)$ is a indicator function such that

$$I(i,t) = \begin{cases} 1 & \text{for } t - e_i \leq 72, \\ 0 & \text{otherwise.} \end{cases}$$

Note that the receiver array has been changed annually; hence we have to estimate the average detection probabilities for each year, given by p_{year_t}.

Data preparation

In our study, the fish are detected by an array of receivers, and the transmission of an acoustic signal from a fish to a receiver takes just a few milliseconds; each detection can be considered as an instantaneous sampling point. There were millions of such detection records in our data set. Hence, we pooled the detection record monthly. If the fish was detected at least once during the month, we recorded the fish as alive during that month.

4.2.4 Model estimation and evaluation

The models were fitted using the Bayesian MCMC approach with 'JAGS' in R using the package 'R2jags' (Su and Yajima 2015). The models were run on Compute Canada, Beluga cluster that uses 2×Intel Gold 6148 Skylake @ 2.4GHz processors with 40 cores in each

node. For each model, three parallel chains were run with 100,000 MCMC iterations and thinning was done by selecting each 5^{th} iteration of the MCMC chain to minimize any possible autocorrelations in the simulated parameter values. We used the Effective Sample Size (ESS) suggested by Kass et al. (1998) and Gelman-Rubin statistics ($\hat{R}$) by Gelman and Rubin (1992) to assess convergence. ESS can be used to measure the amount of independent information in the MCMC chain. We can calculate $\hat{R}$ for the parameter of interest by dividing the total variance of the parameter of interest calculated with multiple MCMC chains combined by the average of the variances within each chain (Kass et al. 1998). Hence, a $\hat{R}$ close to 1 denotes a converged MCMC chain for the parameter.

To check for any identifiability issues, we inspected the posterior distributions, trace plots and pairwise correlations between the parameters generated with MCMC chains. An identifiable model should result in unimodal posterior distributions, trace plots of multiple chains with good mixing (Siekmann et al. 2012; Simpson et al. 2020) and weak correlations between model parameters (Hines et al. 2014).

4.2.5 Model selection

To perform the model selection, we used the deviance information criterion (DIC), which is the most popular predictive measure in Bayesian model selection (Gelman et al. 2013) proposed by Spiegelhalter et al. (2002). DIC accounts for both the model fit and the complexity of the model (Gelman et al. 2013). DIC can be easily obtained using the Bayesian programming language `'JAGS'` (Plummer et al. 2003; Spiegelhalter et al. 2003). In this

work, we used the version of DIC suggested by Gelman et al. (2004) given below:

$$DIC = D(\bar{\theta}) + 2p_V, \tag{4.9}$$

where $\bar{\theta}$ is the posterior mean and p_V is given by

$$p_V = Var(D(\theta))/2, \tag{4.10}$$

and

$$D(\theta) = -2\log p(y|\hat{\theta}) + 2logf(y), \tag{4.11}$$

where, $f(y)$ is the standardizing term that is a function of data (Spiegelhalter et al. 2002).

4.3 Results

The monthly detection variability index exhibited a regular pattern with below-average detection probabilities in summer and above-average detection probabilities in winter (Figure 4.4). This behaviour was similar for all three environments, but the variability was comparatively lower in the estuary environment and higher in freshwater. In the marine environment, we observed a very noticeable drop in the detection probability around September compared to other environments. Also we noticed a higher, almost constant detection probability from December to June in the marine environment.

The full model using all covariates in the survival probability function in (4.8) did not converge, and hence, we dropped the individual random effect (ϵ_i) in all models. The best model with the lowest DIC was the model with surface ice condition and Fulton's condition factor (Table 4.2). The model did not suffer from convergence issues, confirmed by Gelman-Rubin

statistics of almost one and high ESS values ($\geq$ 1900) for all parameters. The model also did not suffer from any identifiability issues since all the posterior densities were unimodal, and the trace plots showed multiple chains mixed well for all the parameters. The 95% credible intervals for all the estimated coefficients for the best model did not contain zero, suggesting that all the coefficients in the model are important in predicting the survival of Arctic char (Table 4.3). The estimated annual detection probabilities were precise, with low standard errors.

The marginal probability densities for the survival probabilities of Arctic char showed a clear difference for different levels of surface ice condition and Fulton's condition factor (Figure 4.5). The survival probability of Arctic char was significantly lower in the open water (when there was less ice) on average compared to when the marine environment was mostly covered in ice. Furthermore, we also notice slightly lower survival for Arctic char with higher Fulton's condition factor (Table 4.4). Finally, the average monthly survival estimates obtained by averaging the simulated survival estimates of the MCMC output showed a noticeable drop in the survival probability of Arctic char in July and August (Figure 4.6).

4.4 Discussion

Disentangling the impacts of environmental and climatic variables on the survival of anadromous and freshwater fishes provides information that is critical for predicting the effects of climate change on population resilience (Caza-Allard et al. 2021; Crossin et al. 2017; Reist et al. 2006). Furthermore, understating the biological drivers impacting survival has implications for understanding population persistence and long-term sustainability. However,

formulating models for the survival of this group of fish is often challenging because many methods (i.e., those based on age) require fish to be sacrificed, or there is a paucity of data for estimating these demographic parameters, and this is especially true for Arctic study systems. Analyses of acoustic telemetry data have recently provided alternative approaches for estimating survival in a variety of taxa; however, covariates, non-static array design and varying detection probabilities have rarely been considered in such models. Here, we present a hierarchical Bayesian approach for estimating survival over seven years in Arctic char from the Cambridge Bay region of Nunavut. Our model incorporates environmental (sea surface temperature and surface ice condition) and biological (Fulton's condition factor and sex) covariates as well varying detection probabilities that account for the changes in the acoustic array from year to year. We found that survival of Arctic char was high across all years, and the surface ice condition and Fulton's condition factor have an influence on the survival probability of Arctic char in the region. The models converged well (three chains each with 100,000 iterations after 20,000 burn-in) without any identifiability issues. To our knowledge, this study was the first to model survival using Bayesian models and acoustic telemetry data with environmental and biological covariates while considering within-year and between-years varying detection probabilities.

Modeling demographic parameters using the Bayesian hierarchical framework is gaining popularity because of its flexibility, ability to incorporate prior knowledge, and the parameter estimates with the Bayesian hierarchical approach frequently yield better precision and lower bias than traditional non-hierarchical models (Calvert et al. 2009; Clark 2005). For example, Gimenez et al. (2007) used a Bayesian state-space modelling approach with CJS models to

estimate survival of on the European dipper (*Cinclus cinclus*). Poole (2002) also incorporated a Bayesian framework to estimate the survival of fulmar petrels (*Fulmaris glacialis*) in Orkney with 13 years of mark-recapture data. The Bayesian approach has rarely been used with acoustic data for estimating demographic parameters and even rare are studies that incorporate environmental and biological covariates. Furthermore, issues with seasonally and annually varying detection probability are rarely considered.

Caza-Allard et al. (2021) previously used the CJS models with maximum likelihood method to understand the influence of the environmental (air temperature and sea ice cover) and biological (sex) covariates on the Arctic char survival in our study area. However, their study was limited to the marine environment, and they did not consider the within-year variation of survival and detection probabilities. They found the sea ice melting date to be the only factor that explained the variability in survival. However, the effect size of the sea ice melting date was not significantly different from zero to establish any effect of this factor on survival. The hierarchical Bayesian framework based on the Cormack–Jolly–Seber we presented here is clearly an effective method for estimating survival in a study system that includes multiple populations, multiple years of data, annual differences in array design, tag characteristics and highly variable detection probabilities. Additionally, this model can be extended to other acoustic telemetry data sets where environmental and biological covariates are available and where detection probabilities vary spatially and temporally within the acoustic array.

In this study, we incorporated covariates in survival estimation and found that the surface ice condition and Fulton's condition factor (K) are associated with the survival probability of Arctic char. Although we only know K at the time of tagging and cannot follow K

across years, this model would still be valuable for short-term studies where K is known and where there are large differences in K among individuals. In general, the fish condition was relatively high in this study (mean=1.02 and SD = 0.27), and we assume fish with high K remained high throughout open water season (when there is no ice) is when fishing pressure would be the highest so it is perhaps not surprising that we found lower survival during this period (Zhu et al. 2014). The K values in this study might not be detrimental to fish survival from a biological standpoint, but fish with larger K (those that are plumper) may be more susceptible to commercial fishing gear or more appealing to predators in the region (such as seals). Furthermore, we found that neither sex nor SST influenced survival. This might be mainly due to the low variability of sea surface temperature having an effect on the survival of Arctic char. The maximum average monthly temperature reported in the region for the study duration is only 8 ^{o}C, which might not be detrimental to Arctic char survival (Harris et al. 2020a). We found no diffidence in survival between sexes. Indeed, in our study area, others have also shown that mortality between sexes is similar for Arctic char in the area (Zhu et al. 2017, 2021).

In multi-year acoustic telemetry studies, often the acoustic array is not consistent over the study period for a variety of reasons (objectives change, lost receivers, etc.). Additionally, detection probabilities are not static and change throughout (within and among years) depending on the habitat occupied (e.g., riverine vs. lacustrine and temporally varying environmental conditions). Despite having an acoustic array that varied annually and detection probabilities that changed monthly and with the environmental conditions of the habitats Arctic char were using, we were able to incorporate varying detection probabilities

and stochastic array design in our model. This allowed us to incorporate all data collected throughout the study period instead of ignoring the data collected by the receivers that were lost, removed or re-positioned during the study period resulting in more precise estimates. Hence, the modelling framework we developed here would be useful for any telemetry study where we know that the detection probabilities change over time and where there are temporal changes in the array design, which is a common feature of acoustic telemetry studies.

In the model estimation, we had to drop the individual variability term in the survival model due to convergence issues. We believe that this might be due to overparameterization that occurred by adding the additional error component to each fish. We may be able to add it back as we collect more data that are not available at the moment. Additional information that might further improve the model is fishing effort information, predator densities and food availability among seasons and habitats. A detailed examination of how additional environmental (e.g., salinity) and biological covariates (e.g., age) influence Arctic char survival remains warranted and necessary for further understanding how Arctic char persist and survive as they encounter multiple habitats that vary substantially.

In this study, we used Bayesian hierarchical models with acoustic telemetry data to estimate survival probabilities for anadromous Arctic char incorporating environmental and individual biological covariates to assess the impact of these factors on survival in this species. The model also accounted for temporally varying detection probabilities which is often not taken into consideration in acoustic telemetry studies. The results of this work should prove valuable for furthering our collective understanding of the environmental and biological drivers of survival in anadromous Arctic char and salmonids in general at high latitudes that use

multiple habitats. Additionally, the proposed approach is very flexible and can be adapted to study other taxa as well. For instance, the proposed Bayesian hierarchical modelling framework can be easily modified to study the survival of animals monitored with a grid of automated observer stations that detect the animal's presence with detection probability affected by temporal and spatial factors. In addition, the proposed model can account for any spatial and temporal changes in the receiver grid as well. Two examples are camera traps with motion sensors and radio tags to study wildlife survival. Finally, the Bayesian hierarchical modelling framework is an extremely flexible and powerful tool that can be used to naturally model complex error structures of ecological data collected using modern animal tracking technologies. With the development of computing power and more efficient MCMC samplers, we are certain that the Bayesian hierarchical modelling framework will be increasingly used as the natural candidate for modelling such data.

Table 4.1: Biological summary of Arctic char tagged in this study including tagging location (Source, EK=Ekalluk River, RB=Roberts Bay, SP=Spawning Lake, WB=Wishbone Lake, FER=Ferguson lake, HT=Heart Lake, see Figure 1), sample size (N) and weight and Fork length information.

Year	Source	Count	Weight		Length	
			Mean	SD	Mean	SD
2013	EK13	30	4013.3	1065.8	717.4	57.0
2014	EK14	30	3156.7	1146.6	666.9	82.4
2015	EK15	72	4174.3	1178.1	735.8	76.6
2016	RB16	21	5319.0	1467.6	783.6	68.1
2016	SP16	22	4605.7	1063.5	724.8	156.0
2016	WB16	18	4244.4	857.1	734.8	57.7
2017	FER17	6	4850.0	2911.4	784.0	81.2
2017	HT17	19	3344.7	698.4	655.7	95.2

Table 4.2: DIC values for fitted models with different covariates for the survival model. The best model is the one with the lowest DIC (marked by '*'). ΔDIC is the difference in the DIC scores from best model. The covariates are sea surface temperature (SST), surface ice condition (SIC), Fulton's condition factor (FC), and sex.

Survival covariates	DIC	ΔDIC
SST,Sex,FC,SIC,(SST×SIC)	8601.0	12.2
SST,FC,SIC,(SST×SIC)	8601.1	12.3
SST,FC,SIC	8604.0	15.2
Sex,FC,SIC	8600.6	11.8
FC,SIC	8588.8*	0

Table 4.3: Parameter estimates for the best model with the lowest DIC. Here, β_0, β_2 and β_3 represent the intercept, coefficients for sea surface condition, and Fulton's condition factor, respectively. $p_1, p_2, \ldots, p_7$ represents the annual detection probabilities. The effective sample size is denoted by ESS, and $\hat{R}$ denotes the Gelman-Rubin statistics.

	Mean	SE	Quantiles		$\hat{R}$	ESS
			2.5%	97.5%		
β_0	5.897	0.366	5.226	6.661	1.002	1900
β_2	-3.555	0.338	-4.263	-2.937	1.002	2300
β_3	-0.477	0.239	-0.966	-0.028	1.001	9700
p_1	0.286	0.038	0.216	0.363	1.001	18000
p_2	0.222	0.021	0.183	0.264	1.001	32000
p_3	0.532	0.017	0.497	0.566	1.001	25000
p_4	0.540	0.013	0.513	0.565	1.001	18000
p_5	0.517	0.012	0.493	0.541	1.001	27000
p_6	0.421	0.015	0.392	0.449	1.001	33000
p_7	0.236	0.019	0.199	0.275	1.001	11000
Deviance	8201.5	27.8	8148.641	8257.8	1.001	12000

Table 4.4: Summary of marginal survival probabilities for different levels of surface ice condition and Fulton's condition factor. The credible intervals were obtained using the $2.5\%^{th}$ percentile and $97.5\%^{th}$ percentile of each marginal density extracted using the MCMC outputs.

		Surface condition	
		Mostly ice covered	Mostly open water
Fulton's conditon factor	<0.9	Median = 0.997	Median = 0.912
		95% CI = (0.995,0.999)	95% CI = (0.872,0.943)
	>0.9	Median = 0.996	Median = 0.866
		95% CI = (0.992,0.998)	95% CI = (0.841,0.888)

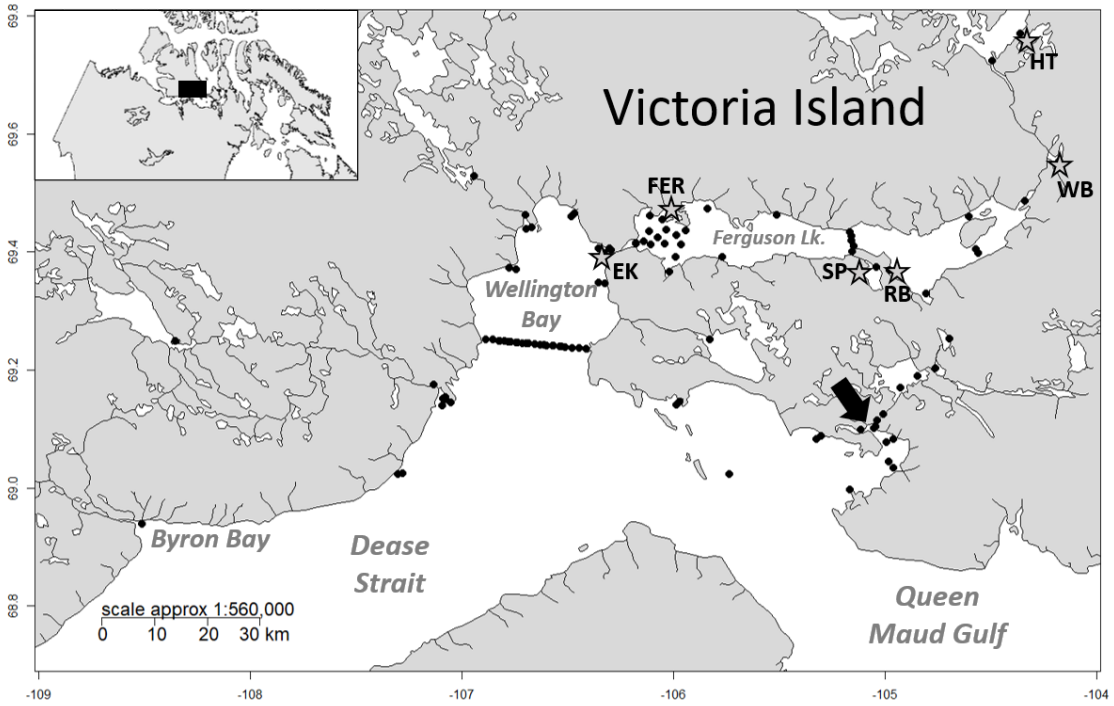

Figure 4.2: Study area on Southern Victoria Island showing all stations within our acoustic telemetry array (black dots) that were used between 2013-2020. Acoustic tagging locations are shown with stars and codes for tagging locations in this study described in Tables 1 . The location of the community of Cambridge Bay is shown with a black arrow. The original map was created with R package 'maps' (Becker et al. 2018) using NAD83 projection, and layers for rivers and lakes were downloaded from the National Topographic Database of Canada.

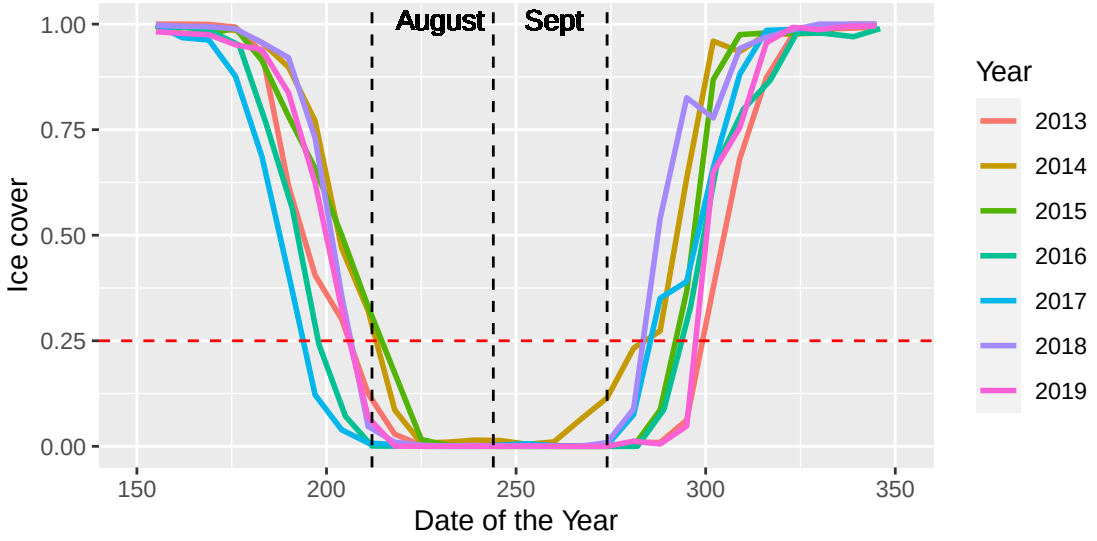

Figure 4.3: Weekly ice cover from 2013 to 2019.

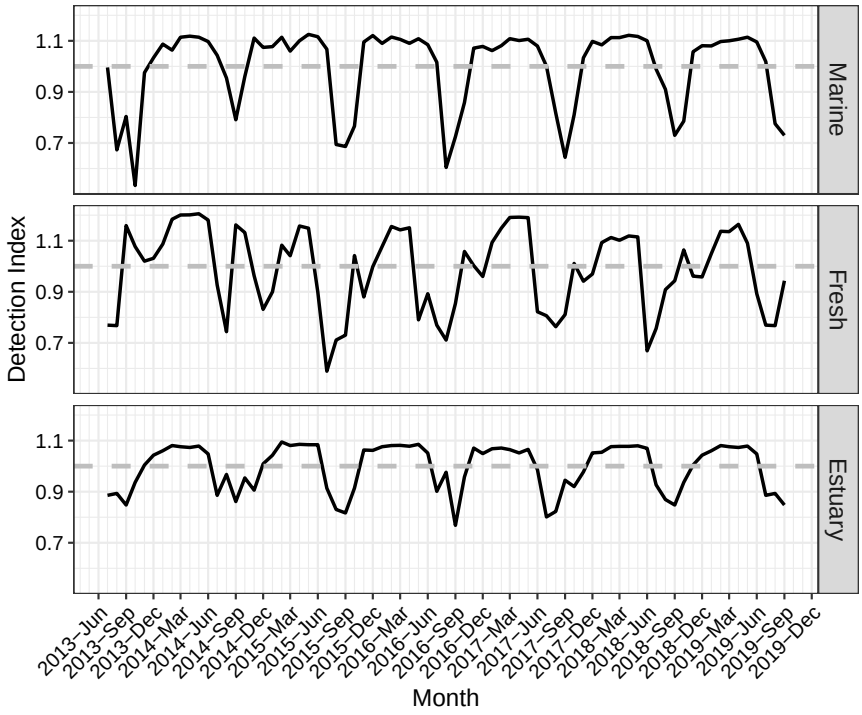

Figure 4.4: Monthly detection variability index (DVI) shown for marine, freshwater and estuarine habitats incorporated in this study (from June-2013 to December 2019). Horizontal lines on each plot represents the average DVI (note that DVI has been scaled for each habitat so that average DVI =1).

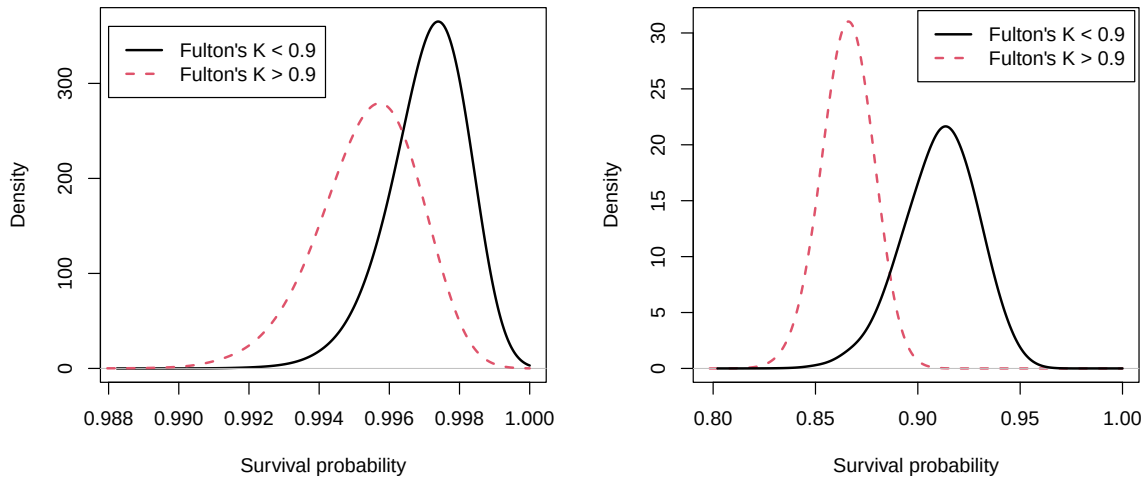

Figure 4.5: Marginal densities of survival probabilities for different levels of Fulton's condition factor and surface ice condition (left - ice-covered, right - open water). All the densities were obtained using kernal density estimation with the Gaussian kernal with arbitrarily selected bandwidths of 0.0005 (left) and 0.005 (right).

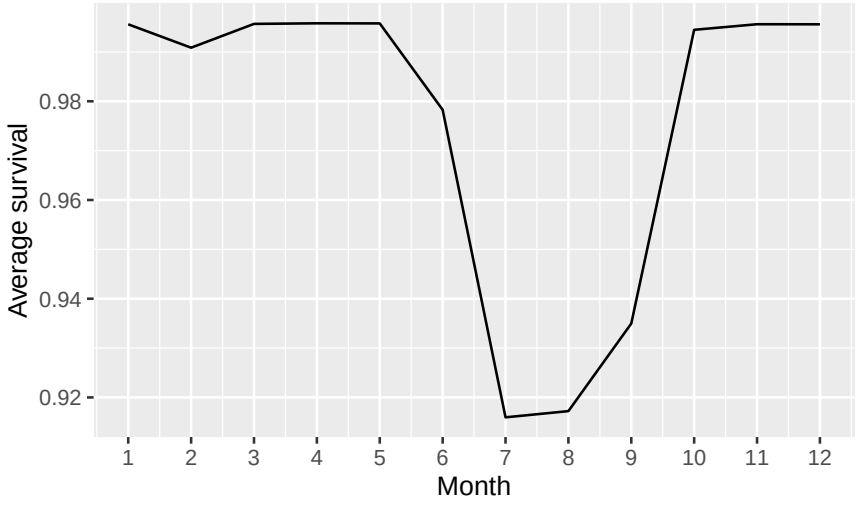

Figure 4.6: Monthly survival estimate obtained by averaging the simulated survival estimates using MCMC outputs.

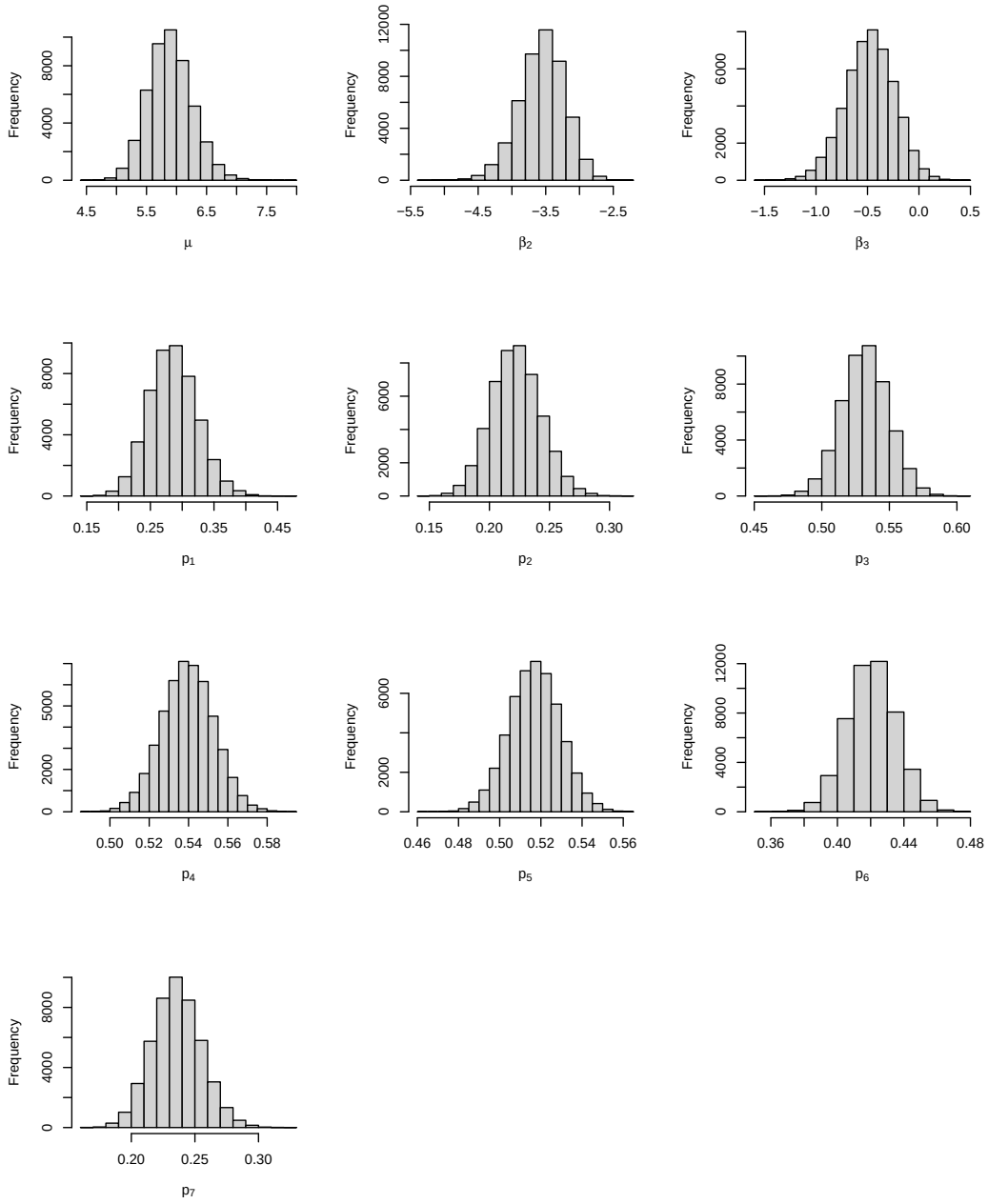

Figure 4.7: Posterior plots of parameter estimates for the best model. Here, β_0, β_2 and β_3 represent the intercept, coefficients for sea surface condition, and Fulton's condition factor respectively. $p_1, p_2, \ldots, p_7$ represents the annual detection probabilities.

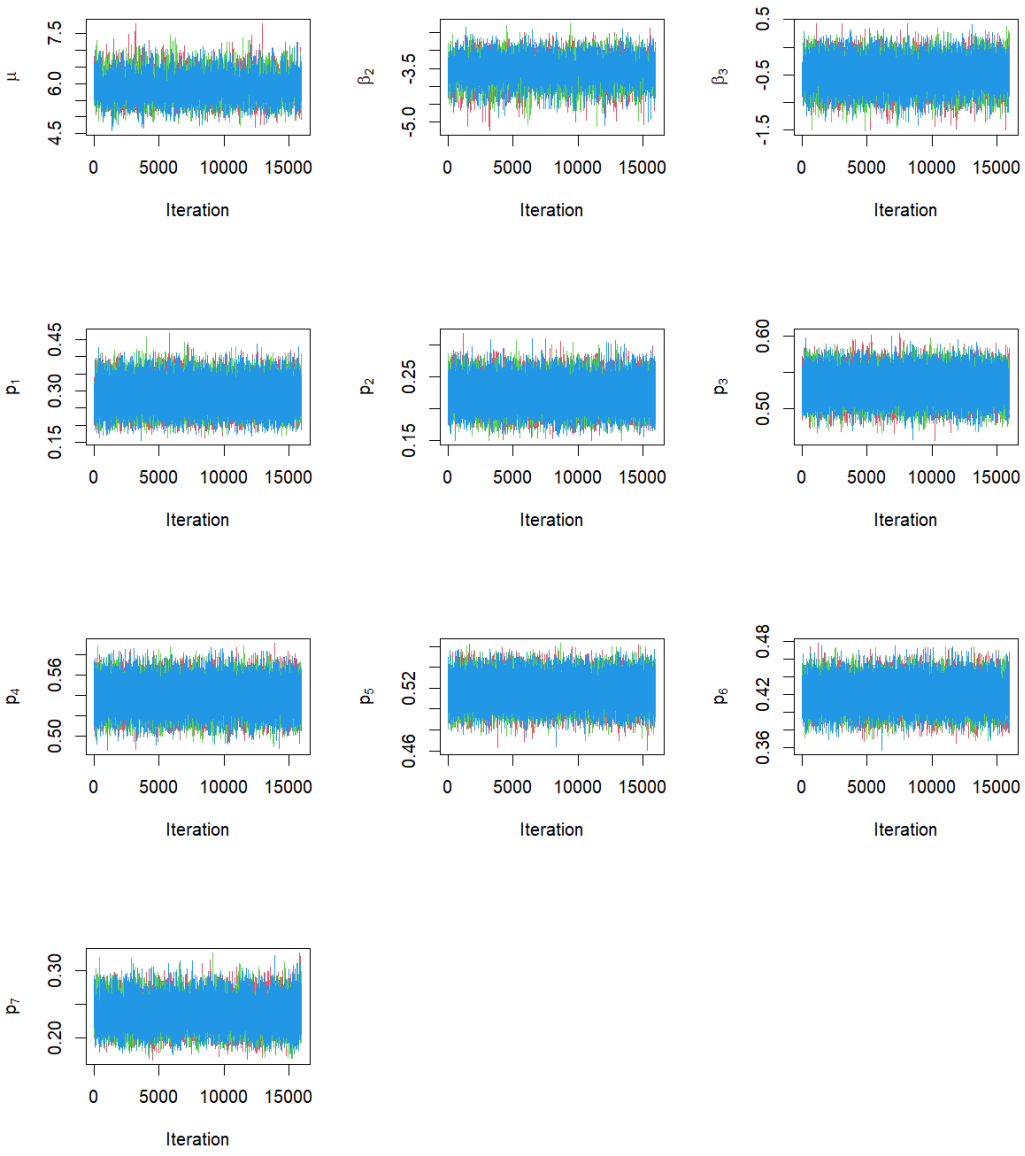

Figure 4.8: Trace plots of parameter estimates for the best model. Here, β_0, β_2 and β_3 represent the intercept, coefficients for sea surface condition, and Fulton's condition factor respectively. $p_1, p_2, \ldots, p_7$ represents the annual detection probabilities.

Chapter 5

Determining vulnerability of walleye to fishing effort using state-space modelling in Lake Winnipeg, Manitoba

Determining vulnerability of walleye to fishing effort using state-space modeling in Lake Winnipeg, Manitoba

Munaweera I[a], Muthukumarana S[a], Gillis D M[a], Watkinson D A[b], Charles C[b],

and Enders E C[b]

[a]University of Manitoba,

Winnipeg R3T 2N2.

[b]Fisheries and Oceans Canada,

501 University Cres.

Winnipeg MB R3T 2N6

To be submitted.

Abstract

Bayesian state-space models coupled with acoustic telemetry can be used as a powerful tool for effective decision-making in fisheries management. Lake Winnipeg supports one of the most important commercial and recreational walleye (*Sander vitreus*) fisheries in North America. Albeit the importance of the fishery, the spatial and temporal patterns of the vulnerability of walleye to commercial fisheries have not been examined due to the lack of information. This study utilized newly available data on walleye movement and walleye landings to develop a novel set of fishery metrics. Specifically, we employed Bayesian state-space models to estimate fish movement paths and incorporated fishing information from Lake Winnipeg, such as the amount of landings and quota assignments to investigate potential interactions between walleye movements and fishing activity in the lake. The developed fishery metrics included the probability of fish presence, probability of encounter, and potential fishing pressure. We observed that in early June and late October, fish are more concentrated near the major harbours and the fishing pressure was higher in early summer making walleye more vulnerable to fishing gear during those time periods. Furthermore, the assumed distance travelled to fish had only a small effect on estimated relative fishing pressure on the lake.

Keywords: Walleye, Fishing Effort, Acoustic Telemetry, Bayesian State-Space Models

5.1 Introduction

Lake Winnipeg, located in Manitoba, Canada, is the tenth largest lake in the world by surface area and accounts for the second-largest freshwater fishery in North America next to Lake Erie (Sheppard et al. 2015; Wassenaar and Rao 2012). Commercial fishing in Lake Winnipeg started in 1872, and it accounts for 40% of Manitoba's fish production (Franzin et al. 2003; Nicholson 2007). Walleye (*Sander vitreus*) is the most valuable species for commercial and recreational fisheries in Lake Winnipeg (Fisheries and Canada 2020; Stewart and Watkinson 2004). Despite the economic and recreational importance of the lake, comparatively little research has been conducted on Lake Winnipeg until recently (Ayles et al. 2011; Espinoza et al. 2011; Johnston et al. 2012). There are growing concerns that the changing conditions in Lake Winnipeg due to invasive species, increasing water demand, nutrient inputs, and continued exploitation by fisheries may result in increased stress for walleye (Environment and Climate Change Canada 2020).

Acoustic telemetry systems are increasingly used to study aquatic animal behaviour in both freshwater and marine ecosystems (Donaldson et al. 2014; Hussey et al. 2015). A systematically deployed two-dimensional array of receivers can be used to understand movements throughout a region (Kraus et al. 2018; Munaweera et al. 2021). However, the data collected by omnidirectional acoustic receivers are subject to large observation errors, especially when the distance between two adjacent receivers in the array is large (Alós et al. 2016). Bayesian state-space models (SSM) are a promising approach in estimating these unobserved animal movements (Alós et al. 2016; Bolker 2008; Patterson et al. 2008). Understanding the spatial and temporal distribution of aquatic species can be used to make effective fishery manage-

ment and fish conservation decisions (Brownscombe et al. 2019; Cooke et al. 2004, 2016). In the case of Lake Winnipeg, paths estimated from acoustic telemetry using Bayesian state-space models allow the study of interactions between fish movement patterns and fishing effort, which could be used to inform fishing regulations and quota allocations in regard to fishing locations and timing.

The Lake Winnipeg Basin Fish Movement Project, conducted by Fisheries and Oceans Canada with provincial agencies and academic partners, is a large-scale, long-term tagging project in the Lake Winnipeg basin. As a part of the Lake Winnipeg Basin Fish Movement Project,399 walleye were tagged, and a two-dimensional array of 148 omnidirectional acoustic receivers was systematically deployed in Lake Winnipeg and some of its major tributaries to detect the movements of tagged fish (Kraus et al. 2018; Munaweera et al. 2021). In our previous work, we presented a framework to estimate individual fish movement paths using the Bayesian state-space modelling approach (Munaweera et al. 2021). The objectives of this study were to use the estimated movement paths using the aforementioned framework to infer the interaction between walleye and commercial fishing activities in the south basin of Lake Winnipeg to describe variation in the potential vulnerability of walleye to commercial fishing pressure during the summer and fall seasons.

5.2 Materials and methods

5.2.1 Lake Winnipeg fishery

From 2000–2010, an annual average of 6.19 million kg of fish (CAD 16.4 million worth on average) were harvested from Lake Winnipeg (Manitoba, Canada) by 850–900 fishermen where walleye is the most harvested fish (Ayles et al. 2011). Since 1971, commercial fishing has been regulated by a quota system for three fish species (lake whitefish (*Coregonus clupeaformis*), walleye, and sauger (*Sander canadensis*) with a total of 6.4 to 7.1 million kg for those three species assigned to 13 community licensing areas around the lake (Figure 5.2). A community licensing area is the defined geographic area in which a fisher is required to have established residency in order to be eligible to acquire a quota entitlement for the adjacent fishing area, as depicted on the various seasonal plans of the Lake Winnipeg commercial fishery. Lake Winnipeg has two open-water fishing seasons (fall and summer) and a winter fishing season. The start date of the summer season changes annually depending on 80% completion of Walleye spawning.

5.2.2 Fishing effort data

For this study, we used the following data sources that are available for Lake Winnipeg to estimate fishing effort: fishing vessel slips (dock locations) from 22 harbours in Lake Winnipeg (Figure 5.1) observed through high-resolution aerial images (Figure 5.3), quota allocation data for 13 licensing areas (Table 5.1 and Figure 5.2), fish landing information obtained from 16 delivery points collected by Manitoba Natural Resources and Northern

Development.

5.2.3 Acoustic telemetry data

Fish were captured using boat electrofishing and tagged with 'Vemco V16-4H' acoustic transmitters (16 mm diameter, 24 g, 6 $\frac{1}{2}$ years expected battery life, with an average transmission delay of 120 s with a pseudo-random uniform interval between 80–160 s). Tagged fish were detected by a grid of Vemco VR2W and VR2Tx acoustic receivers deployed near the bottom of Lake Winnipeg and its major tributaries (Red and Winnipeg rivers). In the Red river, the distance between receivers was 5 km, and in the Winnipeg River, distances between receivers varied between 1.7 and 2.7 km. In the lake, the receivers were placed on a systematic grid varying between 5 km in the southern part of the south basin, 7 km for the rest of the south basin and narrows, and 14 km in the southern part of the north basin (Figure 5.1). Fish movement paths were estimated using Bayesian state-space models with acoustic telemetry data collected with the described grid array of acoustic receivers. Further information on acoustic telemetry setting and path estimation are presented in Munaweera et al. (2021).

5.2.4 Movement path estimation

Movement paths were estimated for 86 Walleye (average weight 3.132 kg with SD 1.004 kg, average total length 655.6 mm and SD 61.1 mm, and average fork length 622.1 mm, and 58.9 mm) that were detected throughout the period of June 1^{st}, 2017, to May 31^{st}, 2018 using the Bayesian state-space modelling (SSM) approach. A complete description of the

movement path estimation can be found in our previous work (Munaweera et al. 2021). Below is the summary of the methodology.

Since the acoustic detection records were in irregular time intervals, first, we made them regular by counting the number of detections recorded by each receiver within regular 3 h time bins. The SSM contains two sub-models; the process model and the observation model. A random walk based on continuous turning angles and step lengths was used as the process model as below.

$$x_{E,t+1} = x_{E,t} + l_t \sin(\Phi_t), \tag{5.1}$$

$$x_{N,t+1} = x_{N,t} + l_t cos(\Phi_t), \tag{5.2}$$

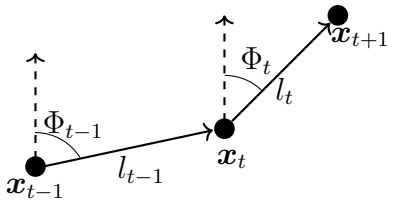

where the true position of the fish (which is unknown) at time t is given by $\boldsymbol{x}_t = \{x_{E,t}, x_{N,t}\}$, are in UTM coordinates. Here, l_t and Φ_t represent the step length and the turning angle at time t. We considered two scenarios for the distribution of l_t.

$$\text{Scenario 1:} \qquad l_t \sim N(\mu_l, 1/\tau_l), \tag{5.3}$$

$$\text{Scenario 2:} \qquad l_t \sim P\phi(\mu_1, \sigma_1^2) + (1-P)\phi(\mu_2, \sigma_2^2). \tag{5.4}$$

In Scenario 1, we considered the step lengths to arise from a single Gaussian distribution with parameters μ_l and τ_l, which represent the average step size and the precision (reciprocal of the variance) of the distribution of step size (l_t), respectively. In the second scenario, l_t was assumed to follow a Gaussian mixture distribution. Here, $\phi(.)$ denotes the Gaussian density and P defines the mixing probability, where μ_1 and μ_2 are the average step length sizes of the two mixing distributions and σ_1, σ_2 are the standard deviations of corresponding

distributions. The ideology behind using the mixture distribution is that fish change their movement behaviour with two-step length distributions at any time step with the probability P. For each fish, the SSM was fitted under both scenarios and the best scenario was selected using the deviance information criterion (DIC) presented by Spiegelhalter et al. (2002).

The observation model, which describes the detection probability, was estimated with the logistic function given by

$$log\left(\frac{\pi_{n,j}}{1-\pi_{n,j}}\right) = \alpha_n + \beta_n d_{n,j}, \tag{5.5}$$

where the distance from the true fish position to the j^{th} acoustic receiver at step n is denoted by $d_{n,j}$ and $\pi_{n,j}$ is the detection probability at j^{th} acoustic receiver at step n. The parameters α_n and β_n were estimated prior to applying the SSM with the non-linear least squares approach using data from a reference tag experiment in Lake Winnipeg (Munaweera et al. 2021).

SSM model estimation was conducted using the Bayesian MCMC approach with `'JAGS'` in R using the package '`R2jags`' (Su and Yajima 2015).

5.2.5 Fishing metrics

To represent the potential interactions between walleye movements (inferred from the SSM paths estimated using the tagged fish) and fishing activity (inferred from harbours and the number of fishing vessels in each harbour), we considered three metrics (probability of presence, probability of encounter, and potential fishing pressure) as described below. Since

we do not have information on how far and in which direction each fishing vessel travels in the lake from the harbour, we assumed a set of plausible regions defined by a set of radii (5 km, 10 km, 15 km and 20 km) by reviewing incident reports from lake Winnipeg by Transport Canada (The Transportation Safety Board of Canada 1999, 2001). However, there were only two reports available on Lake Winnipeg (in October 1999; 6.9 miles away from the harbour, and June 2001; about 14 miles away from the harbour) since they are only generated when there had been an accident or loss of life in the lake.

5.2.6 Probability of presence (PoP)

Assuming fishers travel r linear distance from the harbour for fishing. The probability of presence (PoP) for the ith fish interacting with a potential fishing region in the lake defined by radius r is calculated as

$$\text{PoP}_{i,r} = \frac{\sum_{t=1}^{n} \text{I}(\boldsymbol{x}_{i,t}, r)}{n}, \tag{5.6}$$

where n is the total number of (regular) time steps the fish were observed. Here, $\text{I}(\boldsymbol{x}_{i,t}, r)$ is an indicator function of the i^{th} fish location at time step t in UTM coordinates, $\boldsymbol{x}_{i,t}$ (obtained using the Bayesian SSM approach), and the fishing radius r given by

$$\text{I}(\boldsymbol{x}_t, r) = \begin{cases} 1 & \text{if } \min\limits_{1 \le j \le m} [d(\boldsymbol{x_{i,t}}, \boldsymbol{x_j})] < r, \\ 0 & \text{otherwise,} \end{cases} \tag{5.7}$$

where, $\boldsymbol{x}_j$ is the location of the j^{th} harbour, m is the number of harbours, and $d(\mathbf{.})$ is the Euclidean distance function. $PoP_{i,r}$ represents the probability of the i^{th} fish entering the potential fishing region defined by radius r.

5.2.7 Probability of encounter (PoE)

Assuming a collective fishing region defined by radius r (Union of all fishing regions within radius r from each harbour as shown in Figure 5.5), PoE for the i^{th} fish is calculated as

$$\mathrm{PoE}_{i,r} = \frac{\mathrm{PoP}_{i,r}}{(A_r/A_0)}, \tag{5.8}$$

where (A_r/A_0) is the relative increment of the area of the collective fishing region, A_0 is the area of the fishing region for the smallest assumed radius, and A_r is the area of the fishing region defined by radius r.

5.2.8 Potential fishing pressure (PFP)

PFP for the i^{th} fish interacting with a potential fishing region in the lake defined by radius r is calculated as

$$\mathrm{PFP}_{i,r} = \frac{\sum_{t=1}^{n}\sum_{j=1}^{m}\mathrm{I}(\boldsymbol{x}_{i,t},\boldsymbol{x}_j,r)\times h_j}{n} \times (A_0/A_r), \tag{5.9}$$

where, $\mathrm{I}(\boldsymbol{x}_{i,t},\boldsymbol{x}_j,r)$ is an indicator function of the fish location at time step t ($\boldsymbol{x}_{i,t}$), the j^{th} harbour location ($\boldsymbol{x}_j$) and fishing radius (r) given by

$$\mathrm{I}(\boldsymbol{x}_{i,t}, \boldsymbol{x}_j, r) = \begin{cases} 1 & \text{if } d(\boldsymbol{x_{i,t}}, \boldsymbol{x_j}) < r, \\ 0 & \text{otherwise.} \end{cases} \tag{5.10}$$

Here, h_j represents the fishing effort at harbour j. We used three different approaches to estimate the local intensity of fishing.

1. Using Quota

$$h_j = \text{Quota for harbour } j. \tag{5.11}$$

The quota for harbour j is obtained by dividing the total quota assigned for the licensing area of the fishermen who use the harbour, proportional to the number of commercial slips at the harbour except for the Gull Harbour and Hecla Harbour. Those harbours are used by fishers from both Riverton and Gimli licensing areas. Hence, first, we divided the number of slips in each harbour proportional to the number of fishers at each licensing area and then the quota was separately allocated to each group of slips and and then the sum of those quotas was taken from both licensing areas as the estimated quota for the harbour.

2. Landings approach

$$h_j = \text{Total landings from harbour } j.$$

The total weight of all landings for harbour j is obtained by dividing the weight of total landings reported by the fishermen from the licensing areas proportional to the number of commercial slips at each harbour. Again for the exceptions, Gull harbour and Hecla harbour, the landings were estimated similarly to the quota estimation described above.

3. Combined approach (for weekly metrics)

The quota for a licensing area is allocated for the whole season. In the quota approach we presented above, we assumed that the quota is evenly distributed throughout the fishing season. However, we observed that the number of landings is not constant throughout the seasons. Hence, in the weekly metrics calculation under this approach, we divided the total quota for the season proportional to the number of weekly landings for each week.

$$h_j = \text{Quota for harbour } j \times \frac{\text{Number of landings from harbour } j \text{ during the week}}{\text{Total number of landings during the season}}.$$

5.2.9 Metrics calculation

We obtained all the fishing metrics for the summer and fall fishing seasons for each individual tagged fish. We can identify two major fishing seasons in the lake; in summer, from the last week of May to the second week of July, and in fall, from the first week of September to the end of October. Since we estimated movement paths from June 1st, when calculating PFP for summer under the quota approach, the quota was adjusted for the part of the summer fishing season before June 1, assuming the quota is evenly distributed throughout the fishing season. Furthermore, when the weekly metrics were obtained under the quota approach, the quota was evenly divided between the weeks when the active fishing occurred (June 1–July 16 in Summer and September 1–November 1 in the Fall). In addition to the aforementioned metrics, we also obtained the weekly average distance between fish to document the level of aggregation of fish in the lake. The average distance between fish for week k is given by

$$\overline{D_k} = \frac{\sum_{i=1}^{n} d(\bar{\boldsymbol{x}}_{\boldsymbol{i,k}} - \bar{\bar{\boldsymbol{x}}}_{\boldsymbol{k}})}{N},$$

where N is the total number of fish, $\bar{\boldsymbol{x}}_{\boldsymbol{i,k}}$ is the activity center (average location) of the i^{th} fish during week k, and $\bar{\bar{\boldsymbol{x}}}_{\boldsymbol{k}}$ is the activity center for all fish during week.

5.2.10 Density estimation

Once the fishing metrics were calculated on an individual level, to estimate probability density functions of fishing metrics, we used the kernel density estimation method with the Gaussian kernel using R. To obtain the fish densities on the lake seasonally and weekly, we used two-dimensional kernel density estimation with bi-variate Gaussian kernel using posterior density points obtained from the Markov chain Monte Carlo (MCMC) output of the movement paths of each fish using R.

5.3 Results

The spatial distribution of fish showed clear differences between summer and fall fishing seasons (Figure 5.6). In summer, the fish were more concentrated in the southern part of the southern basin (Riverton region) while they were more spread out in the fall, with some concentration near Hecla and Manigotagan regions. Also, we noticed temporal changes in the fish distribution on weekly densities (Figure 5.7). In early June, fish were more concentrated in Riverton and Hecla regions, and gradually the fish spread throughout the lake until mid-August. Then, they concentrated on the Manigotagan and Victoria Beach regions and returned to the Hecla region again by the end of October. Complete weekly fish densities can be found in the Appendix (Figure C.2). The average distance among fish

during early summer and late fall were lower compared to other weeks (Figure 5.16c).

The densities for the probability of presence (PoP) showed visible differences between the two fishing seasons for larger fishing radius (Figure 5.8). Specifically in the summer, under an assumed fishing radius of 20 km, most fish had PoP close to 1. The average PoP was higher in the summer fishing season compared to the fall fishing season (Figure 5.9). This is explained by the high fish density in the south basin in the summer compared to fall (Figure 5.6). PoP increases as expected as the radius increases, essentially encompassing more area of the lake where walleye occur. The average difference between the two fishing seasons also increases as the fishing radius increases (Figure 5.9). In summer, the fish density was higher in the region between Hecla Island and Gimli, where there are many harbours along the shore. In the fall, we observed a higher spread in the spatial distribution of fish rather than concentrating on a single region and hence, the probability of a fish being inside the fishing region was lower than in the summer.

Densities for the probability of encounter (PoE) for the summer fishing season and the fall fishing season showed some noticeable differences for all fishing radius values (Figure 5.10). In summer, PoE tended to concentrate around 0.1 as the fishing radius increased. In the fall, PoE under a small fishing radius was close to zero and the distribution of PoE again concentrated around 0.8 for 20 km radius. In the summer, the average PoE first increased and then reduced as the fishing radius increased, but the average PoE values for the fall fishing season increased as the radius increased (Figure 5.11). However, the average PoE values for the summer fishing season were larger than those for fall for all the fishing radius. Also, we noticed that the standard errors of those averages decreased with increasing radius.

Seasonal potential fishing pressure (PFP) densities obtained with both quota approach Figure (5.12) and the weight of the landing approach (Figure 5.13) showed some visual differences between the two seasons, especially for 20 km of fishing radius. Under both methods, the PFP increased on average as the radius increased. Overall, the average PFP was larger for the summer fishing season than the fall fishing season for all assumed radius values under both approaches (quota and landings). However, the trend in the two types of metrics (with quota and with landings) was similar (Figure 5.14 and Figure 5.15).

Weekly relative PFP under different approaches also showed visible differences (Figure 5.16f). In metrics calculation, we assumed the quota to be zero for summer weeks when no fishing was recorded and we divided the quota equally between the remaining weeks in summer. Hence, we saw that the metrics under the quota approach were exactly zero during those summer weeks. However, the behaviour in weekly PFP calculated with the daily landings and combined approach were similar to each other but different from the quota approach. Also, we saw that the weekly PFP with the landing method somewhat followed the number of landings (Figure 5.16). However, we noticed a small spike in the fishing pressure under the landing weight approach at the end of October when the fish were more concentrated in the Hecla region (Figure 5.7). Also, we observed that the assumed fishing radius had only a little effect on the relative PFP metrics under all approaches (Figure 5.7).

5.4 Discussion

In this work, we combined the available fishery data with the movement paths estimated with the state-space modelling approach to gain insights into the potential vulnerability of walleye to fishing pressure. The fishing pressure increased as the assumed distance travelled to fish (fishing radius) increased. We observed a higher fishing pressure in summer compared to the fall season, and also, the fishing pressure in Lake Winnipeg showed some connection to the spatial distribution of fish. In early summer and late fall, the fish were more concentrated in the southern part of the southern basin where most of the major harbours are located. Since the amount of fishing effort was also high in early summer, we see a higher fishing pressure in this period compared to the other periods making walleye more vulnerable to fishing gear. Fish were comparatively dispersed in the fall with more activity in the north basin where there is limited fishing effort.

In this study, one of the major assumptions we made was the fishing radius. Our only source of reliable information was two accident reports on Lake Winnipeg by Transport Canada. Hence, we assumed a set of plausible values as the fishing radius in order to calculate the potential fishing pressure. However, interestingly, we noticed that the fishing radius has little effect on our metric of the relative fishing pressure on the lake. Also, a more accurate measure of fishing pressure would require additional information such as how many trips each vessel makes, when and where they lay their nets, how long the nets were in the water, and the specifications of those nets Bordalo-Machado (2006); McCluskey and Lewison (2008); Stewart et al. (2011). Since the movement paths can be estimated with a fine temporal resolution (3 hours in this study), further information such as the exact location and time

of the day fishers fish would allow us to better estimate fishing pressure on fish in different regions of the lake throughout the year. We strongly recommend the collection of this data in fisheries where it is not currently available. Albeit the recreational fishery on Lake Winnipeg is of high economic value, they catch only a small portion of the fish. Hence, we only focused on commercial fishing activities in this study.

Even though this work was based on limited data, including detection records from a sample of mature walleye and approximate fishing effort, the findings of this study will bring light in better understanding of the spatial and temporal distribution of walleye in Lake Winnipeg and the interaction between fishing activities and fish movement paths that can be ultimately used for effective fishery management and conservation decisions making (Brownscombe et al. 2019; Cooke et al. 2004, 2016). Knowing when and where fish are located can be used in implementing regulations and adaptive quota allocation strategies among regions contributing to improved sustainability in the lake's fishery. Hence, this information can be used for both conservation and improving the efficiency of the fishery by informing fishers when and where best to fish. To our knowledge, we do not find a similar study that combines fish movement paths estimated through acoustic telemetry and fishing effort. Hence, this work brings a novel approach to estimating fishing pressure by combining acoustic telemetry data with fishing activities in the study area.

In this work, we used the individual walleye movement paths estimated using Bayesian state-space modelling with acoustic telemetry data and available fishery information to study the vulnerability of walleye to commercial fishery in Lake Winnipeg. Even though acoustic telemetry and Bayesian models are powerful tools that can be used to understand hidden

fish movements, the study was limited due to the availability of fishery information on the lake. Hence, as more fishery information (e.g. vessel information and fishing locations) becomes available, we will be able to make maximum use of these powerful tools.

Table 5.1: Quota allocation and the number of registered fishers per licensing areas.

Licensing Area	Quota (kg)		Number of
	Summer	Fall	Fishers
1. Selkirk	83,110	54,910	21
2. Gimli/Winnipeg Beach	824,090	353,340	143
3. Riverton	270,730	10,0020	57
4. Jackhead/McBeth	591,040	113,630	99
5. Matheson Island	380,820	161,180	68
6. Dauphin River	96,530	85,280	64
7. Grand Rapids	281,574	112,290	104
8. Poplar River	220,930	25,600	39
9. Berens River	382,920	109,200	65
10. Bloodvein	106,290	38,200	19
11. Manigotogan	148,170	103,990	47
12. Victoria Beach	42,200	16,700	13
13. Norway House	269,960	200,000	52

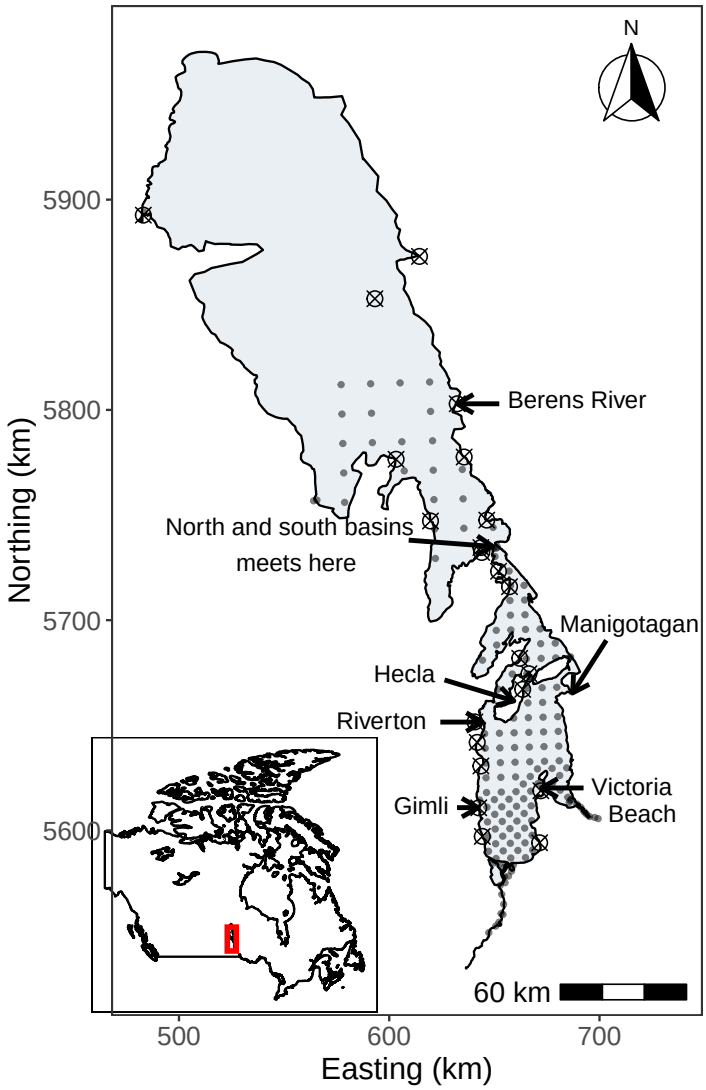

Figure 5.1: Map of Lake Winnipeg. The locations of the acoustic receivers are indicated by '•' and the location of harbours are denoted by '⊗'. The map was made using R with ggplot2. All the harbours below the Berens River were considered in the analysis.

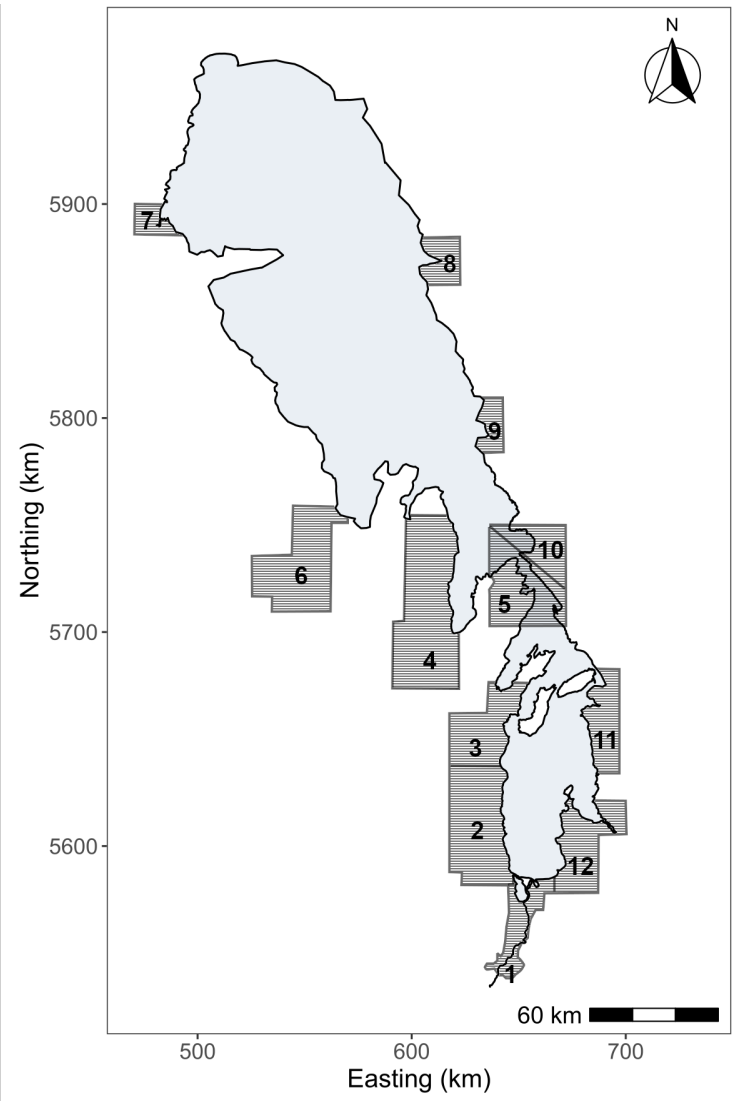

Figure 5.2: Map of community licensing areas in Lake Winnipeg in Table 5.1.

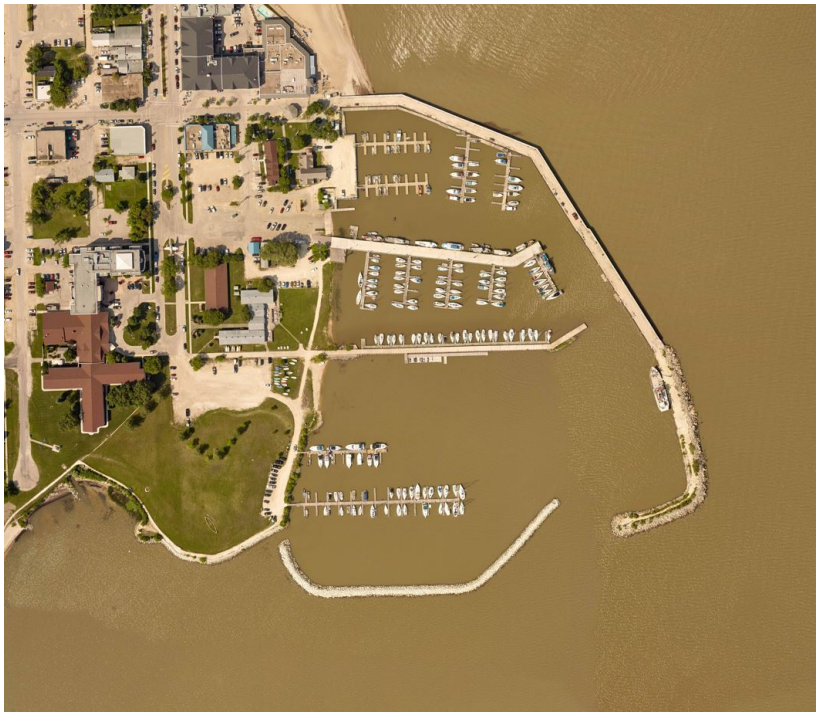

Figure 5.3: High-resolution aerial images were used to obtain fishing vessel information from 22 harbours. The image shown above is the Gimli Harbour.

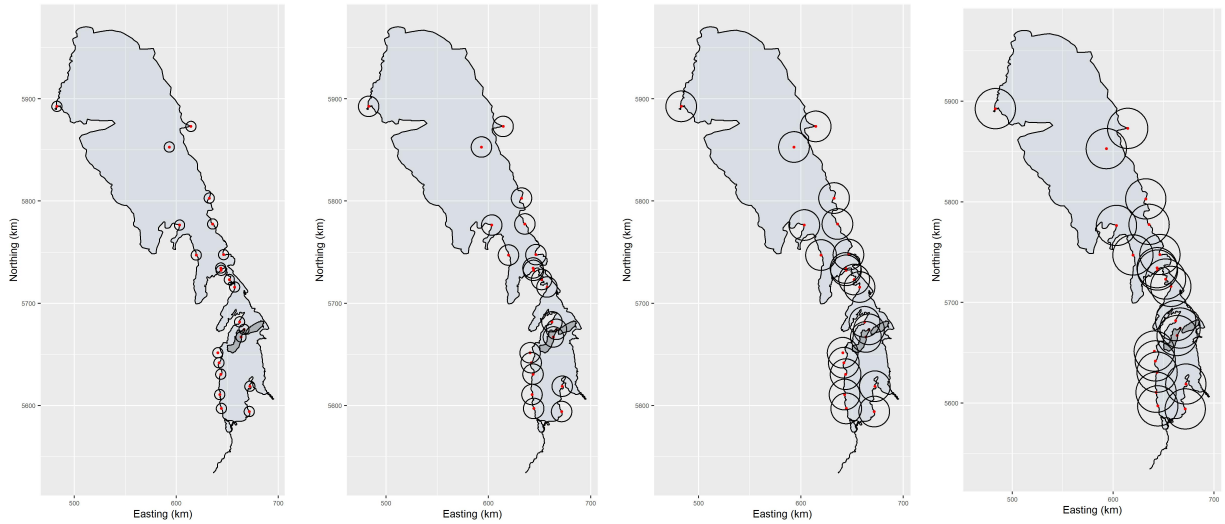

Figure 5.4: Different fishing radii (5 km, 10 km, 15 km, and 20 km) were assumed to study the interaction with fish.

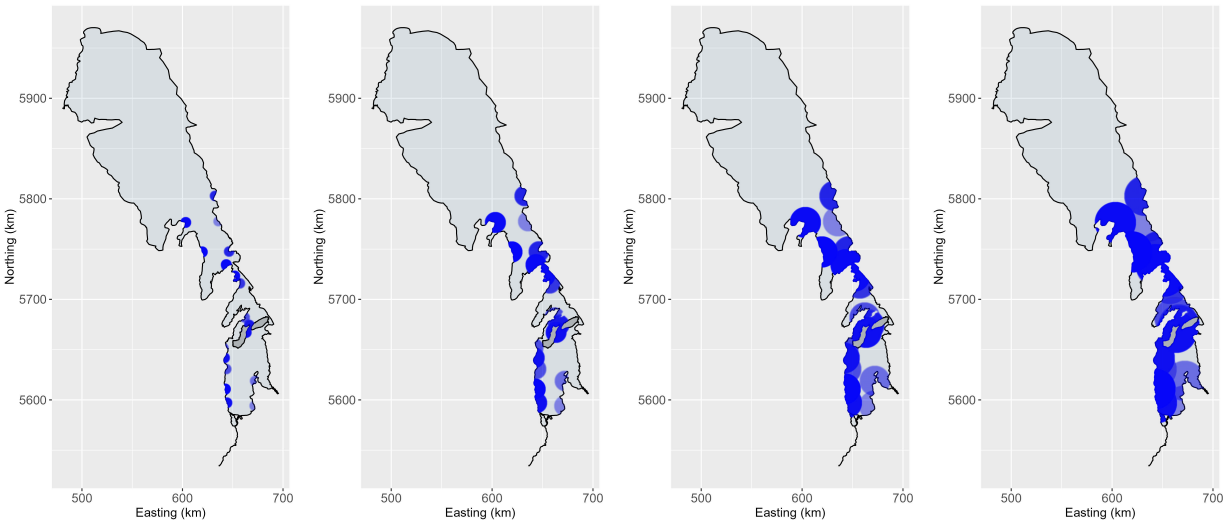

Figure 5.5: Assumed potential fishing regions under different radii (5 km, 10 km, 15 km, and 20 km). The colour intensity in the shaded regions gives an idea of the number of landings from the harbour (i.e., darker regions represent the regions with a higher number of landings).

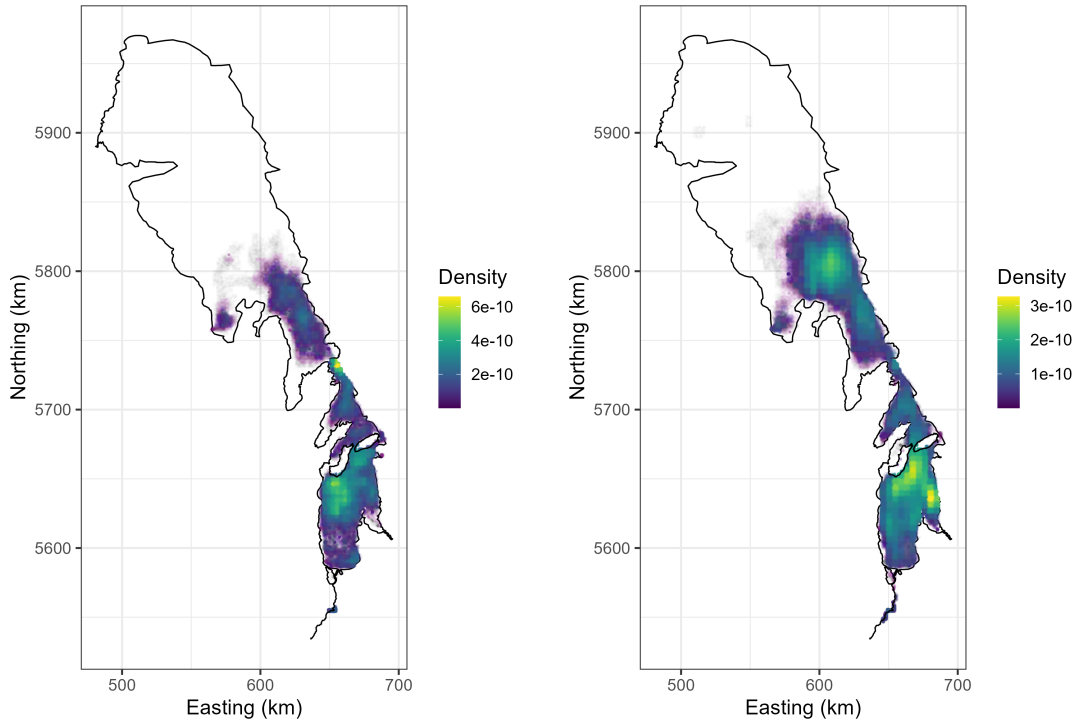

Figure 5.6: Two-dimensional density plots of fish locations in summer (left) and fall (right) fishing seasons, where the two fishing seasons are June 1–July 16, and September 1–November 1 respectively. The density plot was constructed using two-dimensional kernel density estimation with the bi-variate Gaussian kernel applied to posterior density points obtained from the Markov chain Monte Carlo (MCMC) output of the movement paths in R using "kde2d" function.

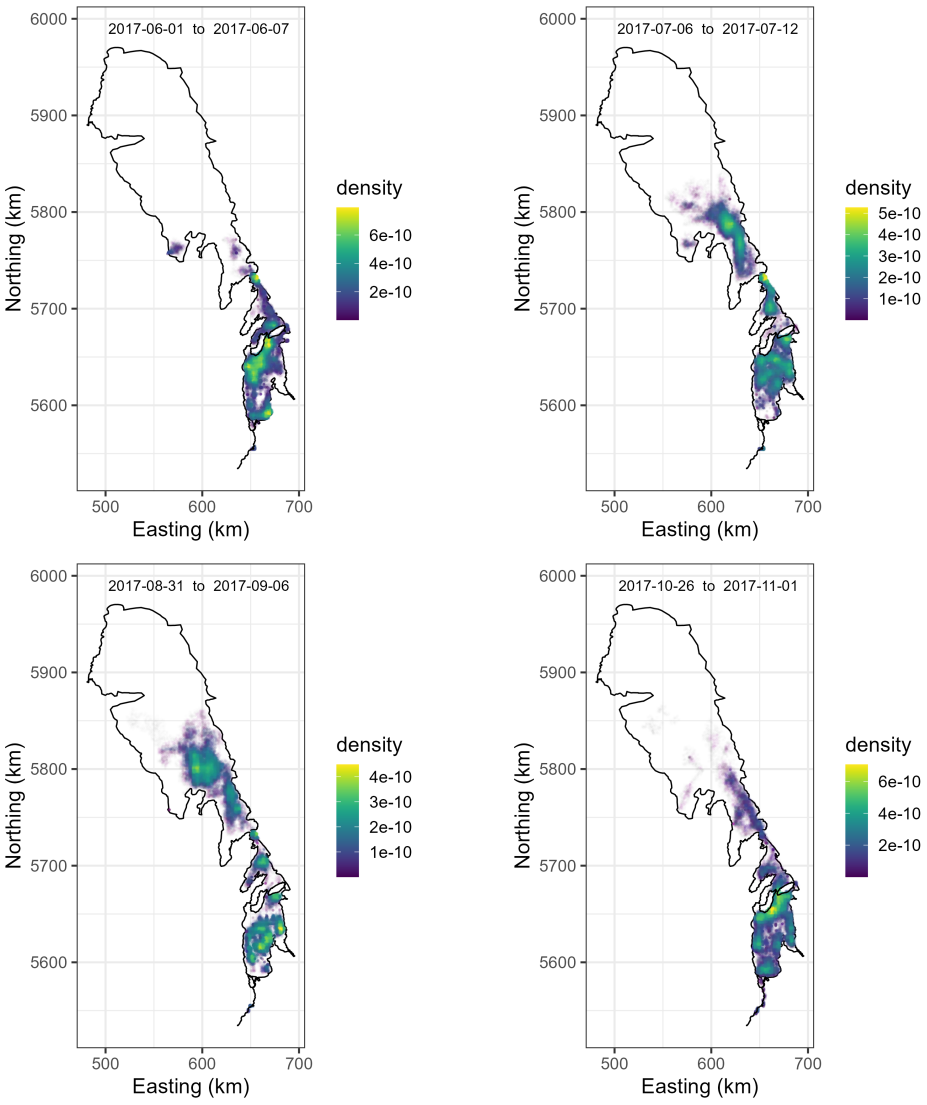

Figure 5.7: Two-dimensional density plots constructed using posterior distributions of walleye movement paths estimated with Bayesian state-space models for selected four weeks of the study duration.

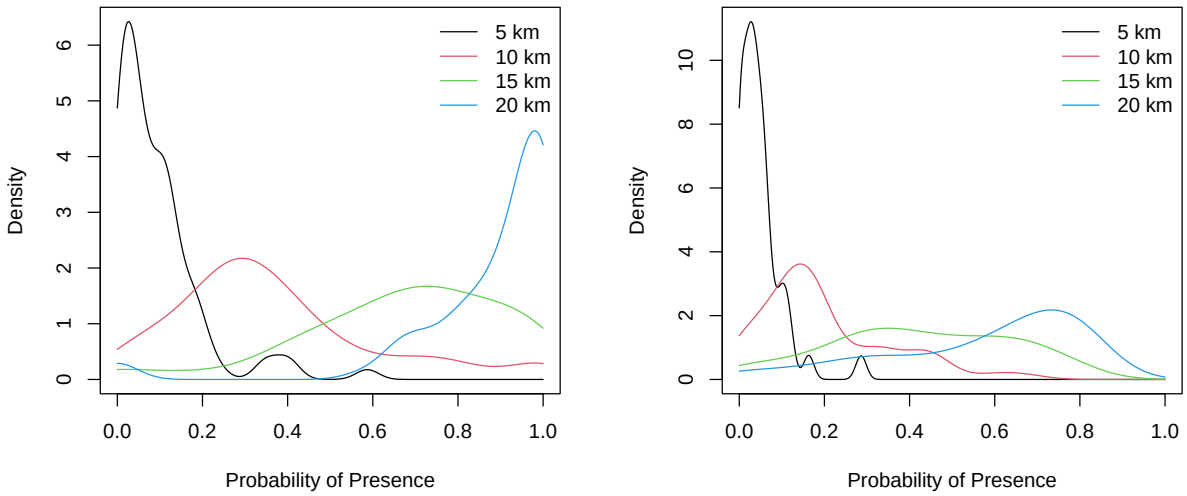

Figure 5.8: Kernel density estimation of the probability of presence for summer fishing season (left) and fall (right), where the two fishing seasons are June 1–July 16, and September 1–November 1 respectively. The density plot was constructed using two-dimensional kernel density estimation with bi-variate Gaussian kernel applied to posterior density points obtained from the Markov chain Monte Carlo (MCMC) output of the movement paths in R using "kde2d" function.

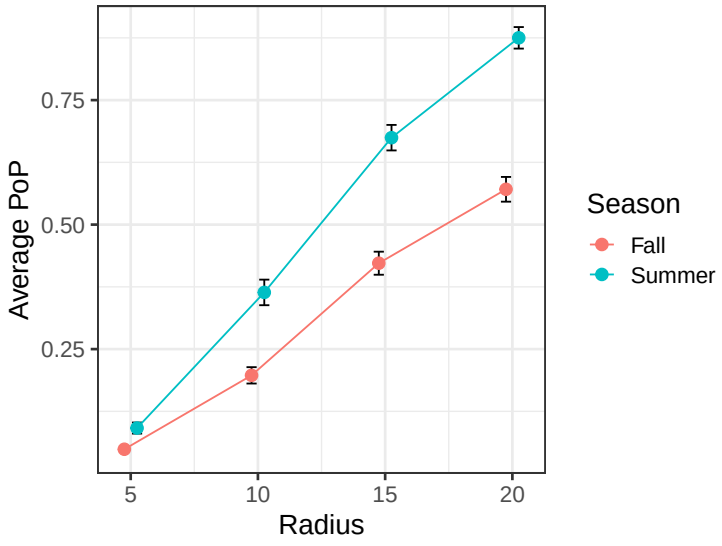

Figure 5.9: Average probability of presence (PoP) and standard errors, where the two fishing seasons are June 1–July 16, and September 1–November 1 respectively.

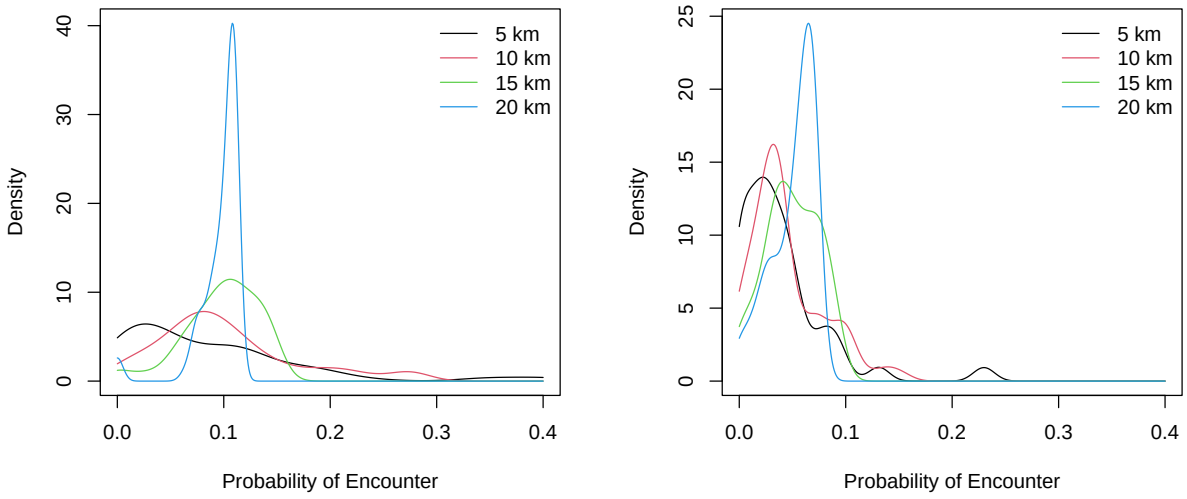

Figure 5.10: Kernel density estimation of probability of encounter for summer fishing season (left) and 2 (right), where the two fishing seasons are June 1–July 16, and September 1–November 1 respectively.

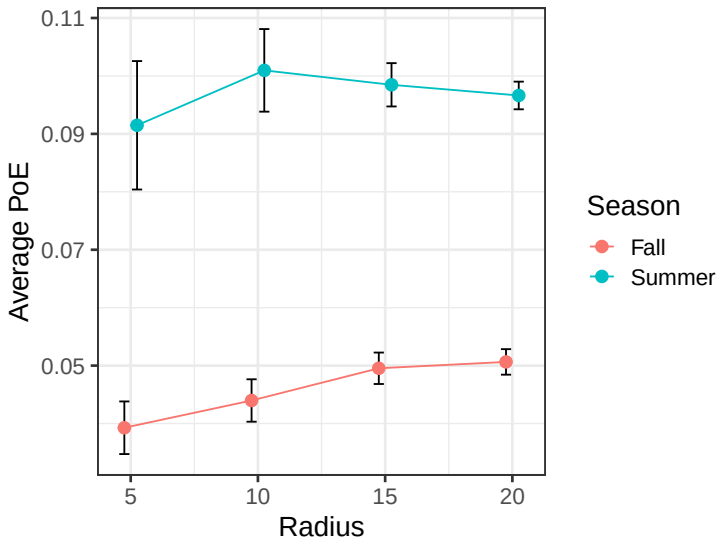

Figure 5.11: Average probability of encounter (PoE) and standard errors, where the two fishing seasons are June 1–July 16, and September 1–November 1 respectively.

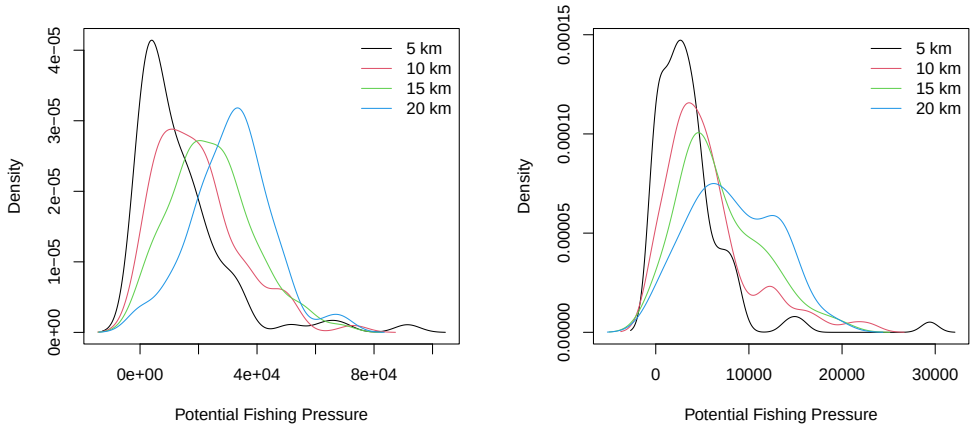

Figure 5.12: Kernel density estimation of potential fishing pressure (PFP) with quota approach for summer fishing season (left) and fall (right), where the two fishing seasons are June 1–July 16, and September 1–November 1 respectively.

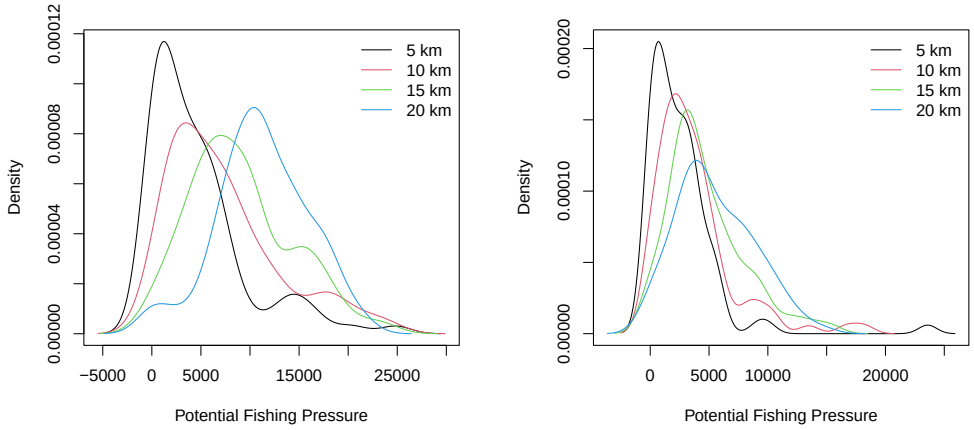

Figure 5.13: Kernel density estimation of potential fishing pressure (PFP) landings approach for summer fishing season (left) and fall (right), where the two fishing seasons are June 1–July 16, and September 1–November 1 respectively.

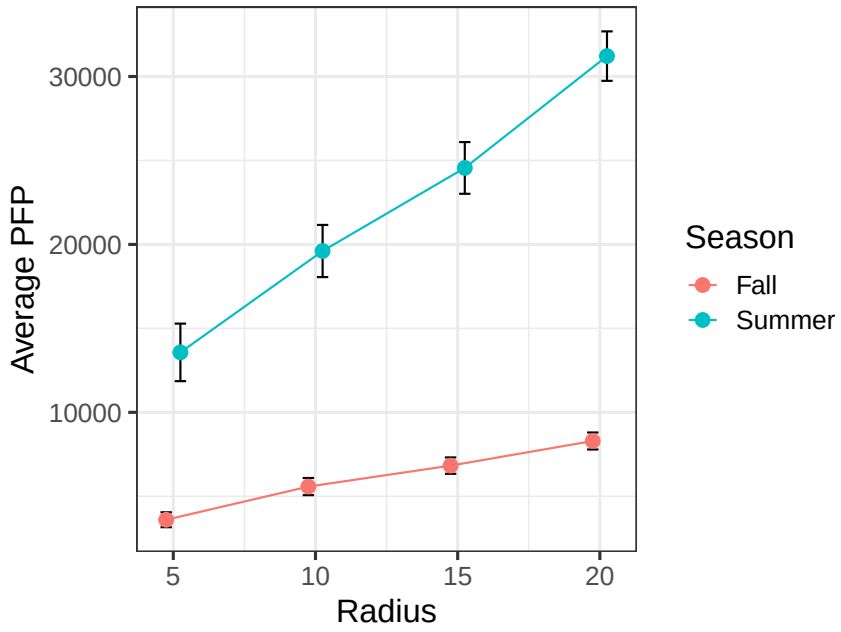

Figure 5.14: Average potential fishing pressure (PFP) and standard errors using quota approach, where the two fishing seasons are June 1–July 16, and September 1–November 1 respectively.

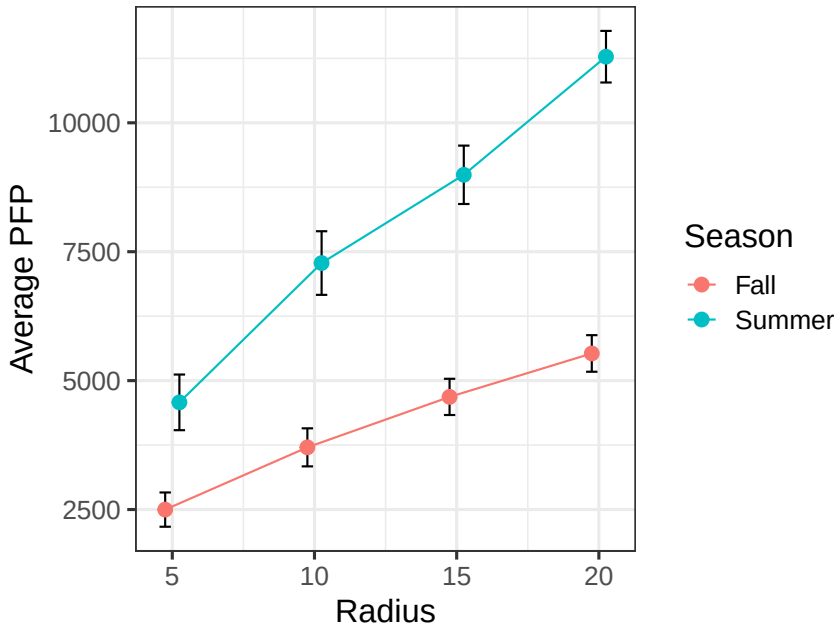

Figure 5.15: Average potential fishing pressure (PFP) and standard errors using landings approach, where the two fishing seasons are June 1–July 16, and September 1–November 1 respectively.

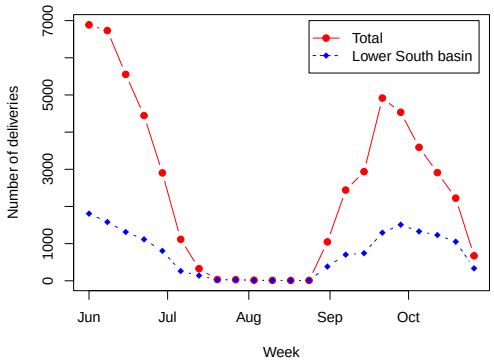

(a) Weekly deliveries

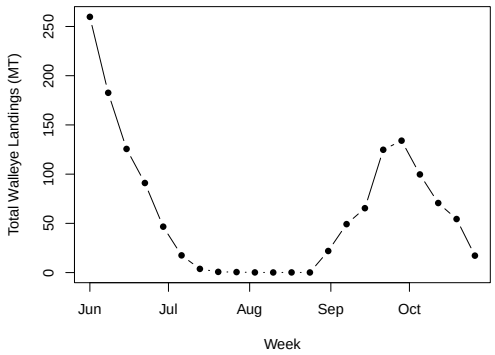

(b) Weekly landings

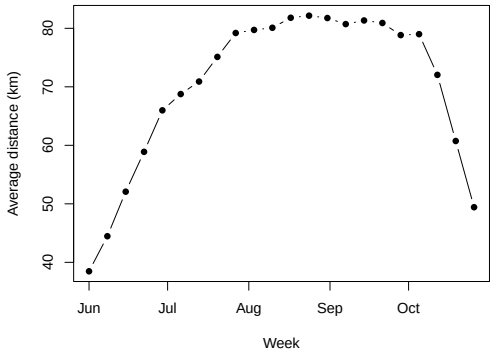

(c) Average distance between fish

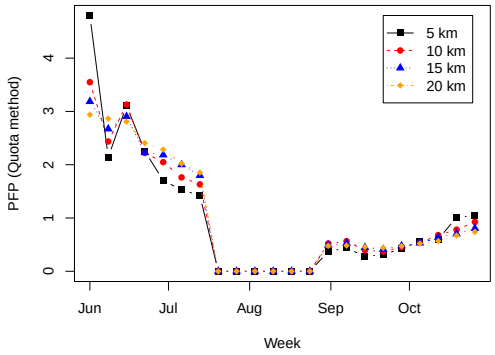

(d) PFP (Quota method)

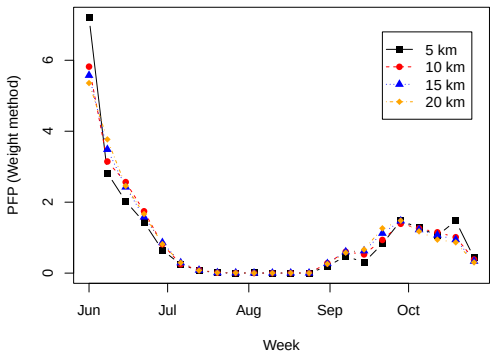

(e) PFP (Landings method)

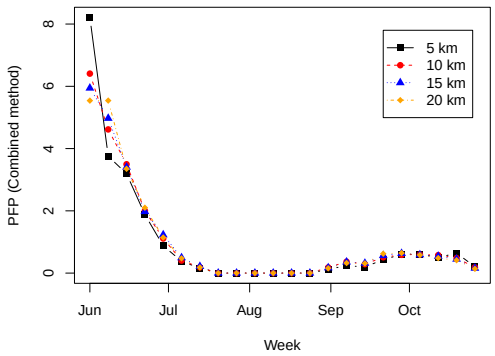

(f) PFP (Combined method)

Figure 5.16: Weekly potential fishing pressure (PFP) metrics under different approaches and other metrics. Figure (a) shows both the weekly total number of deliveries and the deliveries reported at community licensing areas 2, 3, and 11 (Lower south). Note that the weekly PFP values in (d), (e), and (f) have been scaled so that the average PFP is 1.

Chapter 6

Discussion

In this thesis, we developed Bayesian methods for modelling data collected using acoustic telemetry systems. The thesis provides practical solutions for many challenges that will arise from the planning stage of the study to the data analysis stage of widely used omnidirectional acoustic telemetry studies.

In chapter 2, we estimated unobserved movement paths for Walleye using Bayesian SSMs with acoustic telemetry data from a systematically deployed two-dimensional array of receivers in Lake Winnipeg. Compared to the classical smoothing methods, such as kernel smoothing and cross-validated local polynomial regression, the SSM approach resulted in more realistic movement paths well-constrained within the lake. Also, we noticed that the SSM approach has the ability to predict the fish moment path for the periods where there were no detection records by borrowing information from data-rich periods. Furthermore, using an intensive simulation study, we found that the estimated ecological movement metrics using the SSM approach had better accuracy than the classical approaches.

In the manuscript we presented in Chapter 3, we use the Bayesian multi-state mark-recapture modelling approach to estimate the survival and recapture probabilities of Arctic char in the marine, estuary and freshwater environments with data obtained using a traditional acoustic telemetry system. We found that the fish survival rate and recapture probability were generally higher in the freshwater than in the marine and estuary environments. The survival estimates of our study were similar to the previous study done by Caza-Allard et al. (2021); however, the standard errors of survival estimates in our study were much lower than those reported in Caza-Allard et al. (2021), showing the superiority of the Bayesian multi-state mark-recapture modelling approach over classical CJS approach.

In Chapter 4, we examined the effect of environmental (sea surface temperature (SST), surface ice conditions) and individual covariates (Fulton's condition factor and sex of each fish) on the survival probabilities of Cambridge Bay Arctic char using Bayesian hierarchical models. The proposed model can account for the varying detection probability due to the changes to the receiver array across the study duration and any seasonal variation in detection probability due to changing environmental conditions. We noticed that the detection probability of a fish by the receiver is lower in summer than in winter on average in all environments. Furthermore, we found that the surface ice condition and Fulton's condition factor are important in predicting the survival of Arctic char in the region. Moreover, by observing monthly marginal posterior distributions of survival, we notice that Arctic char has a higher mortality rate in summer months compared to winter months.

In the final manuscript in Chapter 5, we developed a novel set of fishery metrics using fish movement paths estimated with the Bayesian SSM approach and available fishing informa-

tion on Lake Winnipeg to study the vulnerability of Walleye to commercial fisheries in the lake. We found that Walleye were more vulnerable to fishing gear during early summer and late Fall periods since the fish were more concentrated near some major harbours. In this study, we had to assume a set of values for fishing radius (distance travelled to fish) due to the lack of data. However, the fishing radius had only a small effect in studying the relative fishing pressure on the lake. Even though we did not have ideal fishing effort information such as how many trips each vessel made, how long and where the nets were placed in the lake, and the specifications of the nets, the metrics we developed in this manuscript using available data will provide valuable information on when and where Walleye are most vulnerable.

Acoustic telemetry is one of the most effective tools in understanding the complex animal behaviour in submerged aquatic ecosystems that would be challenging to monitor otherwise (Cooke et al. 2013; Francisco et al. 2020; Lennox et al. 2017). With the rapid improvement of acoustic telemetry technology, such as miniaturized transmitters, receivers that can remotely offload data, and tags with improved efficiency, some of the main limitations of acoustic telemetry will be removed, and we expect to see the use of such systems more frequently in the near future (Hussey et al. 2015; Lennox et al. 2017). Hence, continuous development of statistical tools that can effectively analyze large and complex data sets generated by telemetry systems is equally important (Cooke et al. 2013; Lennox et al. 2017).

Acoustic telemetry is increasingly used as the primary method for monitoring movements and aquatic animals for informed management and conservation decision making (Crossin et al. 2017; Lees et al. 2021; Matley et al. 2022). The reconstructed paths of walleye presented

in Chapter 2 can be used to gain insights into the behavior and movement patterns of this important fish species, enabling the development of more effective fishing strategies. For example, by analyzing the spatial distribution of female walleye obtained using reconstructed movement paths in Chapter 2, fisheries managers can identify important spawning regions and implement targeted gillnet regulations and mesh sizes to reduce accidental capture of spawning walleye during the spawning season. This can help preserve the walleye population and support sustainable fishing in the lake. Also, the spatial distribution of walleye can reveal when and where fish can be harvested with minimum effort for a viable fishery in the lake under increasing resource costs. In addition, the information can also be used to optimize the grid by repositioning or adding receivers to regions with higher fish density to monitor them closely. Similarly, more precise estimates of the survival of Arctic char in different areas over multiple years and revealing any factors that would affect their survival will lead to better management and conservation decisions. For instance, implementing regulations to reduce mortality during the summer months when we observed low survival probabilities.

The proposed methods in this thesis are very flexible and can be adapted to study other species as well. For instance, the proposed SSM modelling framework in Chapter 2 can be used to model other fish species such as Burbot, Lake Whitefish, Channel Catfish, Lake Sturgeon, and Common Carp in Lake Winnipeg that are already tagged under the Lake Winnipeg Basin fish movement project, with minor adjustments to the priors and the process model. The framework can be easily modified to estimate movement paths for other aquatic or terrestrial animals by utilizing data obtained from fixed automated observer stations that detect the animal presence, such as Radio Frequency Identification (RFID) technology or

camera traps with motion sensors for monitoring wild animals. The Bayesian multi-state mark-recapture models we developed in Chapter 3 can also be used to monitor the survival of study species over multiple habitats using a fixed array of receivers. Furthermore, the proposed Bayesian hierarchical modelling framework in Chapter 4 can be easily adapted to study the impact of environmental and biological factors on the survival of animals monitored with a grid of receivers, where detection probability varies temporally and spatially. Finally, the findings of each project in this thesis offer valuable insights and information for fishery managers, providing them with the tools to make informed decisions regarding the management and conservation of these valuable aquatic species in the corresponding regions.

Appendix A

Appendix for Chapter 2

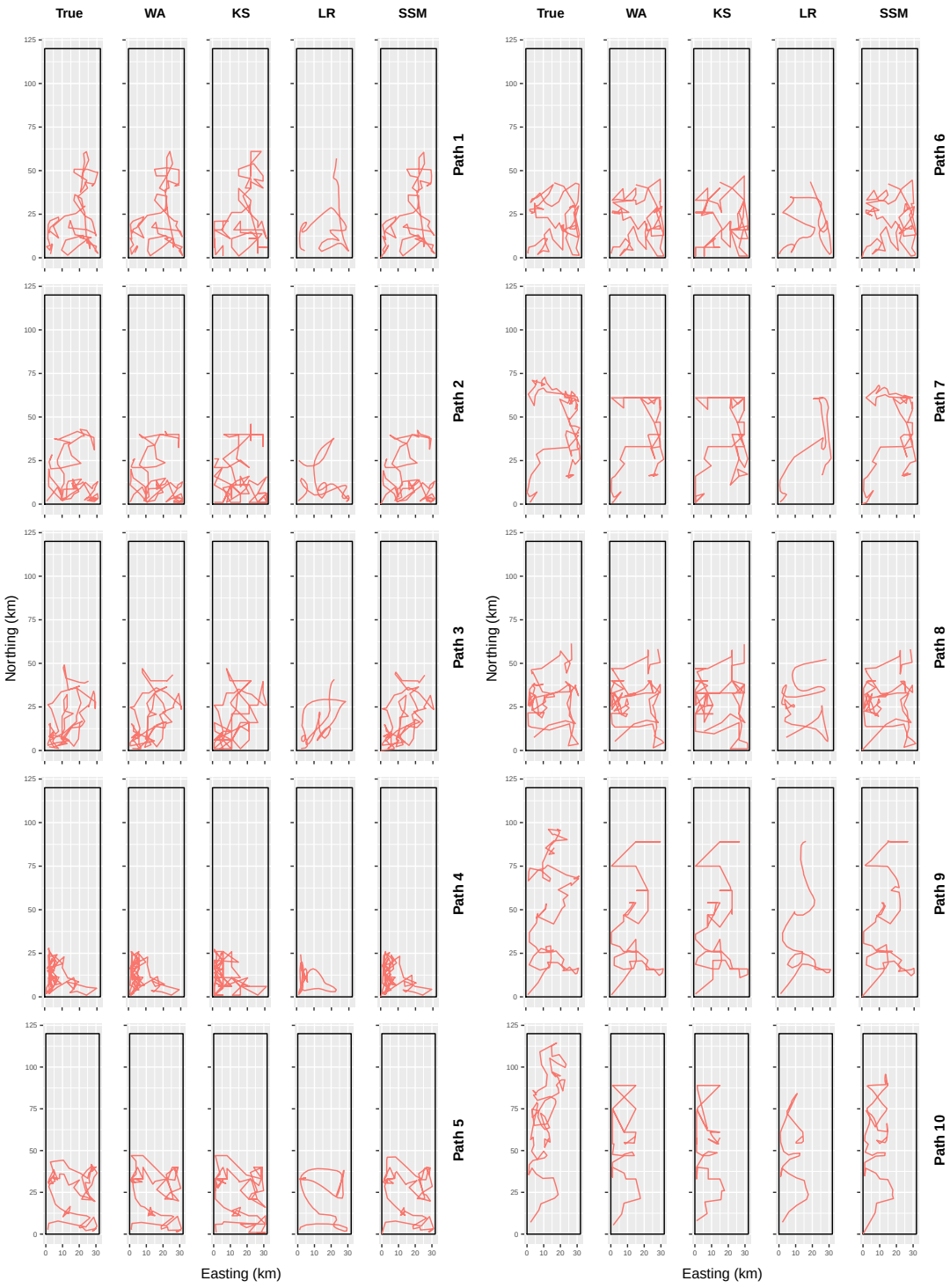

Figure A.1: Reconstructed movement paths with the true average path using three hour time bins, the simple weighted average method (WA), kernel smoothing with the Gaussian kernel (KS), cross-validated local polynomial regression approach (LR), and the state-space modeling approach (SSM) for Simulation 1 (Bin hours = 3 and tracking period = 10 days).

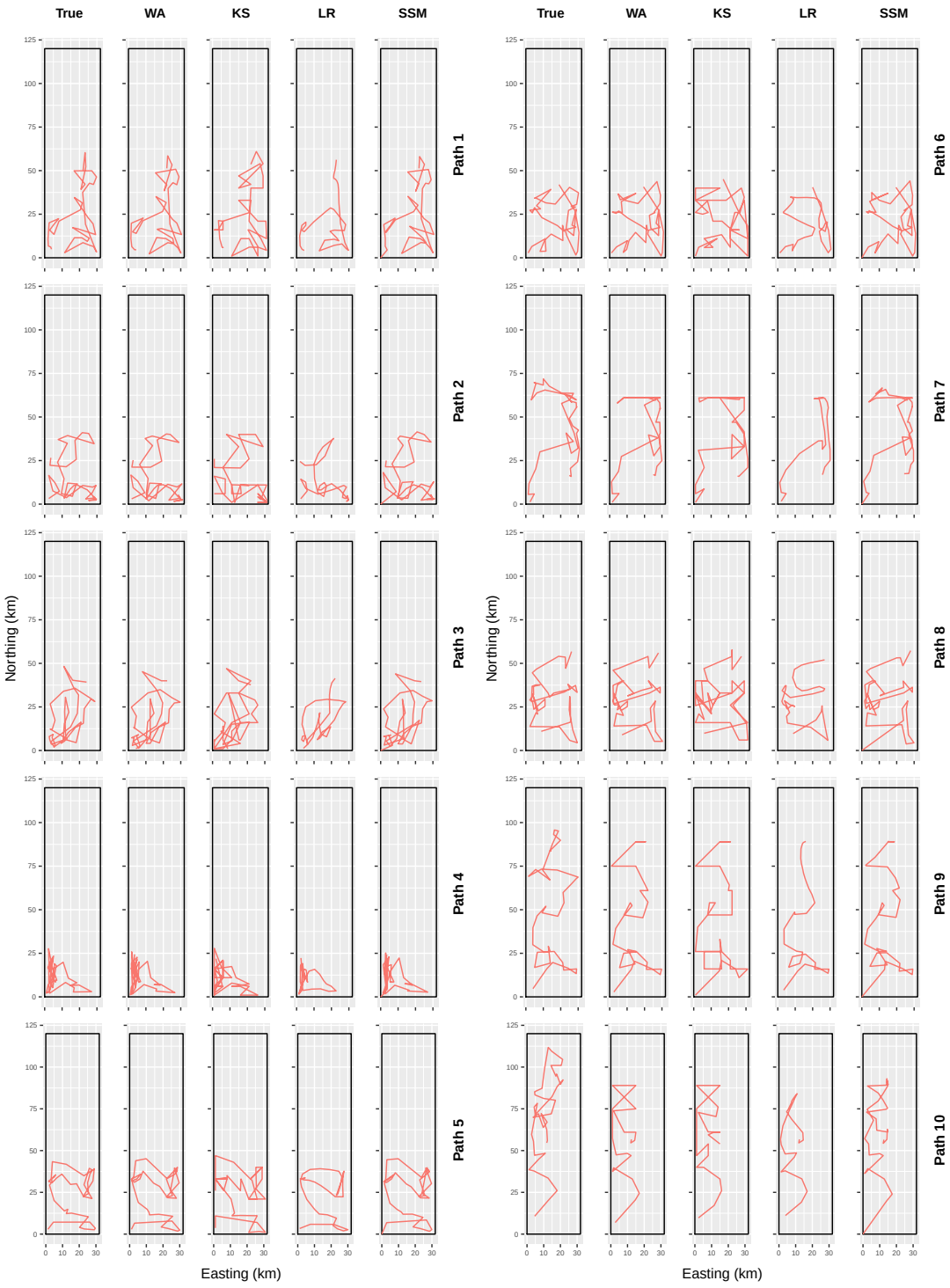

Figure A.2: Reconstructed movement paths with the true average path using six hour time bins, the simple weighted average method (WA), kernel smoothing with the Gaussian kernel (KS), cross-validated local polynomial regression approach (LR), and the state-space modeling approach (SSM) for Simulation 2 (Bin hours = 6 and tracking period = 10 days).

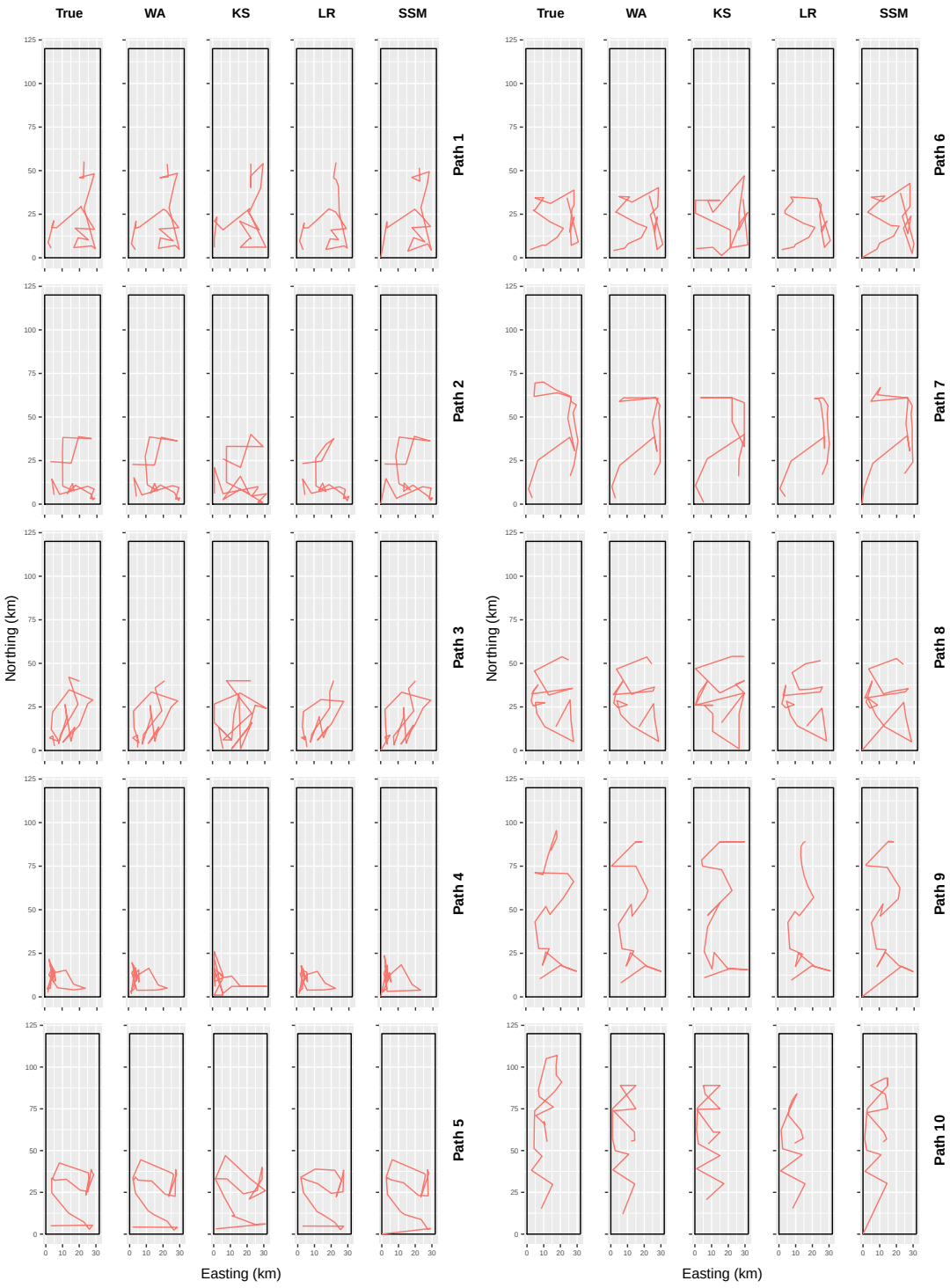

Figure A.3: Reconstructed movement paths with the true average path using 12 hour time bins, the simple weighted average method (WA), kernel smoothing with the Gaussian kernel (KS), cross-validated local polynomial regression approach (LR), and the state-space modeling approach (SSM) for Simulation 3 (Bin hours = 12 and tracking period = 10 days).

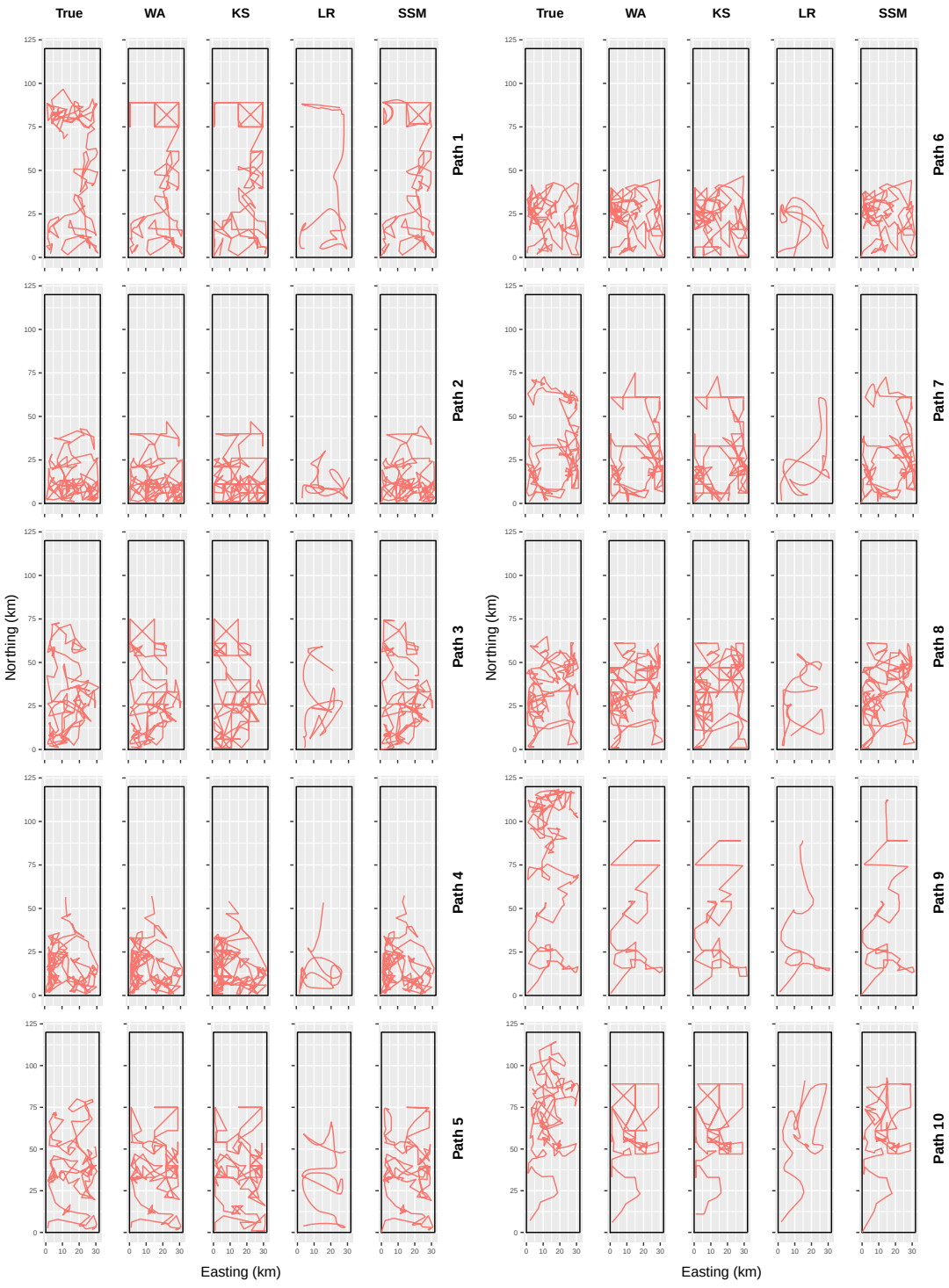

Figure A.4: Reconstructed movement paths with the true average path using three hour time bins, the simple weighted average method (WA), kernel smoothing with the Gaussian kernel (KS), cross-validated local polynomial regression approach (LR), and the state-space modeling approach (SSM) for Simulation 4 (Bin hours = 3 and tracking period = 20 days).

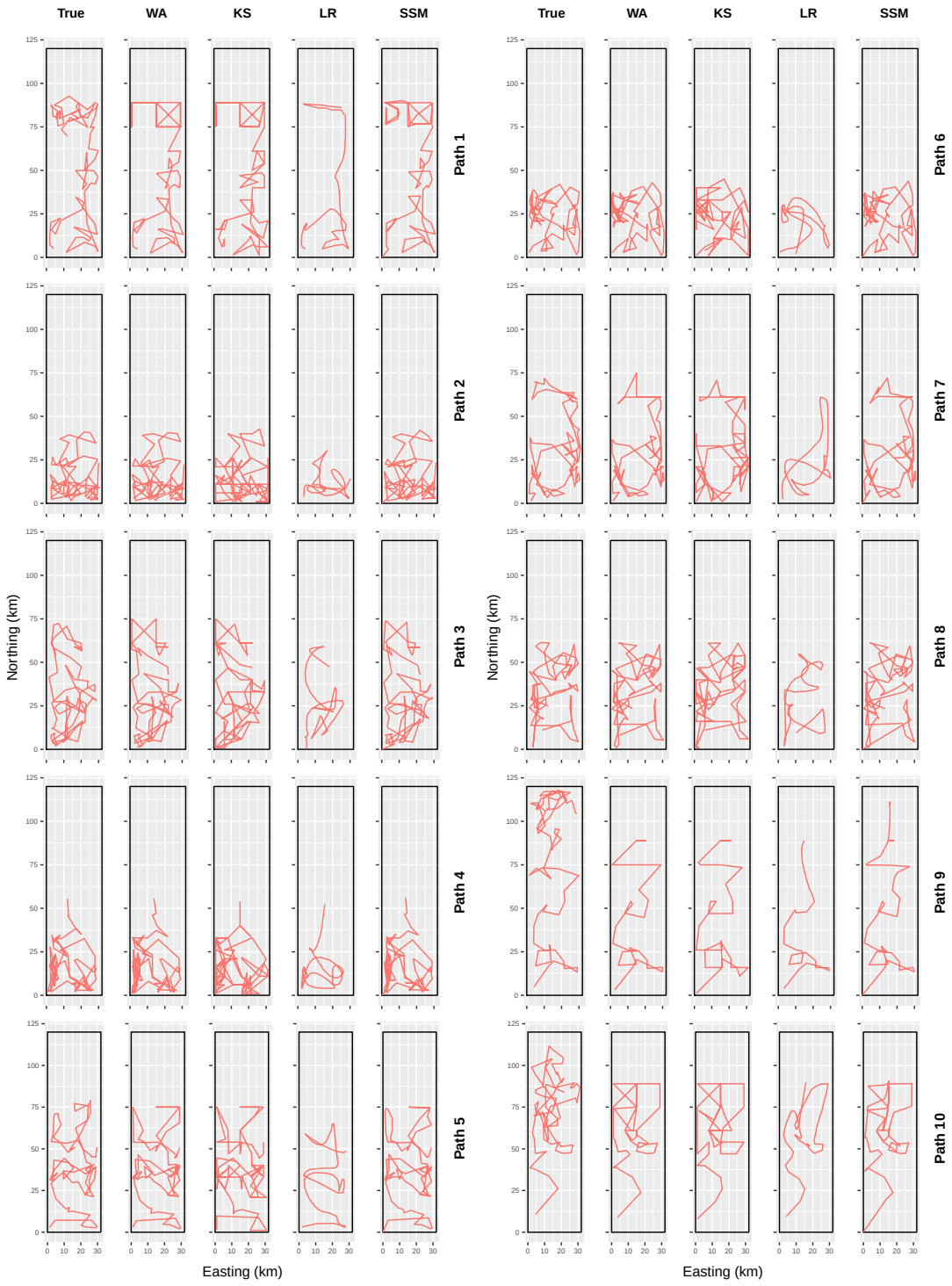

Figure A.5: Reconstructed movement paths with the true average path using six hour time bins, the simple weighted average method (WA), kernel smoothing with the Gaussian kernel (KS), cross-validated local polynomial regression approach (LR), and the state-space modeling approach (SSM) for Simulation 5 (Bin hours = 6 and tracking period = 20 days).

Figure A.6: Reconstructed movement paths with the true average path using 12 hour time bins, the simple weighted average method (WA), kernel smoothing with the Gaussian kernel (KS), cross-validated local polynomial regression approach (LR), and the state-space modeling approach (SSM) for Simulation 6 (Bin hours = 12 and tracking period = 20 days).

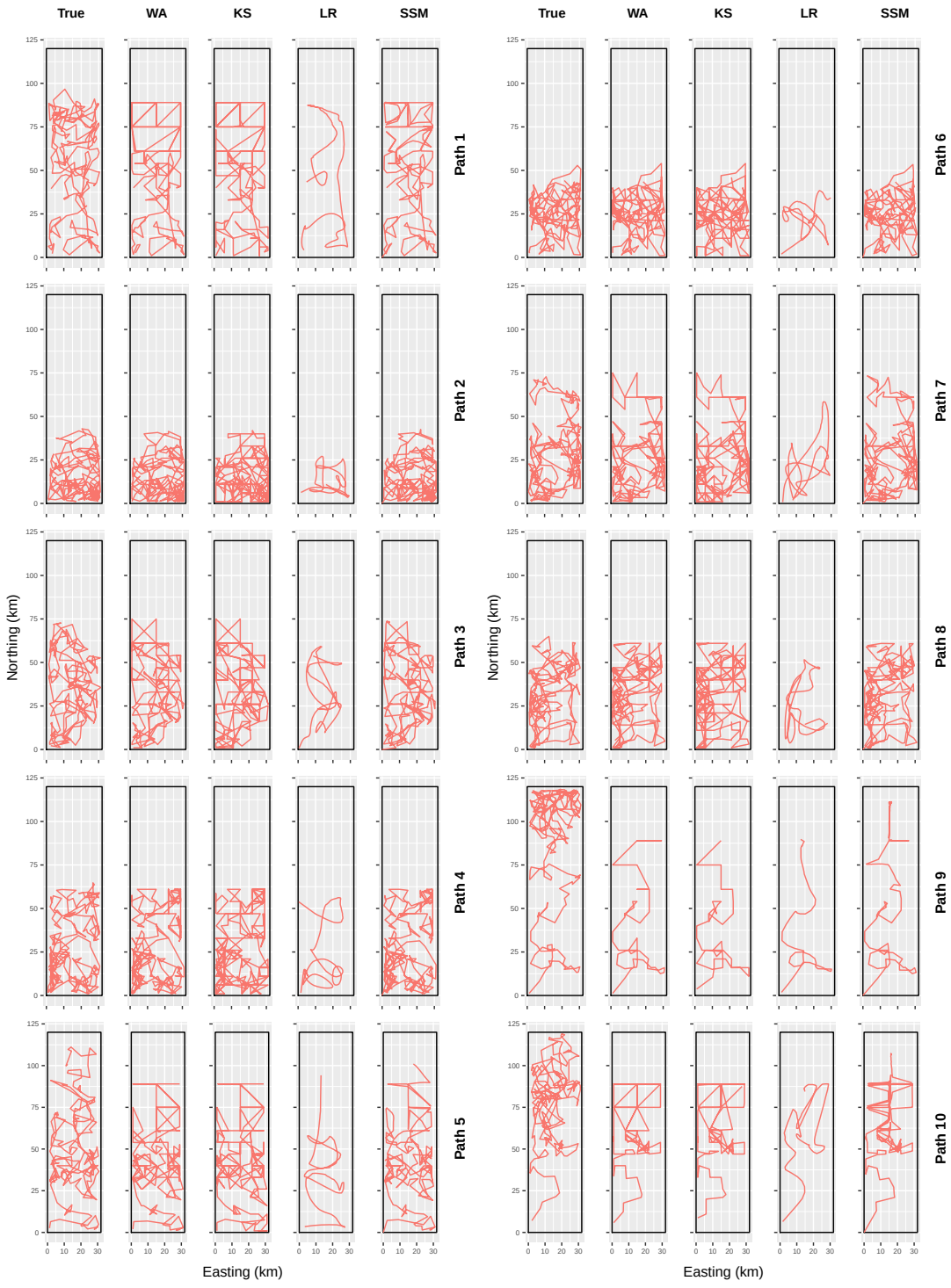

Figure A.7: Reconstructed movement paths with the true average path using three hour time bins, the simple weighted average method (WA), kernel smoothing with the Gaussian kernel (KS), cross-validated local polynomial regression approach (LR), and the state-space modeling approach (SSM) for Simulation 7 (Bin hours = 3 and tracking period = 30 days).

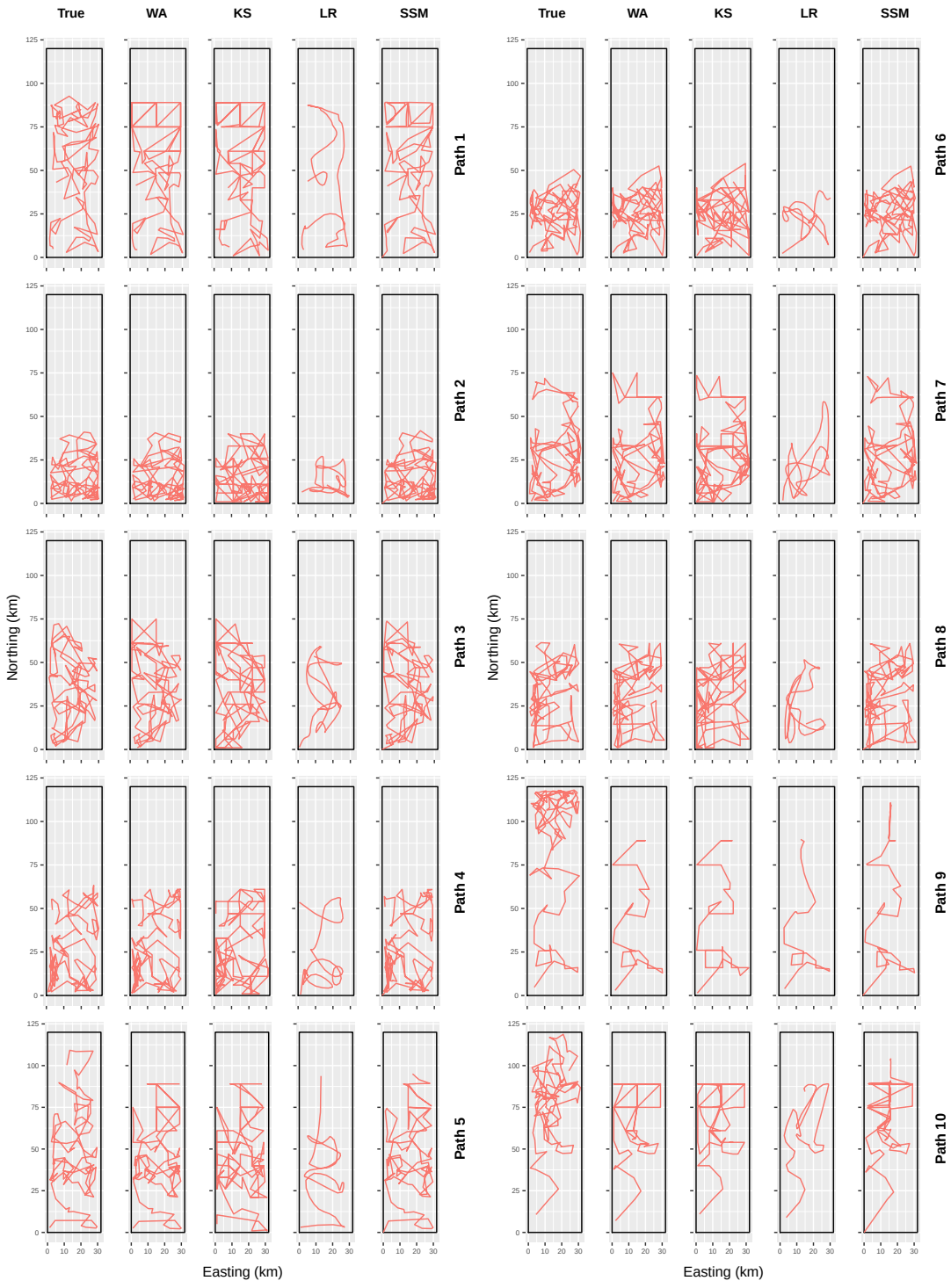

Figure A.8: Reconstructed movement paths with the true average path using six hour time bins, the simple weighted average method (WA), kernel smoothing with the Gaussian kernel (KS), cross-validated local polynomial regression approach (LR), and the state-space modeling approach (SSM) for Simulation 8 (Bin hours = 6 and tracking period = 30 days).

Figure A.9: Reconstructed movement paths with the true average path using 12 hour time bins, the simple weighted average method (WA), kernel smoothing with the Gaussian kernel (KS), cross-validated local polynomial regression approach (LR), and the state-space modeling approach (SSM) for Simulation 9 (Bin hours = 12 and tracking period = 30 days).

Appendix B

Appendix for Chapter 3

Table B.1: Parameter estimates for the model with two environments under Binning scenario 2. Here, ϕ_M and ϕ_F are environment-specific survival probabilities for the marine-estuary environment and freshwater environment while ψ_{MF} and ψ_{FM} are movement probabilities; p_M and p_F are the corresponding detection probabilities. $\hat{R}$ denotes Gelman-Rubin statistics and ESS is the effective sample size. The model was estimated using three MCMC chains each with 50,000 iterations, 10,000 burn-in with thinning by selecting each 5^{th} iteration.

Parameter	Mean	Standard Error	95% Credible Interval		$\hat{R}$	ESS
			Lower	Upper		
p_M	0.26	0.03	0.21	0.31	1.0014	3700
p_F	0.65	0.08	0.52	0.87	1.0014	3800
ϕ_M	0.92	0.01	0.89	0.95	1.0009	12000
ϕ_F	0.98	0.01	0.94	1	1.0014	3600
ψ_{MF}	0.17	0.02	0.13	0.21	1.0012	5400
ψ_{FM}	0.42	0.06	0.32	0.56	1.0017	2400
Deviance	1908.13	39.1	1816.22	1972.07	1.006	2600

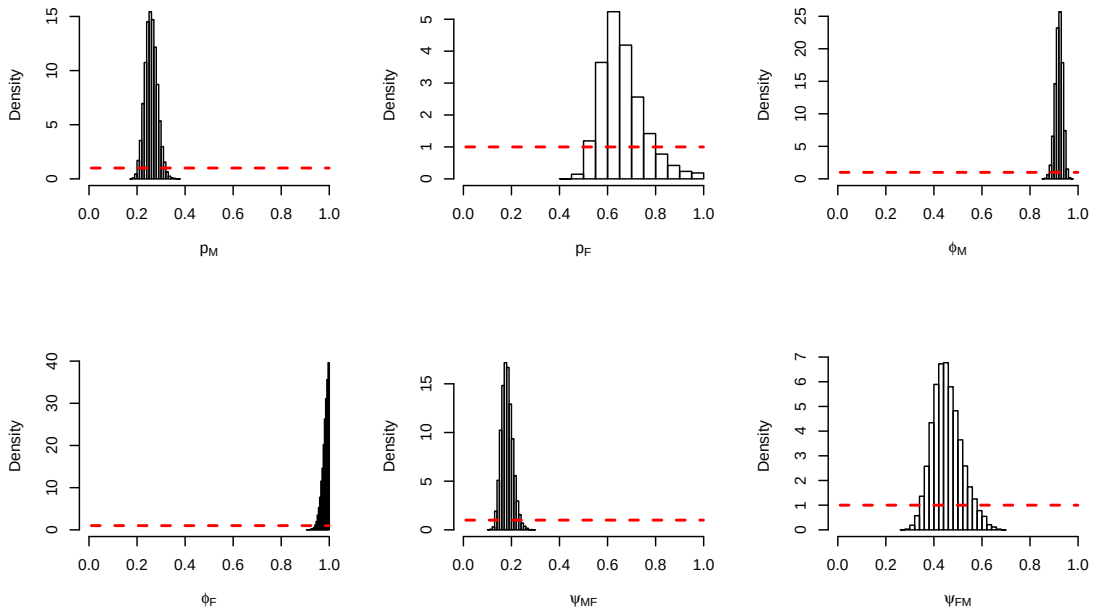

Figure B.1: Posterior plots of parameter estimates for the model with two environments under Binning Scenario 2. Here, ϕ_M and ϕ_F are environment-specific survival probabilities for the marine-estuary environment and freshwater environment while ψ_{MF} and ψ_{FM} are movement probabilities; p_M and p_F are the corresponding detection probabilities. Dashed horizontal lines represent the prior distributions.

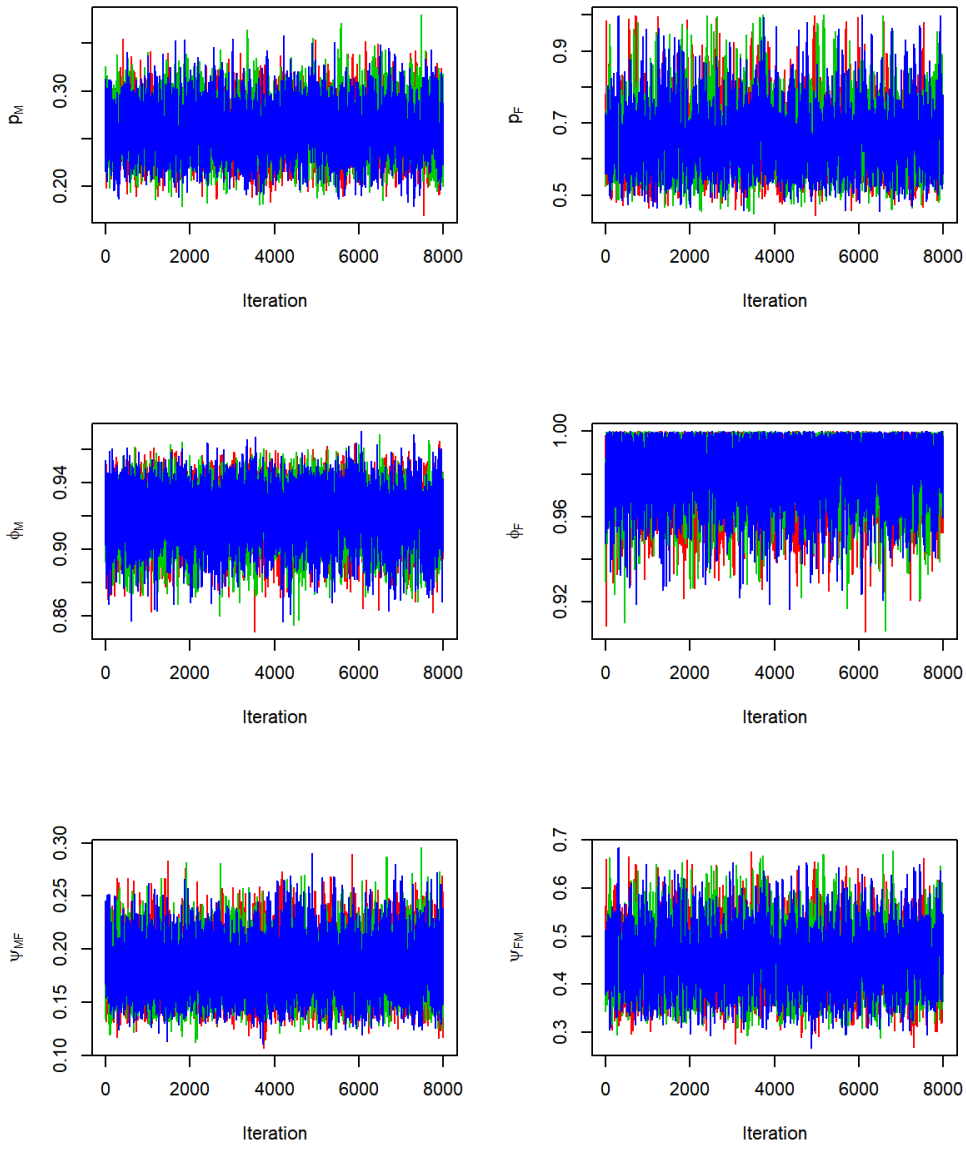

Figure B.2: Trace plots of parameter estimates for the model with two environments under Binning Scenario 2. Here, ϕ_M and ϕ_F are environment-specific survival probabilities for the marine-estuary environment and freshwater environment while ψ_{MF} and ψ_{FM} are movement probabilities; p_M and p_F are the corresponding detection probabilities.

Table B.2: Bivariate correlations between parameters for the model with two environments under Binning Scenario 2. Here, ϕ_M and ϕ_F are environment-specific survival probabilities for the marine-estuary environment and freshwater environment while ψ_{MF} and ψ_{FM} are movement probabilities; p_M and p_F are the corresponding detection probabilities.

	p_M	p_F	ϕ_M	ϕ_F	ψ_{MF}	ψ_{FM}
p_M	1.00					
p_F	-0.66	1.00				
ϕ_M	-0.35	0.29	1.00			
ϕ_F	-0.13	0.03	-0.27	1.00		
ψ_{MF}	0.41	-0.45	-0.27	-0.11	1.00	
ψ_{FM}	-0.62	0.86	0.24	0.11	-0.28	1.00

Table B.3: Parameter estimates for the model with two environments under Binning scenario 3. Here, ϕ_M and ϕ_F are environment-specific survival probabilities for the marine-estuary environment and freshwater environment while ψ_{MF} and ψ_{FM} are movement probabilities; p_M and p_F are the corresponding detection probabilities. $\hat{R}$ denotes Gelman-Rubin statistics and ESS is the effective sample size. The model was estimated using three MCMC chains each with 50,000 iterations, 10,000 burn-in with thinning by selecting each 5^{th} iteration.

Parameter	Mean	Standard Error	95% Credible Interval		$\hat{R}$	ESS
			Lower	Upper		
p_M	0.33	0.02	0.3	0.36	1.0011	11000
p_F	0.95	0.04	0.84	1	1.001	18000
ϕ_M	0.95	0.01	0.93	0.96	1.001	23000
ϕ_F	0.96	0.01	0.94	0.99	1.0013	5900
ψ_{MF}	0.18	0.01	0.15	0.2	1.001	20000
ψ_{FM}	0.51	0.03	0.45	0.56	1.001	24000
Deviance	3379.41	84.06	3232.84	3555.47	1.0014	4600

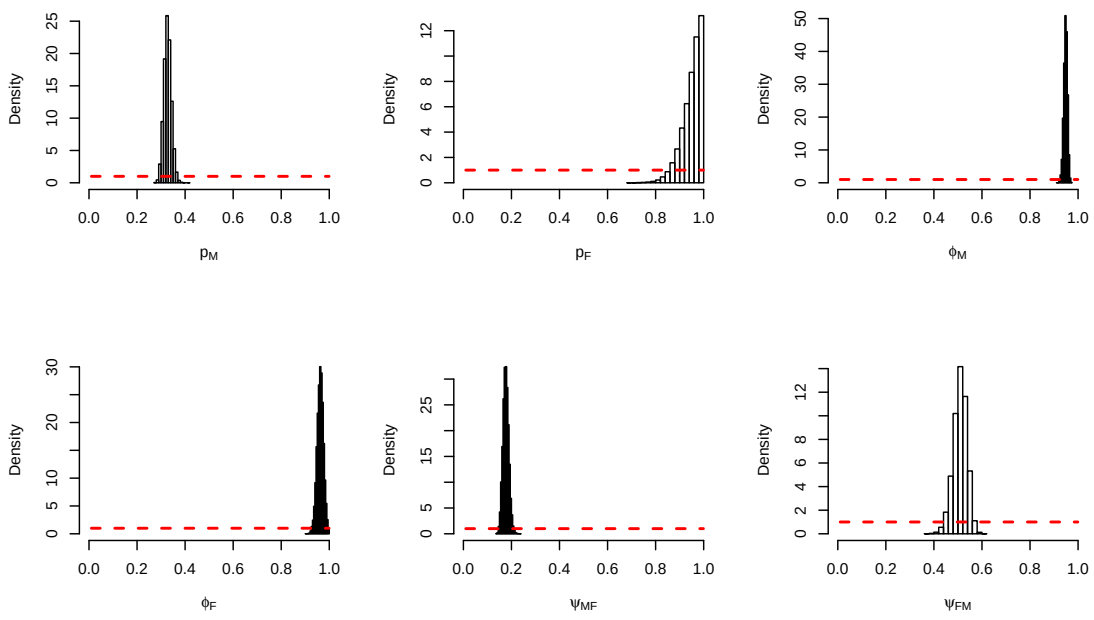

Figure B.3: Posterior plots of parameter estimates for the model with two environments under Binning Scenario 3. Here, ϕ_M and ϕ_F are environment-specific survival probabilities for the marine-estuary environment and freshwater environment while ψ_{MF} and ψ_{FM} are movement probabilities; p_M and p_F are the corresponding detection probabilities. Dashed horizontal lines represent the prior distributions.

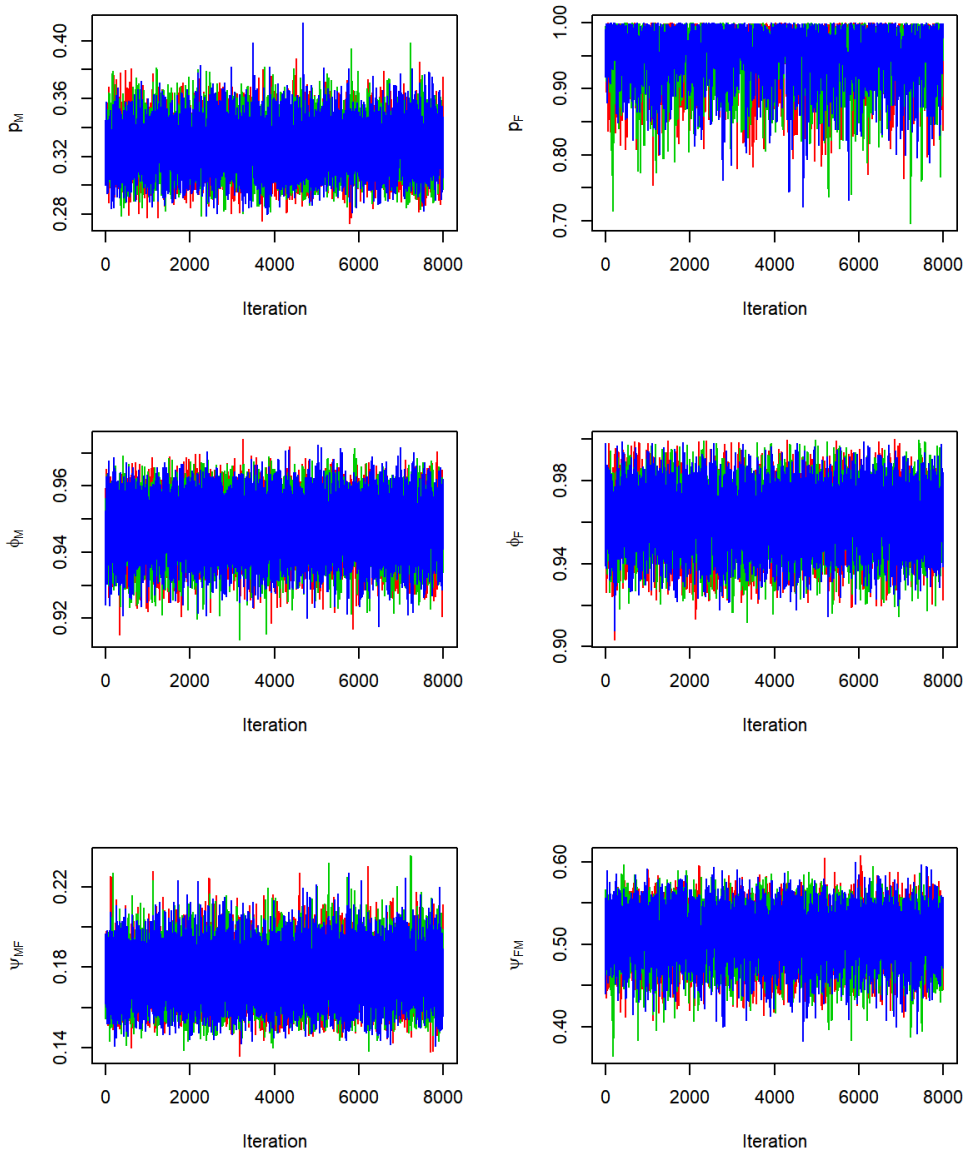

Figure B.4: Trace plots of parameter estimates for the model with two environments under Binning Scenario 3. Here, ϕ_M and ϕ_F are environment-specific survival probabilities for the marine-estuary environment and freshwater environment while ψ_{MF} and ψ_{FM} are movement probabilities; p_M and p_F are the corresponding detection probabilities.

Table B.4: Bivariate correlations between parameters for the model with two environments under Binning Scenario 3. Here, ϕ_M and ϕ_F are environment-specific survival probabilities for the marine-estuary environment and freshwater environment while ψ_{MF} and ψ_{FM} are movement probabilities; p_M and p_F are the corresponding detection probabilities.

	p_M	p_F	ϕ_M	ϕ_F	ψ_{MF}	ψ_{FM}
p_M	1.00					
p_F	-0.34	1.00				
ϕ_M	-0.05	0.06	1.00			
ϕ_F	-0.19	0.01	-0.38	1.00		
ψ_{MF}	0.21	-0.31	-0.04	-0.12	1.00	
ψ_{FM}	-0.30	0.60	-0.03	0.17	-0.18	1.00

Table B.5: Parameter estimates for the model with three environments under Binning scenario 1. Here, ϕ_M, ϕ_E, and ϕ_F are environment-specific survival probabilities for the marine, estuary and freshwater environments respectively while ψ_{ME}, ψ_{MF}, ψ_{EM}, ψ_{EF}, ψ_{FM} and ψ_{FE} are movement probabilities; p_M, p_E, and p_F are the observation probabilities at marine, estuary, and freshwater environments, respectively. $\hat{R}$ denotes Gelman-Rubin statistics and ESS is the effective sample size. The model was estimated using three MCMC chains each with 50,000 iterations, 10,000 burn-in with thinning by selecting each 5^{th} iteration.

Parameter	Mean	Standard Error	95% Credible Interval		$\hat{R}$	ESS
			Lower	Upper		
p_M	0.29	0.04	0.22	0.37	1.0015	3200
p_E	0.92	0.07	0.73	1.00	1.0009	12000
p_F	0.71	0.06	0.62	0.83	1.0009	12000
ϕ_M	0.88	0.03	0.81	0.94	1.0011	8100
ϕ_E	0.82	0.06	0.71	0.93	1.0009	12000
ϕ_F	0.95	0.02	0.91	0.99	1.0015	3100
ψ_{MM}	0.54	0.05	0.44	0.62	1.0010	12000
ψ_{ME}	0.21	0.04	0.15	0.29	1.0010	12000
ψ_{MF}	0.25	0.04	0.18	0.33	1.0012	5400
ψ_{EM}	0.74	0.07	0.60	0.85	1.0009	12000
ψ_{EE}	0.04	0.02	0.01	0.09	1.0011	8300
ψ_{EF}	0.22	0.06	0.12	0.36	1.0009	12000
ψ_{FM}	0.28	0.05	0.19	0.4	1.001	12000
ψ_{FE}	0.07	0.02	0.04	0.11	1.0016	2700
ψ_{FF}	0.66	0.05	0.54	0.74	1.0009	12000
Deviance	1578.85	38.13	1504.25	1652.56	1.0011	9300

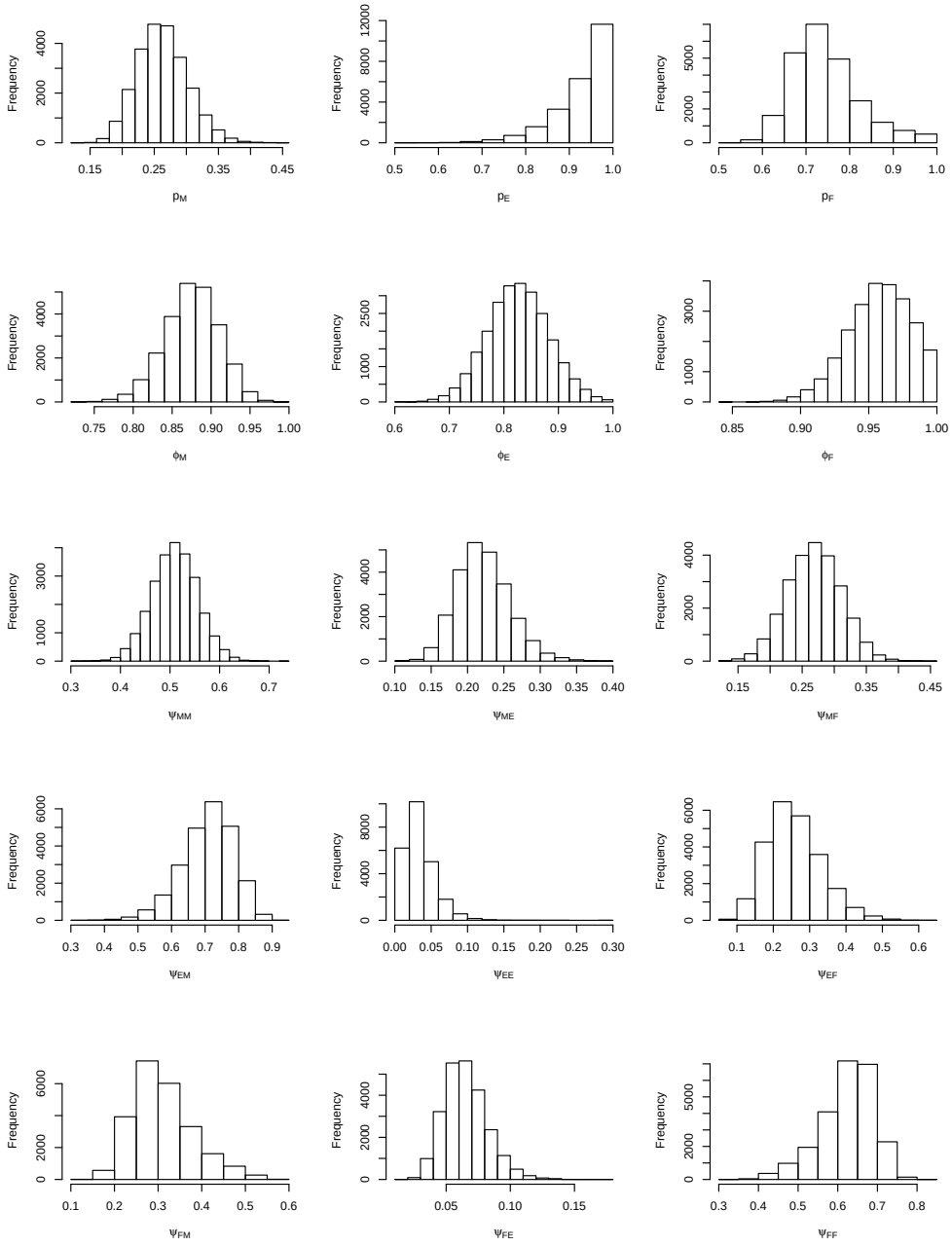

Figure B.5: Posterior plots of parameter estimates for the model with three environments under Binning Scenario 1. Here, ϕ_M, ϕ_E, and ϕ_F are environment-specific survival probabilities for the marine, estuary and freshwater environments respectively while ψ_{ME}, ψ_{MF}, ψ_{EM}, ψ_{EF}, ψ_{FM} and ψ_{FE} are movement probabilities; p_M, p_E, and p_F are the observation probabilities at marine, estuary, and freshwater environments, respectively.

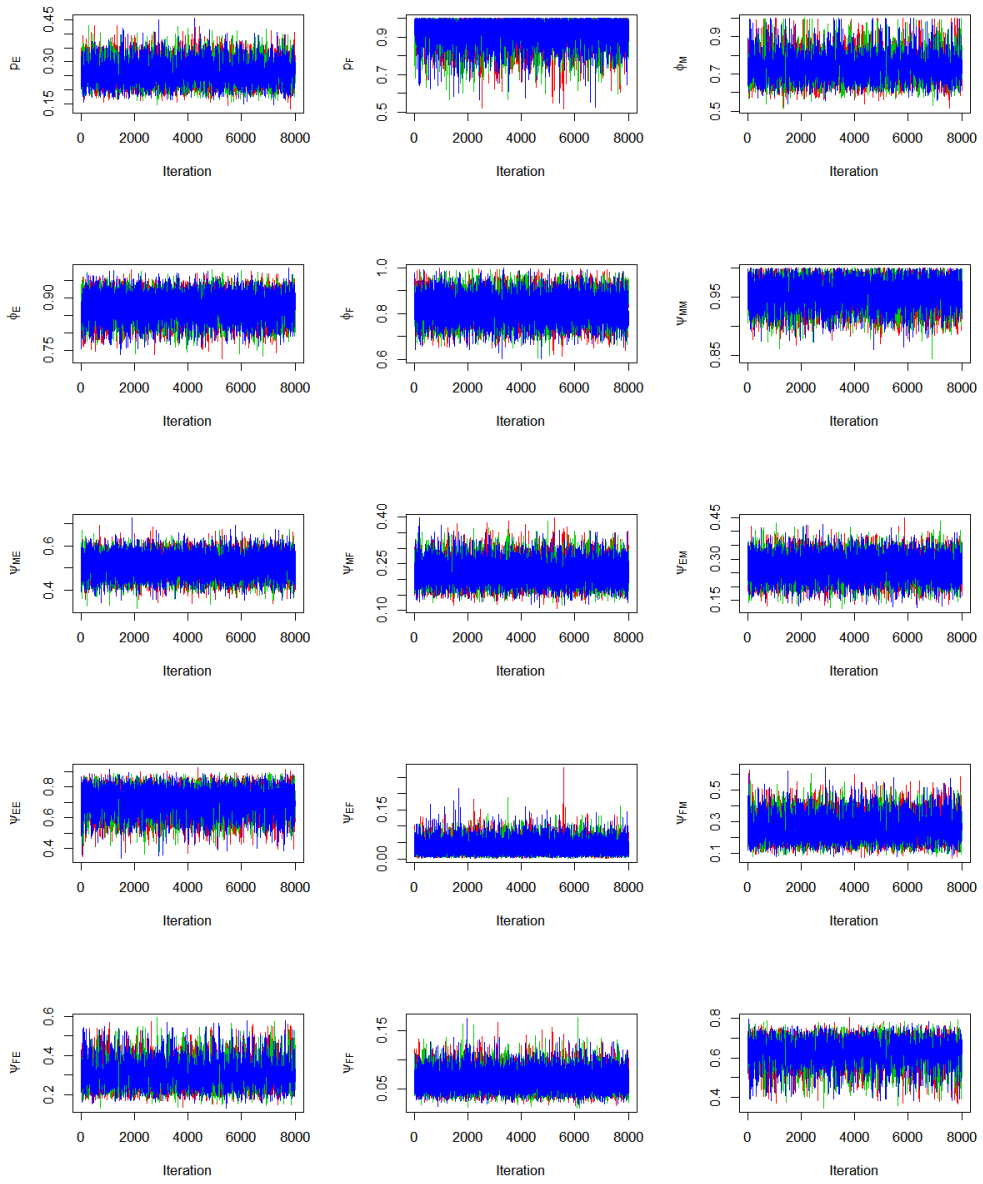

Figure B.6: Trace plots of parameter estimates for the model with three environments under Binning Scenario 1. Here, ϕ_M, ϕ_E, and ϕ_F are environment-specific survival probabilities for the marine, estuary and freshwater environments respectively while ψ_{ME}, ψ_{MF}, ψ_{EM}, ψ_{EF}, ψ_{FM} and ψ_{FE} are movement probabilities; p_M, p_E, and p_F are the observation probabilities at marine, estuary, and freshwater environments, respectively.

Table B.6: Bivariate correlations between parameters for the model with three environments under Binning Scenario 1. Here, ϕ_M, ϕ_E, and ϕ_F are environment-specific survival probabilities for the marine, estuary and freshwater environments respectively while ψ_{ME}, ψ_{MF}, ψ_{EM}, ψ_{EF}, ψ_{FM} and ψ_{FE} are movement probabilities; p_M, p_E, and p_F are the observation probabilities at marine, estuary, and freshwater environments, respectively.

	p_M	p_E	p_F	ϕ_M	ϕ_E	ϕ_F	ψ_{MM}	ψ_{ME}	ψ_{MF}	ψ_{EM}	ψ_{EE}	ψ_{EF}	ψ_{FM}	ψ_{FE}	ψ_{FF}
p_M	1.00														
p_E	-0.06	1.00													
p_F	-0.60	0.04	1.00												
ϕ_M	0.12	-0.10	-0.04	1.00											
ϕ_E	-0.28	0.03	0.11	-0.41	1.00										
ϕ_F	-0.30	-0.09	0.05	-0.38	0.19	1.00									
ψ_{MM}	-0.09	0.14	-0.12	0.02	0.08	0.17	1.00								
ψ_{ME}	0.33	-0.31	-0.30	0.02	-0.13	-0.14	-0.49	1.00							
ψ_{MF}	-0.17	0.10	0.38	-0.05	0.02	-0.08	-0.69	-0.29	1.00						
ψ_{EM}	-0.50	0.12	0.59	-0.14	0.22	0.09	-0.07	-0.25	0.28	1.00					
ψ_{EE}	0.09	-0.18	-0.04	0.07	-0.02	-0.01	-0.03	0.07	-0.02	-0.25	1.00				
ψ_{EF}	0.49	-0.07	-0.60	0.13	-0.22	-0.09	0.08	0.24	-0.29	-0.97	0.01	1.00			
ψ_{FM}	-0.63	0.10	0.88	-0.10	0.14	0.20	-0.12	-0.33	0.40	0.54	-0.04	-0.54	1.00		
ψ_{FE}	0.18	-0.33	-0.16	0.02	-0.05	-0.05	-0.01	0.04	-0.02	-0.14	0.06	0.13	-0.26	1.00	
ψ_{FF}	0.61	-0.03	-0.87	0.10	-0.13	-0.20	0.13	0.33	-0.41	-0.53	0.03	0.54	-0.98	0.05	1.00

Table B.7: Parameter estimates for the model with three environments under Binning scenario 2. Here, ϕ_M, ϕ_E, and ϕ_F are environment-specific survival probabilities for the marine, estuary and freshwater environments respectively while ψ_{ME}, ψ_{MF}, ψ_{EM}, ψ_{EF}, ψ_{FM} and ψ_{FE} are movement probabilities; p_M, p_E, and p_F are the observation probabilities at marine, estuary, and freshwater environments, respectively. $\hat{R}$ denotes Gelman-Rubin statistics and ESS is the effective sample size. The model was estimated using three MCMC chains each with 50,000 iterations, 10,000 burn-in with thinning by selecting each 5^{th} iteration.

Parameter	Mean	Standard Error	95% Credible Interval		$\hat{R}$	ESS
			Lower	Upper		
p_M	0.35	0.06	0.24	0.49	1.001	4000
p_E	0.21	0.03	0.15	0.28	1.003	1200
p_F	0.53	0.04	0.46	0.61	1.001	15000
ϕ_M	0.93	0.03	0.86	0.99	1.002	1600
ϕ_E	0.89	0.03	0.84	0.94	1.002	2700
ϕ_F	0.99	0.01	0.96	1.00	1.002	1400
ψ_{MM}	0.59	0.07	0.43	0.71	1.001	13000
ψ_{ME}	0.18	0.06	0.07	0.32	1.002	2100
ψ_{MF}	0.23	0.05	0.14	0.34	1.001	7800
ψ_{EM}	0.13	0.04	0.06	0.23	1.002	1500
ψ_{EE}	0.72	0.05	0.62	0.80	1.001	11000
ψ_{EF}	0.15	0.04	0.09	0.22	1.002	3300
ψ_{FM}	0.15	0.04	0.09	0.24	1.002	1400
ψ_{FE}	0.12	0.04	0.06	0.19	1.002	1900
ψ_{FF}	0.73	0.04	0.65	0.79	1.001	19000
Deviance	2051.4	33.25	1985.79	2115.47	1.002	1400

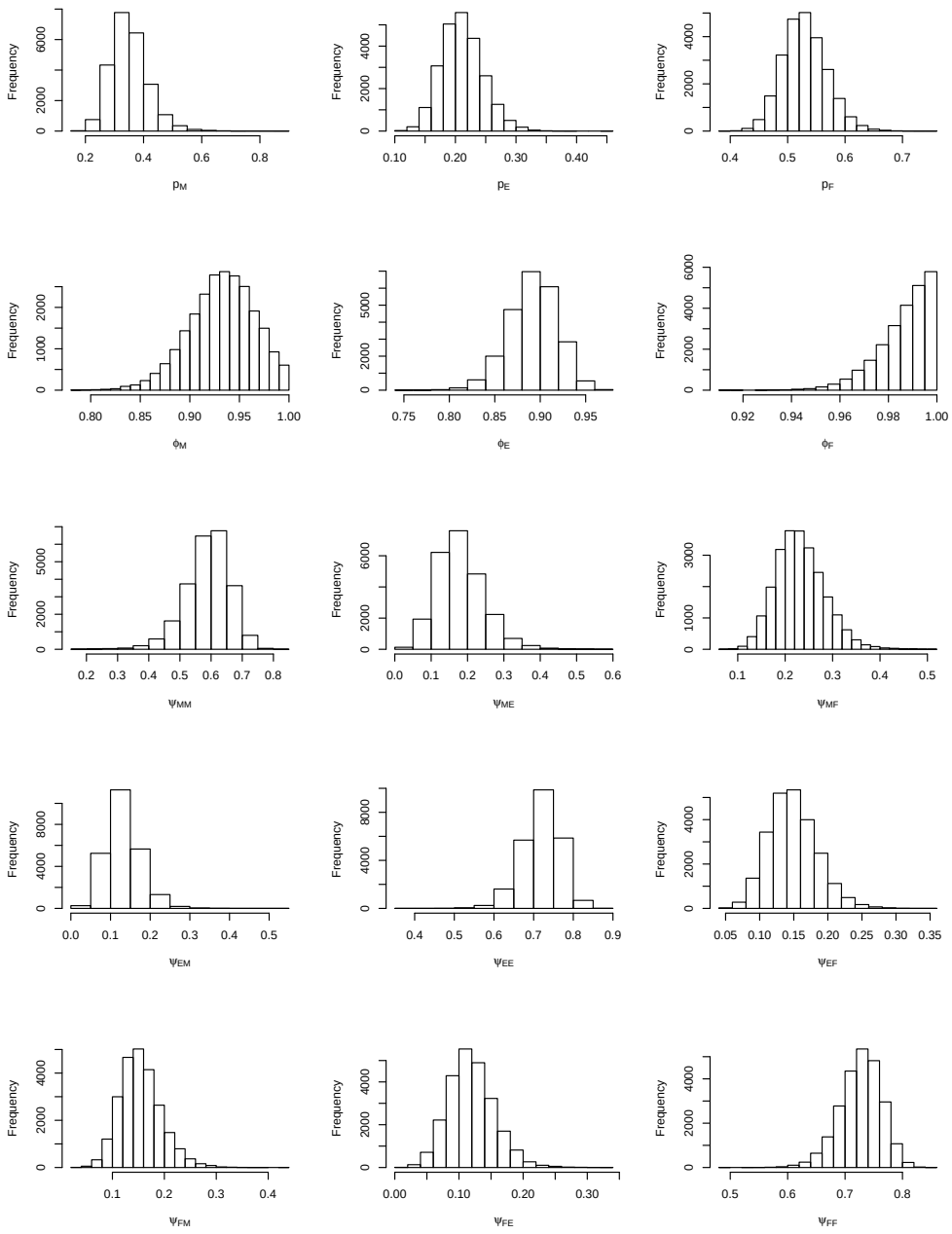

Figure B.7: Posterior plots of parameter estimates for the model with three environments under Binning Scenario 2. Here, ϕ_M, ϕ_E, and ϕ_F are environment-specific survival probabilities for the marine, estuary and freshwater environments respectively while ψ_{ME}, ψ_{MF}, ψ_{EM}, ψ_{EF}, ψ_{FM} and ψ_{FE} are movement probabilities; p_M, p_E, and p_F are the observation probabilities at marine, estuary, and freshwater environments, respectively.

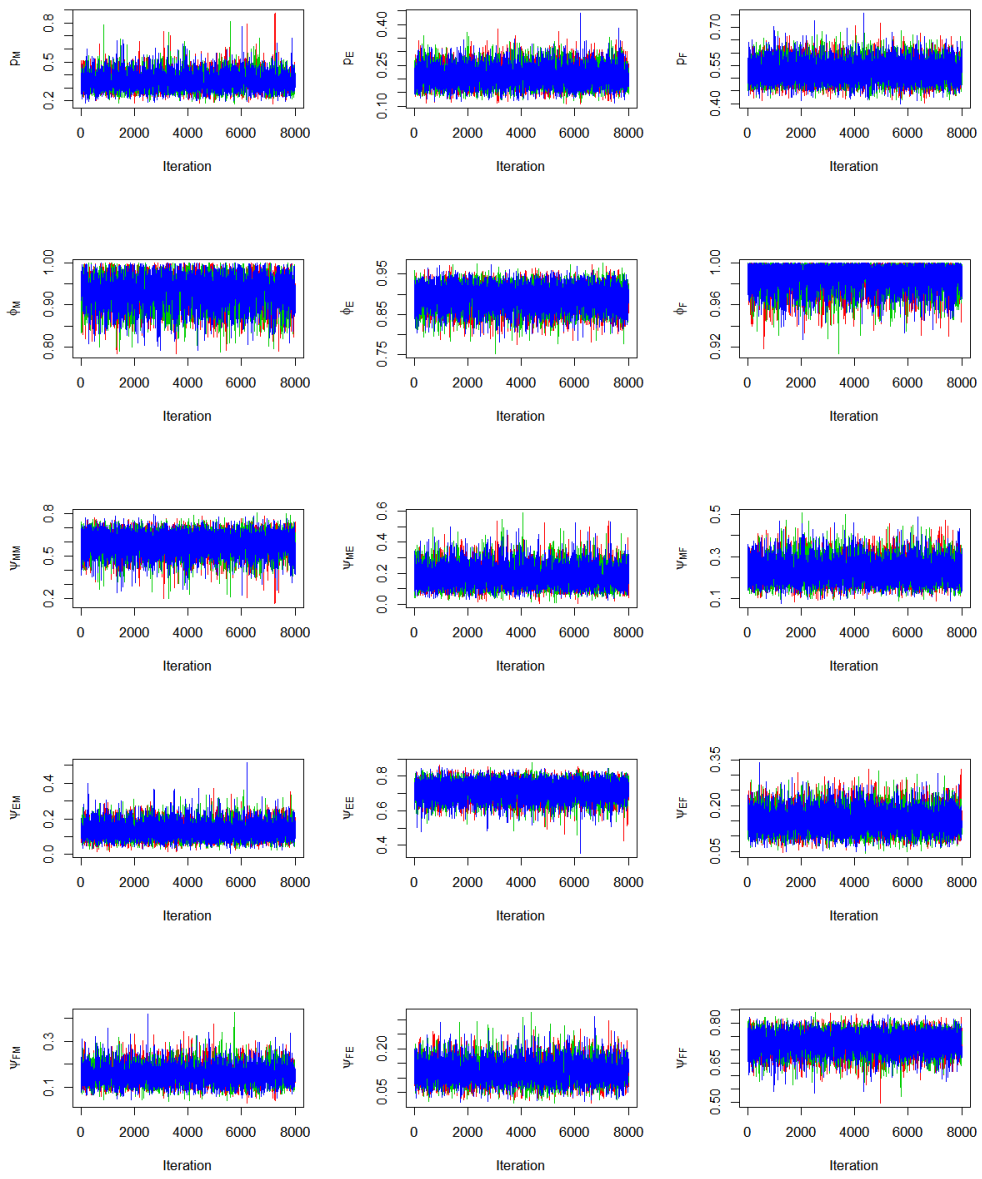

Figure B.8: Trace plots of parameter estimates for the model with three environments under Binning Scenario 2. Here, ϕ_M, ϕ_E, and ϕ_F are environment-specific survival probabilities for the marine, estuary and freshwater environments respectively while ψ_{ME}, ψ_{MF}, ψ_{EM}, ψ_{EF}, ψ_{FM} and ψ_{FE} are movement probabilities; p_M, p_E, and p_F are the observation probabilities at marine, estuary, and freshwater environments, respectively.

Table B.8: Bivariate correlations between parameters for the model with three environments under Binning Scenario 2. Here, ϕ_M, ϕ_E, and ϕ_F are environment-specific survival probabilities for the marine, estuary and freshwater environments respectively while ψ_{ME}, ψ_{MF}, ψ_{EM}, ψ_{EF}, ψ_{FM} and ψ_{FE} are movement probabilities; p_M, p_E, and p_F are the observation probabilities at marine, estuary, and freshwater environments, respectively.

	p_M	p_E	p_F	ϕ_M	ϕ_E	ϕ_F	ψ_{MM}	ψ_{ME}	ψ_{MF}	ψ_{EM}	ψ_{EE}	ψ_{EF}	ψ_{FM}	ψ_{FE}	ψ_{FF}
p_M	1.00														
p_E	-0.27	1.00													
p_F	-0.34	-0.15	1.00												
ϕ_M	-0.14	-0.07	0.08	1.00											
ϕ_E	0.07	-0.21	0.01	-0.36	1.00										
ϕ_F	-0.13	-0.10	-0.01	-0.16	-0.08	1.00									
ψ_{MM}	-0.29	0.19	0.11	-0.11	0.06	-0.03	1.00								
ψ_{ME}	0.12	-0.17	-0.01	0.29	-0.15	0.02	-0.67	1.00							
ψ_{MF}	0.24	-0.05	-0.14	-0.19	0.09	0.01	-0.52	-0.29	1.00						
ψ_{EM}	-0.26	0.15	0.12	0.01	-0.04	0.05	-0.13	0.15	0.00	1.00					
ψ_{EE}	0.17	-0.23	-0.01	-0.02	0.15	0.02	0.12	-0.23	0.11	-0.70	1.00				
ψ_{EF}	0.10	0.13	-0.13	0.01	-0.15	-0.09	0.00	0.13	-0.15	-0.28	-0.49	1.00			
ψ_{FM}	-0.56	0.26	0.29	0.10	-0.10	0.08	-0.07	0.09	0.00	0.00	-0.04	0.06	1.00		
ψ_{FE}	0.27	-0.44	0.21	-0.09	0.12	0.10	0.05	-0.20	0.16	0.05	-0.04	0.00	-0.50	1.00	
ψ_{FF}	0.32	0.15	-0.50	-0.02	-0.02	-0.18	0.03	0.10	-0.15	-0.04	0.08	-0.06	-0.56	-0.44	1.00

Table B.9: Parameter estimates for the model with three environments under Binning scenario 3. Here, ϕ_M, ϕ_E, and ϕ_F are environment-specific survival probabilities for the marine, estuary and freshwater environments respectively while ψ_{ME}, ψ_{MF}, ψ_{EM}, ψ_{EF}, ψ_{FM} and ψ_{FE} are movement probabilities; p_M, p_E, and p_F are the observation probabilities at marine, estuary, and freshwater environments, respectively. $\hat{R}$ denotes Gelman-Rubin statistics and ESS is the effective sample size. The model was estimated using three MCMC chains each with 130,000 iterations, 50,000 burn-in with thinning by selecting each 5^{th} iteration.

Parameter	Mean	Standard Error	95% Credible Interval		$\hat{R}$	ESS
			Lower	Upper		
p_M	0.96	0.03	0.88	1.00	1.0012	9300
p_E	0.17	0.02	0.15	0.21	1.0010	41000
p_F	0.88	0.07	0.73	0.99	1.0010	42000
ϕ_M	0.91	0.02	0.86	0.95	1.0011	13000
ϕ_E	0.95	0.01	0.93	0.97	1.0012	7500
ϕ_F	0.97	0.01	0.94	1.00	1.0017	2800
ψ_{MM}	0.37	0.04	0.30	0.45	1.0011	12000
ψ_{ME}	0.25	0.05	0.15	0.34	1.0011	20000
ψ_{MF}	0.38	0.05	0.29	0.48	1.0010	27000
ψ_{EM}	0.12	0.01	0.10	0.15	1.0010	24000
ψ_{EE}	0.70	0.02	0.66	0.74	1.0011	14000
ψ_{EF}	0.18	0.01	0.15	0.21	1.0010	29000
ψ_{FM}	0.06	0.01	0.04	0.09	1.0010	42000
ψ_{FE}	0.42	0.04	0.34	0.48	1.0011	14000
ψ_{FF}	0.52	0.04	0.45	0.61	1.0011	14000
Deviance	3663.12	110.33	3438.62	3865.78	1.0010	35000

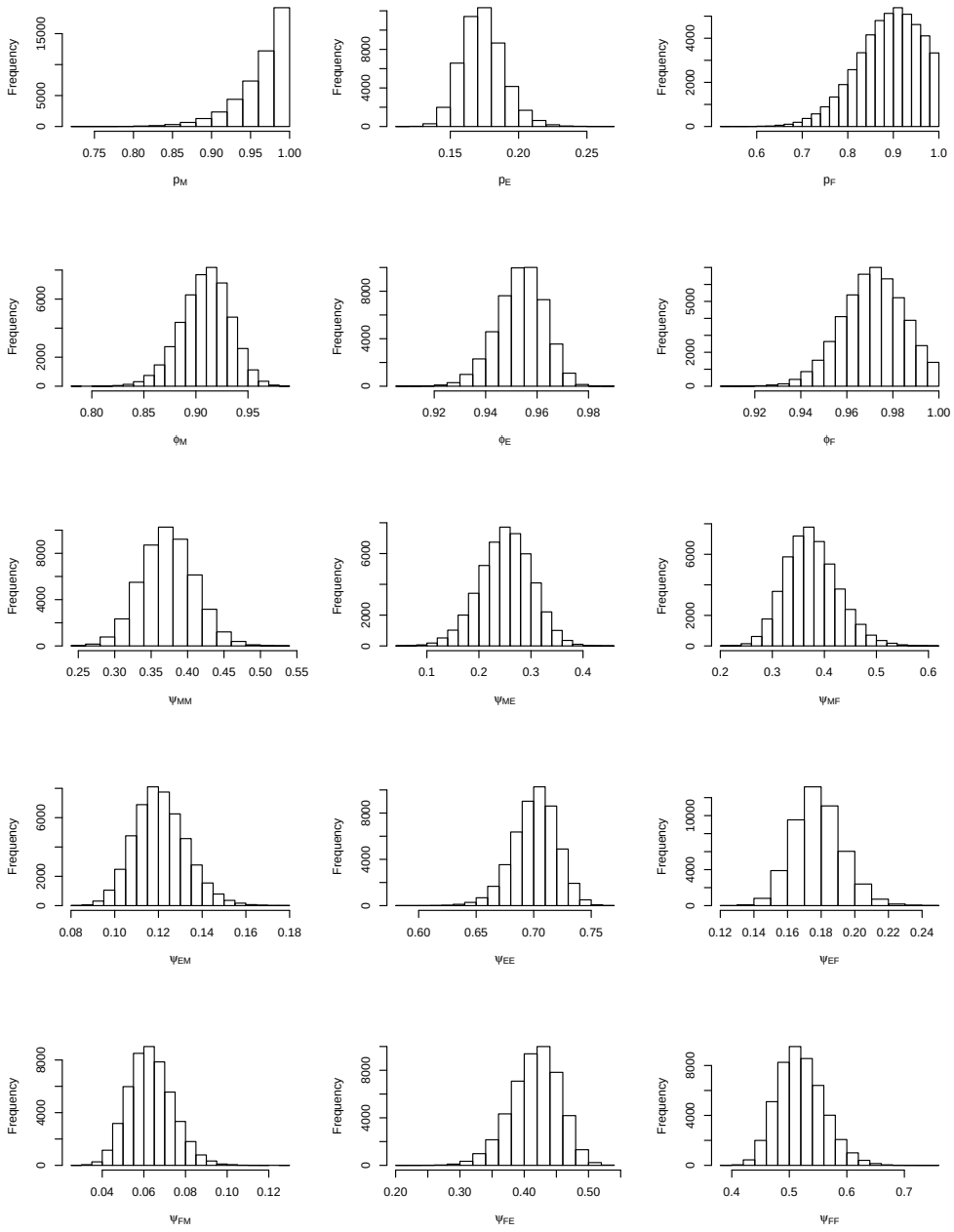

Figure B.9: Posterior plots of parameter estimates for the model with three environments under Binning Scenario 3. Here, ϕ_M, ϕ_E, and ϕ_F are environment-specific survival probabilities for the marine, estuary and freshwater environments respectively while ψ_{ME}, ψ_{MF}, ψ_{EM}, ψ_{EF}, ψ_{FM} and ψ_{FE} are movement probabilities; p_M, p_E, and p_F are the observation probabilities at marine, estuary, and freshwater environments, respectively.

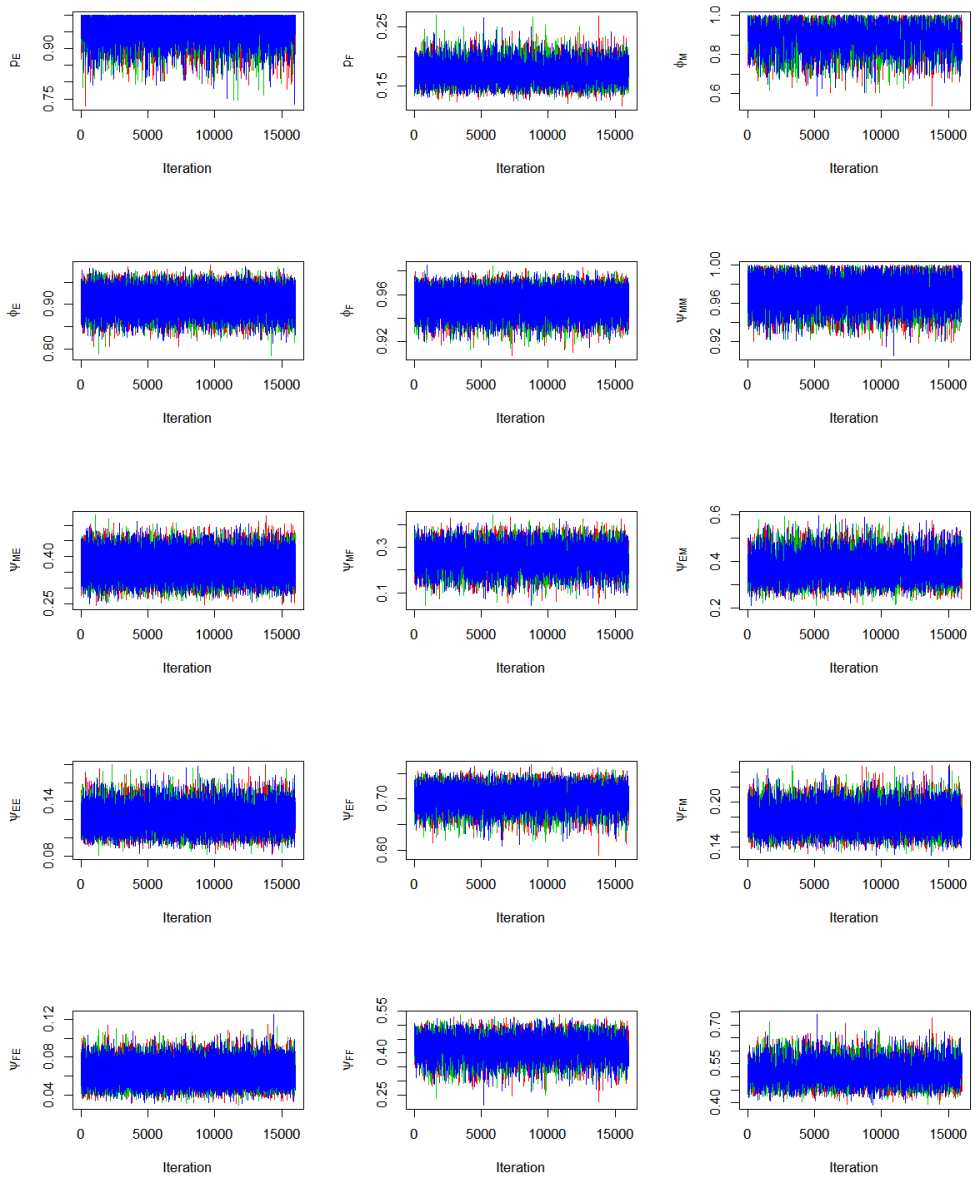

Figure B.10: Trace plots of parameter estimates for the model with three environments under Binning Scenario 3. Here, ϕ_M, ϕ_E, and ϕ_F are environment-specific survival probabilities for the marine, estuary and freshwater environments respectively while ψ_{ME}, ψ_{MF}, ψ_{EM}, ψ_{EF}, ψ_{FM} and ψ_{FE} are movement probabilities; p_M, p_E, and p_F are the observation probabilities at marine, estuary, and freshwater environments, respectively.

Table B.10: Bivariate correlations between parameters for the model with three environments under Binning Scenario 3. Here, ϕ_M, ϕ_E, and ϕ_F are environment-specific survival probabilities for the marine, estuary and freshwater environments respectively while ψ_{ME}, ψ_{MF}, ψ_{EM}, ψ_{EF}, ψ_{FM} and ψ_{FE} are movement probabilities; p_M, p_E, and p_F are the observation probabilities at marine, estuary, and freshwater environments, respectively.

	p_M	p_E	p_F	ϕ_M	ϕ_E	ϕ_F	ψ_{MM}	ψ_{ME}	ψ_{MF}	ψ_{EM}	ψ_{EE}	ψ_{EF}	ψ_{FM}	ψ_{FE}	ψ_{FF}
p_M	1.00														
p_E	-0.08	1.00													
p_F	-0.14	-0.54	1.00												
ϕ_M	0.02	-0.10	0.04	1.00											
ϕ_E	-0.08	0.04	0.04	-0.16	1.00										
ϕ_F	0.08	-0.22	0.05	0.06	-0.45	1.00									
ψ_{MM}	-0.18	0.07	0.00	-0.11	0.09	-0.02	1.00								
ψ_{ME}	0.06	-0.44	0.63	0.18	-0.07	0.08	-0.35	1.00							
ψ_{MF}	0.07	0.38	-0.63	-0.10	0.00	-0.06	-0.38	-0.74	1.00						
ψ_{EM}	-0.20	0.31	-0.31	-0.12	0.05	-0.16	0.03	-0.27	0.25	1.00					
ψ_{EE}	0.04	-0.41	0.45	0.10	-0.05	0.23	-0.04	0.29	-0.26	-0.64	1.00				
ψ_{EF}	0.11	0.27	-0.34	-0.03	0.03	-0.17	0.03	-0.16	0.14	0.02	-0.78	1.00			
ψ_{FM}	-0.19	-0.15	0.31	0.04	0.02	0.02	0.00	0.21	-0.21	-0.07	0.12	-0.10	1.00		
ψ_{FE}	-0.06	-0.51	0.80	0.07	-0.06	0.19	-0.02	0.51	-0.49	-0.30	0.39	-0.26	0.13	1.00	
ψ_{FF}	0.11	0.51	-0.83	-0.08	0.05	-0.18	0.02	-0.53	0.51	0.30	-0.39	0.27	-0.38	-0.96	1.00

Appendix C

Appendix for Chapter 5

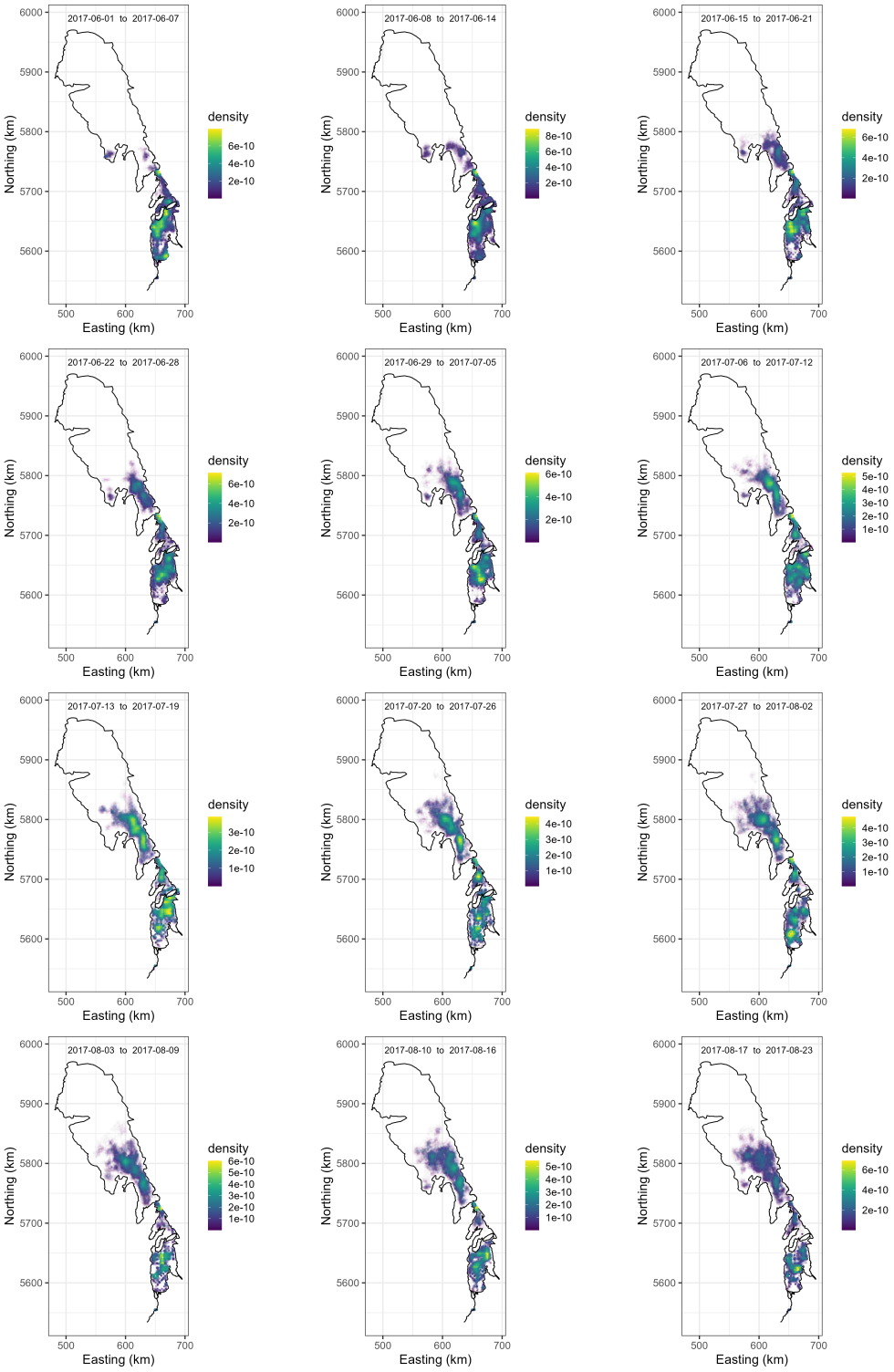

Figure C.1: Weekly fish densities constructed constructed using posterior distributions of walleye movement paths estimated with Bayesian state-space models.

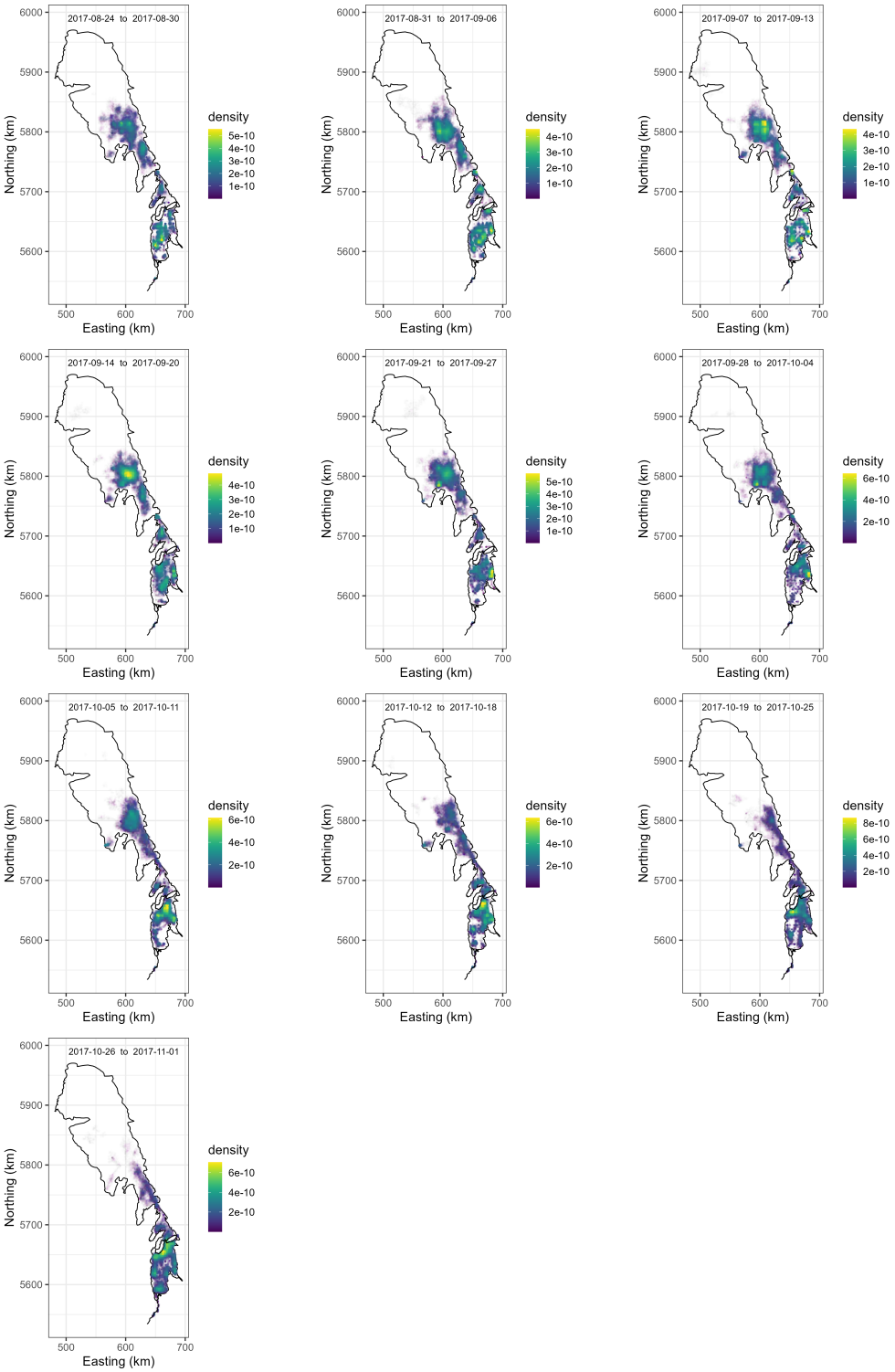

Figure C.2: Weekly fish densities constructed constructed using posterior distributions of walleye movement paths estimated with Bayesian state-space models.

Bibliography

Aanes, S., Engen, S., Sæther, B.-E. and Aanes, R. (2007), 'Estimation of the parameters of fish stock dynamics from catch-at-age data and indices of abundance: can natural and fishing mortality be separated?', *Canadian Journal of Fisheries and Aquatic Sciences* **64**(8), 1130–1142.

Aeberhard, W., Flemming, J. and Nielsen, A. (2018), 'Review of state-space models for fisheries science', *Annual Review of Statistics and Its Application* **5**, 215–235.

Albertsen, C. M., Whoriskey, K., Yurkowski, D., Nielsen, A. and Flemming, J. M. (2015), 'Fast fitting of non-gaussian state-space models to animal movement data via template model builder', *Ecology* **96**(10), 2598–2604.

Alós, J., Palmer, M., Balle, S. and Arlinghaus, R. (2016), 'Bayesian state-space modelling of conventional acoustic tracking provides accurate descriptors of home range behavior in a small-bodied coastal fish species', *PloS one* **11**(4), e0154089.

Apputhurai, P. and Stephenson, A. (2013), 'Spatiotemporal hierarchical modelling of extreme precipitation in western australia using anisotropic gaussian random fields', *Environmental and Ecological Statistics* **20**.

Arnason, A. N. (1972), 'Parameter estimates from mark-recapture experiments on two populations subject to migration and death', *Researches on population ecology* **13**(2), 97–113.

Auger-Méthé, M., Newman, K., Cole, D., Empacher, F., Gryba, R., King, A. A., Leos-Barajas, V., Mills Flemming, J., Nielsen, A., Petris, G. and Thomas, L. (2021), 'A guide to state–space modeling of ecological time series', *Ecological Monographs* **91**(4), e01470.

Ayles, G., Campbell, K., Gillis, D., Saunders, L., Scott, K., Tallman, R. and Traverse, N. (2011), *Technical Assessment of the Status, Health and Sustainable Harvest Levels of the Lake Winnipeg Fisheries Resource*, Lake Winnipeg Quota Review Task Force.

Banzon, V., Smith, T. M., Chin, T. M., Liu, C. and Hankins, W. (2016), 'A long-term record of blended satellite and in situ sea-surface temperature for climate monitoring, modeling and environmental studies', *Earth System Science Data* **8**(1), 165–176.

Barber, D. G., Lukovich, J. V., Keogak, J., Baryluk, S., Fortier, L. and Henry, G. H. R. (2008), 'The changing climate of the arctic', *Arctic* **61**, 7–26.

Becker, R. A., Wilks, A. R., Brownrigg, R. and Minka, T. P. D. A. (2018), 'maps: Draw Geographical Maps'. Available at https://cran.r-project.org/package=maps, version 3.3.0.

Benhamou, S. (2004), 'How to reliably estimate the tortuosity of an animal's path:: straightness, sinuosity, or fractal dimension?', *Journal of theoretical biology* **229**(2), 209–220.

Block, B. (2011), Fish migrations — tracking oceanic fish, *in* A. P. Farrell, ed., 'Encyclopedia of Fish Physiology', Academic Press, San Diego, pp. 1928–1936.

Bolker, B. M. (2008), *Ecological models and data in R*, Princeton University Press.

Bordalo-Machado, P. (2006), 'Fishing effort analysis and its potential to evaluate stock size', *Reviews in Fisheries Science* **14**(4), 369–393.

Bowman, A. W. and Azzalini, A. (2018), *R package* `sm`*: nonparametric smoothing methods (version 2.2-5.6)*, University of Glasgow, UK and Università di Padova, Italia.
URL: *http://www.stats.gla.ac.uk/ adrian/sm/*

Breed, G. A., Golson, E. A. and Tinker, M. T. (2017), 'Predicting animal home-range structure and transitions using a multistate ornstein-uhlenbeck biased random walk', *Ecology* **98**(1), 32–47.

Brooks, S. P., Catchpole, E. A. and Morgan, B. J. T. (2000), 'Bayesian animal survival estimation', *Statistical Science* **15**(4), 357–376.
URL: *http://www.jstor.org/stable/2676830*

Brownie, C., Hines, J. E., Nichols, J. D., Pollock, K. H. and Hestbeck, J. B. (1993), 'Capture-recapture studies for multiple strata including non-markovian transitions', *Biometrics* **49**(4), 1173–1187.

Brownscombe, J. W., Lédée, E. J., Raby, G. D., Struthers, D. P., Gutowsky, L. F., Nguyen, V. M., Young, N., Stokesbury, M. J., Holbrook, C. M., Brenden, T. O. et al. (2019), 'Conducting and interpreting fish telemetry studies: considerations for researchers and resource managers', *Reviews in Fish Biology and Fisheries* **29**(2), 369–400.

Brunskill, G., Elliott, S. and Campbell, P. (1980), Morphometry, hydrology, and watershed

data pertinent to the limnology of Lake Winnipeg, Canadian manuscript report of fisheries and aquatic science no. 1556, Department of Fisheries and Oceans,Winnipeg, Manitoba.

Calenge, C. (2011), 'Analysis of animal movements in r: the adehabitatlt package', *R Foundation for Statistical Computing: Vienna, Austria* .

Calvert, A. M., Bonner, S. J., Jonsen, I. D., Flemming, J. M., Walde, S. J. and Taylor, P. D. (2009), 'A hierarchical Bayesian approach to multi-state mark–recapture: simulations and applications', *Journal of Applied Ecology* **46**(3), 610–620.

Caza-Allard, I., Mazerolle, M. J., Harris, L. N., Malley, B. K., Tallman, R. F., Fisk, A. T. and Moore, J.-S. (2021), 'Annual survival probabilities of anadromous arctic char remain high and stable despite interannual differences in sea ice melt date', *Arctic Science* **7**(2), 575–584.

Chib, S. and Greenberg, E. (1995), 'Hierarchical analysis of sur models with extensions to correlated serial errors and time-varying parameter models', *Journal of Econometrics* **68**(2), 339–360.

Clark, J. S. (2005), 'Why environmental scientists are becoming Bayesians', *Ecology letters* **8**(1), 2–14.

Clark, R. G. (2016), 'Statistical efficiency in distance sampling', *PloS one* **11**(3).

Codling, E. A., Plank, M. J. and Benhamou, S. (2008), 'Random walk models in biology', *Journal of the Royal society interface* **5**(25), 813–834.

Congdon, P. D. (2010), *Applied Bayesian Hierarchical Methods (1st ed.)*, Chapman and Hall/CRC.

Cooke, S. J., Hinch, S. G., Wikelski, M., Andrews, R. D., Kuchel, L. J., Wolcott, T. G. and Butler, P. J. (2004), Biotelemetry: a mechanistic approach to ecology. trends in ecology, *in* 'Evolution', Citeseer.

Cooke, S. J., Iverson, S. J., Stokesbury, M. J., Hinch, S. G., Fisk, A. T., VanderZwaag, D. L., Apostle, R. and Whoriskey, F. (2011), 'Ocean tracking network canada: a network approach to addressing critical issues in fisheries and resource management with implications for ocean governance', *Fisheries* **36**(12), 583–592.

Cooke, S. J., Midwood, J. D., Thiem, J. D., Klimley, P., Lucas, M. C., Thorstad, E. B., Eiler, J., Holbrook, C. and Ebner, B. C. (2013), 'Tracking animals in freshwater with electronic tags: past, present and future', *Animal Biotelemetry* **1**(1), 1–19.

Cooke, S., Martins, E., Struthers, D., Gutowsky, L., Doka, S., Dettmers, J., Crook, D., Lucas, M., Holbrook, C. and Krueger, C. (2016), 'A moving target—incorporating knowledge of the spatial ecology of fish into the assessment and management of freshwater fish populations', *Environmental Monitoring and Assessment* **188**.

Cormack, R. (1964), 'Estimates of survival from the sighting of marked animals', *Biometrika* **51**(3/4), 429–438.

Crossin, G. T., Heupel, M. R., Holbrook, C. M., Hussey, N. E., Lowerre-Barbieri, S. K., Nguyen, V. M., Raby, G. D. and Cooke, S. J. (2017), 'Acoustic telemetry and fisheries management', *Ecological Applications* **27**(4), 1031–1049.

Day, A. C. and Harris, L. N. (2013), *Information to support an updated stock status of commercially harvested Arctic Char (Salvelinus alpinus) in the Cambridge Bay region of Nunavut, 1960-2009*, Canadian Science Advisory Secretariat.

DFO (2014), *Integrated fisheries management plan, Cambridge Bay Arctic Char commercial fishery, Nunavut Settlement area*, Fisheries and Oceans Canada, Central Arctic Region, Resource Management and Aboriginal Affairs, Winnipeg, Canada.

Donaldson, M. R., Hinch, S. G., Suski, C. D., Fisk, A. T., Heupel, M. R. and Cooke, S. J. (2014), 'Making connections in aquatic ecosystems with acoustic telemetry monitoring', *Frontiers in Ecology and the Environment* **12**(10), 565–573.

Dudgeon, C. L., Pollock, K. H., Braccini, J. M., Semmens, J. M. and Barnett, A. (2015), 'Integrating acoustic telemetry into mark–recapture models to improve the precision of apparent survival and abundance estimates', *Oecologia* **178**(3), 761–772.

Environment and Climate Change Canada (2020), *State of Lake Winnipeg, 2nd Edition*, Manitoba Agriculture and Resource Development.

Espinoza, M., Farrugia, T. J., Webber, D. M., Smith, F. and Lowe, C. G. (2011), 'Testing a new acoustic telemetry technique to quantify long-term, fine-scale movements of aquatic animals', *Fisheries Research* **108**(2-3), 364–371.

Fisheries and Canada, O. (2020), 'Freshwater landings, 2018', https://www.dfo-mpo.gc.ca/stats/commercial/land-debarq/freshwater-eaudouce/2018-eng.htm. [Online; accessed 12-Feb-2021].

Fouley, J.-L. (2013), 'The bugs book: A practical introduction to bayesian analysis'.

Francisco, F. A., Nührenberg, P. and Jordan, A. (2020), 'High-resolution, non-invasive animal tracking and reconstruction of local environment in aquatic ecosystems', *Movement ecology* **8**(1), 1–12.

Franzin, W., Stewart, K., Hanke, G. and Heuring, L. (2003), *The fish and fisheries of Lake Winnipeg: the first 100 years*, Can. Tech. Rep. Fish. Aquat. Sci. 2398: v + 53p.
URL: *https://publications.gc.ca/collections/collection*$_2$014/$mpo - dfo/Fs97 - 6 - 2398 - eng.pdf$

Friedman, J. H. (1984), A variable span smoother, Technical report, Stanford Univ CA Lab for Computational Statistics.

Fuentes, M. and Raftery, A. (2005), 'Model evaluation and spatial interpolation by bayesian combination of observations with outputs from numerical models', *Biometrics* **61**, 36–45.

Gelman, A., Carlin, J. B., Stern, H. S., Dunson, D. B., Vehtari, A. and Rubin, D. B. (2013), *Bayesian Data Analysis (3rd ed.)*, Chapman and Hall/CRC.

Gelman, A., Carlin, J. B., Stern, H. S. and Rubin, D. B. (2004), *Bayesian Data Analysis (2nd ed.)*, Chapman and Hall/CRC.

Gelman, A., Hwang, J. and Vehtari, A. (2014), 'Understanding predictive information criteria for bayesian models', *Statistics and computing* **24**(6), 997–1016.

Gelman, A. and Rubin, D. B. (1992), 'Inference from Iterative Simulation Using Multiple Sequences', *Statistical Science* **7**(4), 457 – 472.

Geyer, C. J. (1992), 'Practical Markov Chain Monte Carlo', *Statistical Science* **7**(4), 473 – 483.

Gimenez, O., Morgan, B. and Brooks, S. (2009), 'Weak identifiability in models for mark-recapture-recovery data', *Modeling Demographic Processes in Marked Populations* **3**, 1055–1067.

Gimenez, O., Rossi, V., Choquet, R., Dehais, C., Doris, B., Varella, H., Vila, J.-P. and Pradel, R. (2007), 'State-space modelling of data on marked individuals', *Ecological Modelling* **206**(3), 431–438.

Goodchild, G. A. (2004), 'Fish habitat is everyone's business, Canada's fish habitat management programme', *Fisheries Management and Ecology* **11**(3–4), 277–281.

Government of Nunavut (2016), *Nunavut fisheries strategy: 2016-2020. GN, Department of Environment, Fisheries and Sealing Division. 47 pp.*

Grenier, G. and Tallman, R. F. (2021), 'Lifelong divergence of growth patterns in arctic charr life history strategies: implications for sustainable fisheries in a changing climate', *Arctic Science* **7**(2), 454–470.

Grieve, R., Nixon, R. and Thompson, S. G. (2010), 'Bayesian hierarchical models for cost-effectiveness analyses that use data from cluster randomized trials', *Medical Decision Making* **30**(2), 163–175. PMID: 19675321.

URL: *https://doi.org/10.1177/0272989X09341752*

Halpern, B. (2003), 'The impact of marine reserves: Do reserves work and does reserve size matter?', *Ecological Applications* **13**, 117–137.

Hammer, L. J., Hussey, N. E., Marcoux, M., Pettitt-Wade, H., Hedges, K., Tallman, R. and Furey, N. B. (2022), 'Arctic char *Salvelinus alpinus* movement dynamics relative to ice breakup in a high arctic embayment', *Marine Ecology Progress Series* **682**, 221–236.

Harley, S. J. and Myers, R. A. (2001), 'Hierarchical bayesian models of length-specific catchability of research trawl surveys', *Canadian Journal of Fisheries and Aquatic Sciences* **58**(8), 1569–1584.

Harris, L., Malley, B., Moore, J.-S. and Tallman, R. (2020b), *A Dressed Weight to Round Weight Conversion Factor for Commercially Harvested Arctic Char (Salvelinus alpinus) from the Halokvik River, Nunavut*, Fisheries and Oceans Canada.

Harris, L. N., Cahill, C. L., Jivan, T., Zhu, X. and Tallman, R. F. (2021), *Updated stock status of commercially harvested Arctic Char (Salvelinus alpinus) from the Jayko and Halokvik rivers, Nunavut: A summary of harvest, catch-effort and biological information*, Canadian Science Advisory Secretariat.

Harris, L. N., Yurkowski, D. J., Gilbert, M. J., Else, B. G., Duke, P. J., Ahmed, M. M., Tallman, R. F., Fisk, A. T. and Moore, J.-S. (2020a), 'Depth and temperature preference of anadromous Arctic Char, *Salvelinus alpinus*, in the Kitikmeot Sea - a shallow and low salinity area of the Canadian Arctic', *Marine Ecology Progress Series* **634**, 175–197.

Harris, L. N., Yurkowski, D. J., Malley, B. K., Jones, S. F., Else, B. G., Tallman, R. F., Fisk, A. T. and Moore, J.-S. (2022), 'Acoustic Telemetry Reveals the Complex Nature of Mixed-Stock Fishing in Canada's Largest Arctic Char (Salvelinus alpinus) Commercial Fishery', *North American Journal of Fisheries Management* **42**(5), 1250–1268.

Hartman, G. (2009), 'A biological synopsis of walleye (sander vitreus)', *Canadian Manuscript Report of Fisheries and Aquatic Sciences 2888* **v+48p**.

Harwood, J. and Stokes, K. (2003), 'Coping with uncertainty in ecological advice: lessons from fisheries', *Trends in Ecology & Evolution* **18**(12), 617–622.

Hedger, R. D., Martin, F., Dodson, J. J., Hatin, D., Caron, F. and Whoriskey, F. G. (2008), 'The optimized interpolation of fish positions and speeds in an array of fixed acoustic receivers', *ICES Journal of Marine Science* **65**(7), 1248–1259.

Hestbeck, J. B., Nichols, J. D. and Malecki, R. A. (1991), 'Estimates of movement and site fidelity using mark-resight data of wintering Canada geese', *Ecology* **72**(2), 523–533.

Heupel, M. R. and Simpfendorfer, C. A. (2002), 'Estimation of mortality of juvenile blacktip sharks, carcharhinus limbatus, within a nursery area using telemetry data', *Canadian Journal of Fisheries and Aquatic Sciences* **59**(4), 624–632.

Hines, K., Middendorf, T. and Aldrich, R. (2014), 'Determination of parameter identifiability in nonlinear biophysical models: A Bayesian approach', *The Journal of General Physiology* **143**, 401–416.

Hollins, J., Pettitt-Wade, H., Gallagher, C. P., Lea, E. V., Loseto, L. L. and Hussey, N. E. (2022), 'Distinct freshwater migratory pathways in arctic char, salvelinus alpinus, coincide with separate patterns of marine spatial habitat-use across a large coastal landscape', *Canadian Journal of Fisheries and Aquatic Sciences* **Just-IN**.

Hostetter, N. J. and Royle, J. A. (2020), 'Movement-assisted localization from acoustic telemetry data', *Movement Ecology* **8**, 1–13.

How, J. R. and de Lestang, S. (2012), 'Acoustic tracking: issues affecting design, analysis and interpretation of data from movement studies', *Marine and Freshwater Research* **63**(4), 312–324.

Huang, B., Liu, C., Freeman, J., Graham, G., Smith, T. and Zhang, H.-M. (2021), 'Assessment and intercomparison of noaa daily optimum interpolation sea surface temperature (doisst) version 2.1', *Journal of Climate* **34**, 1–57.

Hussey, N. E., Hedges, K. J., Barkley, A. N., Treble, M. A., Peklova, I., Webber, D. M., Ferguson, S. H., Yurkowski, D. J., Kessel, S. T., Bedard, J. M. and Fisk, A. T. (2017), 'Movements of a deep-water fish: establishing marine fisheries management boundaries in coastal Arctic waters', *Ecological Applications* **27**(3), 687–704.

Hussey, N. E., Kessel, S. T., Aarestrup, K., Cooke, S. J., Cowley, P. D., Fisk, A. T., Harcourt, R. G., Holland, K. N., Iverson, S. J., Kocik, J. F. et al. (2015), 'Aquatic animal telemetry: a panoramic window into the underwater world', *Science* **348**(6240), 1255642.

Jensen, A. J., Finstad, B. and Fiske, P. (2019), 'The cost of anadromy: marine and freshwater mortality rates in anadromous Arctic char and brown trout in the Arctic region of Norway', *Canadian Journal of Fisheries and Aquatic Sciences* **76**(12), 2408–2417.

Johnson, L. (1980), *The Arctic char, Salvelinus alpinus. In: Balo EK, ed. Charrs: Salmonid Fishes of the genus Salvelinus.*, The Hague, Netherlands: W Junk Publishers.

Johnston, T. A., Lysack, W. and Leggett, W. C. (2012), 'Abundance, growth, and life history characteristics of sympatric walleye (sander vitreus) and sauger (sander canadensis) in lake winnipeg, manitoba', *Journal of Great Lakes Research* **38**, 35–46.

Jolly, G. M. (1965), 'Explicit estimates from capture-recapture data with both death and immigration-stochastic model', *Biometrika* **52**(1/2), 225–247.

Jonsen, I. D., Flemming, J. M. and Myers, R. A. (2005), 'Robust state–space modeling of animal movement data', *Ecology* **86**(11), 2874–2880.

Jonsen, I. D., Myers, R. A. and Flemming, J. M. (2003), 'Meta-analysis of animal movement using state-space models', *Ecology* **84**(11), 3055–3063.

Kantorová, V., Wheldon, M. C., Ueffing, P. and Dasgupta, A. N. Z. (2020), 'Estimating progress towards meeting women's contraceptive needs in 185 countries: A bayesian hierarchical modelling study', *PLOS Medicine* **17**.

Kass, R. E., Carlin, B. P., Gelman, A. and Neal, R. M. (1998), 'Markov Chain Monte Carlo in practice: A roundtable discussion', *The American Statistician* **52**(2), 93–100.
URL: *http://www.jstor.org/stable/2685466*

Kéry, M. and Schaub, M. (2011), *Bayesian population analysis using WinBUGS: a hierarchical perspective*, Academic Press.

King, R. (2012), 'A review of Bayesian state-space modelling of capture-recapture-recovery data', *Interface focus* **2**, 190–204.

Klimley, A. P., Voegeli, F., Beavers, S. C. and Le Boeuf, B. J. (1998), 'Automated listening stations for tagged marine fishes', *Marine Technology Society Journal* **32**(1), 94–101.

Klinard, N. V., Halfyard, E. A., Matley, J. K., Fisk, A. T. and Johnson, T. B. (2019),

'The influence of dynamic environmental interactions on detection efficiency of acoustic transmitters in a large, deep, freshwater lake', *Animal Biotelemetry* **7**(1), 17.

Kneebone, J., Hoffman, W. S., Dean, M. J., Fox, D. A. and Armstrong, M. P. (2014), 'Movement patterns and stock composition of adult striped bass tagged in Massachusetts coastal waters', *Transactions of the American Fisheries Society* **143**(5), 1115–1129.

Kraus, R. T., Holbrook, C. M., Vandergoot, C. S., Stewart, T. R., Faust, M. D., Watkinson, D. A., Charles, C., Pegg, M., Enders, E. C. and Krueger, C. C. (2018), 'Evaluation of acoustic telemetry grids for determining aquatic animal movement and survival', *Methods in Ecology and Evolution* **9**(6), 1489–1502.

Kruschke, J. (2014), *Doing Bayesian data analysis: A tutorial with R, JAGS, and Stan, second edition*, London, UK ; San Diego, CA : Academic Press.

Lea, J. S. E., Humphries, N. E., von Brandis, R. G., Clarke, C. R. and Sims, D. W. (2016), 'Acoustic telemetry and network analysis reveal the space use of multiple reef predators and enhance marine protected area design', *Proceedings of the Royal Society B: Biological Sciences* **283**(1834), 20160717.

Lees, K., MacNeil, M., Hedges, K. and Hussey, N. (2021), 'Estimating demographic parameters for fisheries management using acoustic telemetry', *Reviews in Fish Biology and Fisheries* pp. 1–27.

Lehnherr, I., St.Louis, V., Sharp, M., Gardner, A., Smol, J., Schiff, S., Muir, D., Mortimer, C., Michelutti, N., Tarnocai, C., St.Pierre, K., Emmerton, C., Wiklund, J., Köck, G.,

Lamoureux, S. and Talbot, C. (2018), 'The world's largest high arctic lake responds rapidly to climate warming', *Nature communications* **9**, 1290.

Lele, S. R. and Dennis, B. (2009), 'Bayesian methods for hierarchical models: Are ecologists making a faustian bargain?', *Ecological Applications* **19**(3), 581–584.
URL: *http://www.jstor.org/stable/27645998*

Lennox, R., Aarestrup, K., Cooke, S., Cowley, P., Deng, Z., Fisk, A., Harcourt, R., Heupel, M., Hinch, S., Holland, K., Hussey, N., Iverson, S., Kessel, S., Kocik, J., Lucas, M., Flemming, J., Nguyen, V., Stokesbury, M., Vagle, S. and Young, N. (2017), 'Envisioning the future of aquatic animal tracking: Technology, science, and application', *BioScience* **67**, 884–896.

Link, W. A. and Eaton, M. J. (2012), 'On thinning of chains in MCMC', *Methods in Ecology and Evolution* **3**(1), 112–115.

Maceachern, S. N. and Berliner, L. M. (1994), 'Subsampling the Gibbs sampler', *The American Statistician* **48**(3), 188–190.

Matley, J. K., Klinard, N. V., Barbosa Martins, A. P., Aarestrup, K., Aspillaga, E., Cooke, S. J., Cowley, P. D., Heupel, M. R., Lowe, C. G., Lowerre-Barbieri, S. K., Mitamura, H., Moore, J.-S., Simpfendorfer, C. A., Stokesbury, M. J., Taylor, M. D., Thorstad, E. B., Vandergoot, C. S. and Fisk, A. T. (2022), 'Global trends in aquatic animal tracking with acoustic telemetry', *Trends in Ecology & Evolution* **37**(1), 79–94.

McCluskey, S. M. and Lewison, R. L. (2008), 'Quantifying fishing effort: a synthesis of current methods and their applications', *Fish and Fisheries* **9**(2), 188–200.

McMichael, G. A., Eppard, M. B., Carlson, T. J., Carter, J. A., Ebberts, B. D., Brown, R. S., Weiland, M., Ploskey, G. R., Harnish, R. A. and Deng, Z. D. (2010), 'The juvenile salmon acoustic telemetry system: A new tool', *Fisheries* **35**(1), 9–22.

Meredith, M. (2013), 'SECR in BUGS/JAGS with patchy habitat '. https://mmeredith.net/blog/2013/1309_SECR_in_JAGS_patchy_habitat.htm, visited 2023-01-04.

Moore, J.-S., Harris, L. N., Kessel, S. T., Bernatchez, L., Tallman, R. F. and Fisk, A. T. (2016), 'Preference for nearshore and estuarine habitats in anadromous arctic char (*Salvelinus alpinus*) from the Canadian high Arctic (Victoria Island, Nunavut) revealed by acoustic telemetry', *Canadian Journal of Fisheries and Aquatic Sciences* **73**(9), 1434–1445.

Moore, J. W. (1975), 'Distribution, movements, and mortality of anadromous arctic char, salvelinus alpinus l., in the cumberland sound area of baffin island', *Journal of Fish Biology* **7**(3), 339–348.

URL: *https://onlinelibrary.wiley.com/doi/abs/10.1111/j.1095-8649.1975.tb04608.x*

Morris, S. R., Larracuente, A. M., Covino, K. M., Mustillo, M. S., Mattern, K. E., Liebner, D. A. and Sheets, H. D. (2006), 'Utility of open population models: Limitations posed by parameter estimability in the study of migratory stopover', *The Wilson Journal of Ornithology* **118**(4), 513–526.

Mulder, I. M., Morris, C. J., Dempson, J. B., Fleming, I. A. and Power, M. (2018), 'Winter movement activity patterns of anadromous arctic charr in two Labrador lakes', *Ecology of Freshwater Fish* **27**(3), 785–797.

Munaweera, I., Harris, L., Moore, J.-S., Tallman, R., Fisk, A., Gillis, D. and Muthuku-

marana, S. (2022), 'Estimating survival probabilities of cambridge bay arctic char using acoustic telemetry data and bayesian multi-state capture-recapture models', *Canadian Journal of Fisheries and Aquatic Sciences* **79**.

Munaweera, I., Muthukumarana, S., Gillis, D., Watkinson, D., Charles, C. and Enders, E. (2021), 'Assessing movement patterns using Bayesian state space models on Lake Winnipeg walleye', *Canadian Journal of Fisheries and Aquatic Sciences* **78**(10), 1407–1421.

Murray, D. L. and Patterson, B. R. (2006), 'Wildlife survival estimation: Recent advances and future directions', *The Journal of Wildlife Management* **70**(6), 1499–1503.
URL: *http://www.jstor.org/stable/4128082*

Muthukumarana, S., Schwarz, C. J. and Swartz, T. B. (2008), 'Bayesian analysis of mark-recapture data with travel time-dependent survival probabilities', *Canadian Journal of Statistics* **36**(1), 5–21.
URL: *https://onlinelibrary.wiley.com/doi/abs/10.1002/cjs.5550360103*

Nathan, R., Getz, W. M., Revilla, E., Holyoak, M., Kadmon, R., Saltz, D. and Smouse, P. E. (2008), 'A movement ecology paradigm for unifying organismal movement research', *Proceedings of the National Academy of Sciences* **105**(49), 19052–19059.

Nicholson, K. (2007), *A history of Manitoba's commercial fishery 1872 - 2005*, Historic Resources Branch, Manitoba Government.
URL: *https://www.gov.mb.ca/chc/hrb/internal$_r$eports/pdfs/Fishery$_M$B$_C$ommercial.pdf*

Nicosia, A., Duchesne, T., Rivest, L.-P. and Fortin, D. (2017), 'A general hidden state

random walk model for animal movement', *Computational Statistics & Data Analysis* **105**, 76–95.

O'Brien, S., Robert, B. and Tiandry, H. (2005), 'Consequences of violating the recapture duration assumption of mark–recapture models: a test using simulated and empirical data from an endangered tortoise population', *Journal of Applied Ecology* **42**(6), 1096–1104.

Patterson, T. A., Parton, A., Langrock, R., Blackwell, P. G., Thomas, L. and King, R. (2017), 'Statistical modelling of individual animal movement: an overview of key methods and a discussion of practical challenges', *AStA Advances in Statistical Analysis* **101**(4), 399–438.

Patterson, T. A., Thomas, L., Wilcox, C., Ovaskainen, O. and Matthiopoulos, J. (2008), 'State–space models of individual animal movement', *Trends in ecology & evolution* **23**(2), 87–94.

Peake, S., McKinley, R. S. and Scruton, D. A. (2000), 'Swimming performance of walleye (stizostedion vitreum)', *Canadian Journal of Zoology* **78**(9), 1686–1690.
URL: *https://doi.org/10.1139/z00-097*

Pedersen, M. W. and Weng, K. C. (2013), 'Estimating individual animal movement from observation networks', *Methods in Ecology and Evolution* **4**(10), 920–929.

Peklova, I., Hussey, N., Hedges, K., Treble, M. and Fisk, A. (2012), 'Depth and temperature preferences of the deepwater flatfish Greenland halibut Reinhardtius hippoglossoides in an Arctic marine ecosystem', *Marine Ecology Progress Series* **467**, 193–205.

Pithan, F. and Mauritsen, T. (2014), 'Arctic amplification dominated by temperature feedbacks in contemporary climate models', *Nature Geoscience* **7**(3), 181–184.

Plummer, M. et al. (2003), Jags: A program for analysis of bayesian graphical models using gibbs sampling, *in* 'Proceedings of the 3rd international workshop on distributed statistical computing', Vol. 124, Vienna, Austria., p. 10.

Pollock, K. H., Jiang, H. and Hightower, J. E. (2004), 'Combining telemetry and fisheries tagging models to estimate fishing and natural mortality rates', *Transactions of the American Fisheries Society* **133**(3), 639–648.

Pollock, K. H., Nichols, J. D., Brownie, C. and Hines, J. E. (1990), 'Statistical inference for capture-recapture experiments', *Wildlife Monographs* (107), 3–97.

Poole, D. (2002), 'Bayesian estimation of survival from mark-recapture data', *Journal of Agricultural, Biological, and Environmental Statistics* **7**(2), 264–276.
URL: *http://www.jstor.org/stable/1400699*

Prevost, T. C., Abrams, K. R. and Jones, D. R. (2000), 'Hierarchical models in generalized synthesis of evidence: an example based on studies of breast cancer screening', *Statistics in Medicine* **19**(24), 3359–3376.

Priest, H. and Usher, P. (2004), 'The nunavut wildlife harvest study: Final report', *Iqaluit: Nunavut Wildlife Management Board* .

Prowse, T. D., Wrona, F. J., Reist, J. D., Gibson, J. J., Hobbie, J. E., Lévesque, L. M. and Vincent, W. F. (2006), 'Climate change effects on hydroecology of arctic freshwater ecosystems', *AMBIO: A Journal of the Human Environment* **35**(7), 347–358.

R Core Team (2020), *R: A Language and Environment for Statistical Computing*, R Foun-

dation for Statistical Computing, Vienna, Austria.

URL: *https://www.R-project.org/*

Reist, J. D., Wrona, F. J., Prowse, T. D., Dempson, J. B., Power, M., Köck, G., Carmichael, T. J., Sawatzky, C. D., Lehtonen, H. and Tallman, R. F. (2006), 'Effects of climate change and UV radiation on fisheries for arctic freshwater and anadromous species', *AMBIO: A Journal of the Human Environment* **35**(7), 402–410.

Reubens, J., Verhelst, P., van der Knaap, I., Deneudt, K., Moens, T. and Hernandez, F. (2019), 'Environmental factors influence the detection probability in acoustic telemetry in a marine environment: results from a new setup', *Hydrobiologia* **845**(1), 81–94.

Reynolds, R., Smith, T., Liu, C., Chelton, D. and Casey, K. (2007), 'Daily high-resolution-blended analyses for sea surface temperature', *Journal of Climate* **20**.

Richardson, S. and Best, N. (2003), 'Bayesian hierarchical models in ecological studies of health–environment effects', *Environmetrics* **14**(2), 129–147.

Rivot, E. and Prevost, E. (2002), 'Hierarchical bayesian analysis of capture–mark–recapture data', *Canadian Journal of Fisheries and Aquatic Sciences* **59**(11), 1768–1784.

Ropert-Coudert, Y. and Wilson, R. P. (2005), 'Trends and perspectives in animal-attached remote sensing', *Frontiers in Ecology and the Environment* **3**(8), 437–444.

Royle, J. A. and Dorazio, R. M. (2008), *Hierarchical modeling and inference in ecology: the analysis of data from populations, metapopulations and communities*, Academic Press.

Royle, J. A. and Dorazio, R. M. (2009), 1 - conceptual and philosophical considerations in

ecology and statistics, *in* J. A. Royle and R. M. Dorazio, eds, 'Hierarchical Modeling and Inference in Ecology', Academic Press, San Diego, pp. 1–26.

Sahu, S., Yip, S. and Holland, D. (2009), 'Improved space–time forecasting of next day ozone concentrations in the eastern us', *Atmospheric Environment* **43**, 494–501.

Seber, G. A. (1965), 'A note on the multiple-recapture census', *Biometrika* **52**(1/2), 249–259.

Seidel, D. P., Dougherty, E., Carlson, C. and Getz, W. M. (2018), 'Ecological metrics and methods for gps movement data', *International Journal of Geographical Information Science* **32**(11), 2272–2293.

Shaddick, G. and Zidek, J. V. (2015), *Spatio-temporal methods in environmental epidemiology*, CRC Press.

Sheppard, K. T., Davoren, G. K. and Hann, B. J. (2015), 'Diet of walleye and sauger and morphological characteristics of their prey in lake winnipeg', *Journal of Great Lakes Research* **41**(3), 907–915.

Siekmann, I., Sneyd, J. and Crampin, E. (2012), 'MCMC can detect nonidentifiable models', *Biophysical journal* **103**, 2275–86.

Simpfendorfer, C. A., Heupel, M. R. and Hueter, R. E. (2002), 'Estimation of short-term centers of activity from an array of omnidirectional hydrophones and its use in studying animal movements', *Canadian Journal of Fisheries and Aquatic Sciences* **59**(1), 23–32.

Simpson, M. J., Baker, R. E., Vittadello, S. T. and Maclaren, O. J. (2020), 'Practical parameter identifiability for spatio-temporal models of cell invasion', *Journal of The Royal*

Society Interface **17**(164), 20200055.

URL: *https://royalsocietypublishing.org/doi/abs/10.1098/rsif.2020.0055*

Smith, R. L. (2020), Migration timing and overwintering habitat of anadromous Arctic char (*Salvelinus alpinus*) near Kugluktuk, Nunavut, Master's thesis, Department of Biology, University of Waterloo, Ontario.

Spiegelhalter, D. J., Best, N. G., Carlin, B. P. and Van Der Linde, A. (2002), 'Bayesian measures of model complexity and fit', *Journal of the royal statistical society: Series b (statistical methodology)* **64**(4), 583–639.

Spiegelhalter, D., Thomas, A., Best, N. and Lunn, D. (2003), 'Winbugs user manual version 1.4 january 2003', *Upgraded to version* **1**(3).

Stewardship, M. W. et al. (2011), State of lake winnipeg: 1999 to 2007, Technical report, Environment Canada and Manitoba Water Stewardship.

Stewart, K. R., Lewison, R. L., Dunn, D. C., Bjorkland, R. H., Kelez, S., Halpin, P. N. and Crowder, L. B. (2011), 'Characterizing fishing effort and spatial extent of coastal fisheries', *PLOS ONE* **5**(12), 1–8.

Stewart, K. W. and Watkinson, D. A. (2004), *The freshwater fishes of Manitoba*, Univ. of Manitoba Press.

Su, Y.-S. and Yajima, M. (2015), *Package 'R2jags'*. Available at `http://CRAN.R-project.org/package=R2jags`, version 0.5-7.

The Transportation Safety Board of Canada (1999), *MARINE INVESTIGATION REPORT M99C0048*.

The Transportation Safety Board of Canada (2001), *MARINE INVESTIGATION REPORT REPORTM01C0029*.

Thorstensen, M. J., Wiens, L. M., Jeffrey, J. D., Klein, G. M., Jeffries, K. M. and Treberg, J. R. (2020), 'Morphology and blood metabolites reflect recent spatial and temporal differences among lake winnipeg walleye, sander vitreus', *Journal of Great Lakes Research* . **URL:** *https://www.sciencedirect.com/science/article/pii/S0380133020301374*

Tim, S., J., P., Benjamin, G., Chi, L., Simon, H., Mark, M., Pierre, K., Felipe, C., Vardis, T., Steven L.H., T., Alexandre, A.-d.-S. and Simon, N. (2015), 'Using movement data from electronic tags in fisheries stock assessment: A review of models, technology and experimental design', *Fisheries Research* **163**, 152–160.

Ulrich, K. L. and Tallman, R. F. (2021), 'Multi-indicator evidence for habitat use and trophic strategy segregation of two sympatric forms of Arctic char from the Cumberland Sound region of Nunavut, Canada', *Arctic Science* **7**(2), 1–33.

Vandergoot, C. S., Murchie, K. J., Cooke, S. J., Dettmers, J. M., Bergstedt, R. A. and Fielder, D. G. (2011), 'Evaluation of two forms of electroanesthesia and carbon dioxide for short-term anesthesia in walleye', *North American Journal of Fisheries Management* **31**(5), 914–922.

Villegas-Ríos, D., Freitas, C., Moland, E., Thorbjørnsen, S. H. and Olsen, E. M. (2020),

'Inferring individual fate from aquatic acoustic telemetry data', *Methods in Ecology and Evolution* **11**(10), 1186–1198.

Wassenaar, L. I. and Rao, Y. R. (2012), 'Lake winnipeg: The forgotten great lake', *Journal of Great Lakes Research* **38**, 1–5.

Whoriskey, K., Martins, E. G., Auger-Méthé, M., Gutowsky, L. F. G., Lennox, R. J., Cooke, S. J., Power, M. and Mills Flemming, J. (2019), 'Current and emerging statistical techniques for aquatic telemetry data: A guide to analysing spatially discrete animal detections', *Methods in Ecology and Evolution* **10**(7), 935–948.

Wickham, H. (2016), *ggplot2: Elegant Graphics for Data Analysis*, Springer-Verlag New York.

Wikle, C. K. (2003), 'Hierarchical models in environmental science', *International Statistical Review* **71**(2), 181–199.

Wu, G. and Holan, S. H. (2017), 'Bayesian hierarchical multi-population multistate jolly–seber models with covariates: Application to the pallid sturgeon population assessment program', *Journal of the American Statistical Association* **112**(518), 471–483.

Yano, A., Nicol, B., Jouanno, E., Quillet, E., Fostier, A., Guyomard, R. and Guiguen, Y. (2013), 'The sexually dimorphic on the y-chromosome gene (sdy) is a conserved male-specific y-chromosome sequence in many salmonids', *Evolutionary Applications* **6**(3), 486–496.

Ying, J., Kuo, L. and Seow, G. S. (2005), 'Forecasting stock prices using a hierarchical bayesian approach', *Journal of Forecasting* **24**(1), 39–59.

Zhu, X., Day, A. C., Carmichael, T. J. and Tallman, R. F. (2014), *Hierarchical Bayesian Modeling for Cambridge Bay Arctic Char, Salvelinus Alpinus (L.), Incoporated with Precautionary Reference Points*, Canadian Science Advisory Secretariat (CSAS).

Zhu, X., Gallagher, C., Howland, K., Harwood, L. and Tallman, R. (2017), 'Multimodel assessment of population production and recommendations for sustainable harvest levels of anadromous Arctic Char, Salvelinus alpinus (L.), from the Hornaday River, Northwest Territories', *DFO Can. Sci. Advis. Sec. Res. Doc. 2016/116. v + 81 p.* .

Zhu, X., Harris, L., Cahill, C. and Tallman, R. (2021), *Assessing population dynamics of Arctic Char, Salvelinus alpinus, from the Halokvik and Jayko Rivers, Cambridge Bay, Nunavut, Canada*, DFO Can. Sci. Advis. Sec. Res. Doc. 2021/016. iv + 34 p.